



Strål
säkerhets
myndigheten

Swedish Radiation Safety Authority

Report

Investigation of risk assessment for decommissioning waste to Fortum's landfill at Norrtorp

2023:02

Authors: Shulan Xu ¹⁾, Ryk Klos ²⁾

¹⁾ Xu Environmental Consulting AB, Sweden

²⁾ Aleksandria Sciences Ltd, UK

Report number: 2023:02

ISSN: 2000-0456

Available at www.ssm.se

SSM perspektiv

Bakgrund

I och med avveckling och rivning av ett flertal kärnkraftsreaktorer i Sverige har Strålsäkerhetsmyndigheten identifierat att ansökningar om dispens, så kallad riktad friklassning, för att deponera lågaktivt avfall (VLLW) kan komma att öka. En avfallsdeponi som tagit emot ett flertal omgångar med avfall från riktade friklassningar godkända av myndigheten är Fortum Waste Solution AB:s deponi för farligt avfall i Norrtorp, Kumla. En förutsättning för dispens att deponera lågaktivt avfall (VLLW) är att den planerade hanteringen inte kan antas medföra en oacceptabel risk för att människor eller miljön utsätts för skadlig verkan av strålning (enligt 7 kap. 6 § strålskyddsförordningen). Eftersom det ofta rör sig om mycket låga beräknade stråldoser till allmänheten har varje enskilt inkommet ärende med dispensansökan hittills endast riskbedömts var för sig av myndigheten inför beslut om riktad friklassning. Men utifrån att denna typ av avfallsströmmar kan komma att öka i närtid i och med avveckling av ett flertal reaktorer finns ett behov på myndigheten att få en översikt av hur hela riskbilden ser ut för deponin. Myndigheten har därför finansierat ett uppdrag om att utföra en platsspecifik biosfärsmodell för Fortums deponi i Norrtorp som en del av en radiologisk riskbedömning av det lågaktiva avfall som redan deponerats hos Fortum och vilka marginaler ur strålskyddssynpunkt som finns för att bevilja att ytterligare avvecklingsrelaterat avfall deponeras där.

Syfte

Uppdraget omfattade att utföra en radiologisk riskbedömning av deponering av avvecklingsrelaterat avfall på Fortums deponi i Norrtorp inklusive att utveckla en platsspecifik biosfärsmodell för deponin och att presentera detta i en rapport. Riskbedömningen skulle omfatta risk för människans hälsa och miljön till följd av joniserande strålning och ta hänsyn till tidigare deponerat avfall på deponin som har godkänts av myndigheten för att få en helhetssyn i konsekvensanalysen för sådant avfall. Den platsspecifika biosfärsmodellen för deponin skulle inkludera platsspecifika parametrar så som till exempelvis deponins utformning, deponins utveckling, deponeringsplatser för aktuellt och tidigare deponerat avfall, utloppsvägar för lakvatten och recipienter i omgivningen. Uppdraget genomfördes med syftet att vara ett stöd för myndigheten i pågående och kommande granskning av ansökningar om deponering av radioaktivt förorenat avfall vid Fortums deponi i Norrtorp.

Resultat

Uppdraget utfördes av Xu Environmental Consulting AB och Aleksandria Sciences Ltd. Metoder som använts för den utförda radiologiska riskbedömningen är en kombination av dokumentgranskning, reproducering av modeller och oberoende modellering. Rapporter från tidigare dispensansökningar och avfallsdeponering vid Fortums

deponi i Norrtorp har granskats och modellering utfördes med syfte att reproducera resultat från tidigare dosberäkningar i tre hanterade ärenden. Resultaten visar på god överensstämmelse med skillnaden att för de reproducerade resultaten användes fördelningskoefficienter (Kd) istället för urlakningsfaktorer samt att antaganden och valda parametrar skulle kunna motiveras tydligare i de granskade modellerna.

I den utförda oberoende modelleringen har ISAM och BIOMASS metoder använts. Recipienten, också kallad biosfärsobjekt eller landskapsdosobjekt, har identifierats för dosberäkningar med hjälp av plats specifika data inhämtade från bl. a. SMHI, Lantmäteriet och SGU. Ett flertal scenarion och beräkningsfall redovisas här i en radiologisk riskbedömning av Fortums deponi i Norrtorp. Extrema förhållanden har antagits för att studera osäkerheter och känslighet i både deterministiska och probabilistiska beräkningar. Syftet med detta har varit att lyfta fram nyckelfaktorer som kan ha en signifikant effekt på dosberäkningarna och att föreslå att SSM fokuserar på dessa nyckelfaktorer i kommande granskningar av ansökningar om riktad friklassning för deponering. Exempel på sådana nyckelfaktorer är infiltrationshastighet genom avfallet, grundvattenflöde och antagen utspädning i brunnscenariot.

Stråldoser till miljön, speciellt fisk, beräknades med ERICA-verktyget vara långt under screeningvärdet 10 mikroGy/h. Stråldoser till allmänheten för det uppskattade inventariet av redan deponerat avfall beräknades vara under kriteriet 10 mikroSv per år i 100 000 år i beräkningsfallet med extremt låg utspädning och en konstant infiltrationshastighet. I andra beräkningsfall överstegs kriteriet vid olika tidpunkter. De olika beräkningsfallen ska dock inte tolkas som att deponin inte är strålsäker utan syftar till att identifiera viktiga parametrar i dosberäkningarna. Osäkerheten i beräkningarna ökar även över tid, speciellt efter 1000 år, eftersom konstanta biosfärsförhållanden har antagits i dessa modeller.

Slutsatser

Modelleringen som utfördes i detta uppdrag har använt nya tekniker med tillgängliga platsdata för att karakterisera landskapsdosobjektet. Detta har resulterat i en platsbeskrivning som representerar den specifika platsen i en större utsträckning än i tidigare dosberäkningar. En vidare utveckling av dosmodellering för denna plats skulle ha nytta av en noggrannare studie av den ytnära hydrologin i området och en bättre förståelse av faktiska utsläpp av radionuklider från avfallet som deponerats i deponin. En strukturerad vägledning från SSM för ansökningar om riktad friklassning för deponering kan även vara värdefullt.

Projektinformation

Kontaktperson SSM: Karolina Stark
Referens: SSM2021-1098



Strål
säkerhets
myndigheten

Swedish Radiation Safety Authority

Authors: Shulan Xu ¹⁾, Ryk Klos ²⁾
¹⁾ Xu Environmental Consulting AB, Sweden
²⁾ Aleksandria Sciences Ltd, UK

2023:02

Investigation of risk assessment for
decommissioning waste to Fortum's
landfill at Norrtorp

Date: January 2023

Report number: 2023:02

ISSN: 2000-0456

Available at www.stralsakerhetsmyndigheten.se

Content

| | |
|--|-----------|
| 1. Introduction | 3 |
| 2. Methodology | 5 |
| 2.1 Assessment method | 5 |
| 2.2 ISAM methodology | 5 |
| 2.3 Methodology for biosphere assessment | 7 |
| 3. Site description of the Fortum landfill at Norrtorp | 8 |
| 3.1 Methodology | 8 |
| 3.2 Regional scale | 9 |
| 3.3 Site scale | 12 |
| 3.4 Dose assessment model | 18 |
| 4. Preparation of independent risk assessment | 22 |
| 4.1 Description of the assessment based on ISAM methodology | 22 |
| 4.1.1 Assessment context | 22 |
| 4.1.2 Description of the disposal system..... | 22 |
| 4.1.3 Generation of scenarios and calculation cases | 26 |
| 4.2 Formulation of models | 28 |
| 4.2.1 Descriptions of ISAM models | 30 |
| 4.2.2 Site-specific biosphere models..... | 34 |
| 4.2.3 Models for the alternative and human intrusion scenarios | 35 |
| 4.2.4 Non-human biota dose rate calculations..... | 37 |
| 5. Analysis of results | 39 |
| 5.1 Reproducing results of Kemakta's assessment | 39 |
| 5.1.1 Ranstad waste disposal case..... | 39 |
| 5.1.2 WSE waste disposal case | 41 |
| 5.1.3 Cyclife waste disposal case | 43 |
| 5.2 Independent dose risk assessment | 45 |
| 5.2.1 Main scenario | 45 |
| 5.2.2 Alternative scenarios | 55 |
| 5.2.3 Human intrusion scenarios..... | 56 |
| 5.2.4 Non-human biota | 57 |
| 5.2.5 Dose conversion factors (DCF)..... | 58 |
| 6. Discussion and conclusions | 60 |
| 7. References | 63 |
| Appendix A – Hydrology of the biosphere model | 66 |
| Appendix B – Numerical data | 68 |
| Appendix C – Dose Conversion Factors | 75 |

1. Introduction

The quantity of waste in the category of very low-level waste (VLLW) that is subject to conditional clearance applications will increase in the future as a result of, among other things, the decommissioning of a number of nuclear power reactors in Sweden. Such VLLW can contain such low levels of radioactive substances that the waste can be treated as conventional waste, thereby being exempt from regulatory consideration. However, materials with a higher content of radioactive materials can be disposed in landfill via *conditional clearance*. SSM's regulations SSMFS 2018:3 (SSM 2018) require that any such application for disposal of radioactive wastes in exceedance of the clearance levels in a conventional landfill shall contain an analysis of alternatives to the requested clearance, a description of the circumstances that justify disposal of a higher level of radioactive contamination, as well as an assessment of the radiological consequences of the disposal. According to the Radiation protection ordinance (2018:506) chap. 7 section 6, an exemption from regulation may not be granted if it can be assumed to entail an unacceptable risk to people or the environment being exposed to the harmful effects of radiation. For conditional clearance of material the EU-radiation protection directive (2013/59/Euratom), incorporated into Swedish law, states in appendix VII that a dose criteria in the order of 10 μSv in a year should be used as an acceptable level for clearance from regulatory control to account for the possibility of exposures arising from disposals or activities at other sites.

A conventional landfill that has received several rounds of waste by conditional clearance decisions from SSM is Fortum Waste Solution AB's landfill for hazardous waste at Norrortorp, Kumla. Each individual case received by the authority with a conditional clearance application has so far only been risk assessed separately before a decision. Calculated doses in risk assessment models in applications are often very low for each case. However, based on the fact that this type of waste streams may increase in the near future, there is a need for SSM to carry out an investigation with a compilation of all application cases with conditional clearance to get an overview of the entire risk picture in terms of the potential impact of the general public and the environment from this type of disposal at the landfill in question. This is so that SSM can also assess the scope from a radiation protection perspective that may exist when reviewing future applications for conditional clearance including disposal of waste at Fortum's landfill at Norrortorp. This assignment contributes to support SSM's investigation of this matter.

There are a number of objectives for this assignment. The first is to perform a radiological risk assessment of disposals of decommissioning-related waste as landfill at Fortum's Norrortorp site.

The second objective is to perform a risk assessment to evaluate the risk to human health and the environment as a result of ionizing radiation, taking into account previously deposited waste at the landfill that has been previously approved by SSM. Combined with the first objective this provides a holistic view of radiological risk for waste disposed as landfill at Norrortorp.

The third objective is to identify representative biosphere dose objects through an extensive analysis of site-specific data obtained from several national institutes such as Swedish Meteorological and Hydrological Institute (SMHI), Swedish mapping, cadastral and land registration authority (Lantmäteriet) and the Geological Survey of Sweden (SGU).

This inclusion of site-specific information allows the development of a representative biosphere dose assessment model for the site. The approach used defines a template for how to define dose assessment models using available site descriptive material.

The fourth objective is to document the results and findings in a report including recommendations to SSM.

The assessment is based on the material obtained from SSM relating to earlier assessments of activities at the site:

- Kemakta AR 2020-02
- SKB DokumentID 1579757
- Kemakta AR 2015-42
- Kemakta AR 2014-21
- Kemakta AR 2005-01
- SSM Dokumentnr: 21-1773

Chapter 2 describes the method used to perform the assessment and IAEA's ISAM methodology¹ which is recommended by SSG-23 (IAEA 2012) for use in post-closure radiological risk assessment for near-surface radioactive waste disposal facilities. In this chapter descriptions are also given of BIOMASS² methodology because this methodology is closely related to the biosphere assessment in the ISAM methodology.

Chapter 3 gives site description of Norrtorp based on collected site-specific data from national institutes such as SMHI, Lantmäteriet and SGU. Based on the analysis of the obtained site-specific data representative biosphere dose object(s) are identified.

In Chapter 4 models used in independent modelling are described. Moreover, a dynamic biosphere model, developed based on site-specific data, is described.

In Chapter 5 independent risk assessment for radioactive wastes deposited at the conventional landfill at Norrtorp is presented. Chapter 5 gives a holistic view of what the entire risk picture looks like for the general public and the environment due to wastes deposited at the landfill at Norrtorp and our recommendations to SSM for the review of applications of potential cases in the future.

Finally, Chapter 6 discusses the findings and presents conclusions.

¹ In 1997, IAEA launched a research project on Improvement of Safety Assessment Methodologies for Near Surface Disposal Facilities (ISAM). The particular objectives of the project were to provide a critical evaluation of the approaches and tools used in post-closure safety assessment for proposed and existing near-surface radioactive waste disposal facilities.

² The IAEA Biosphere Modelling and Assessment (BIOMASS) project, which ran from 1996 to 2001, developed the reference biosphere methodology, drawing on experience of its application and through development of several illustrative examples (IAEA 2003a).

2. Methodology

2.1 Assessment method

The method used in the risk assessment is a combination of document review and independent modelling, which consists of the following steps:

- Review of the various documents concerning operations and waste disposals at Norrtorp
- Modelling intended to reproduce the results of Kemakta's assessment (AR 2014-21, AR-2015-42, AR 2020-02)
- Independent modelling

Document review is performed based on the reports related to three cases of applications of conditional clearance for disposal of waste at Fortum's landfill at Norrtorp as given in Chapter 1.

Reproducing the results of Kemakta's assessment was conducted using Kemakta's models and data, however, in this case the release of radionuclides from the waste matrix is described using a so-called K_d concept model instead of the leaching model used by Kemakta. In this way insight into the working of Kemakta's assessment model has been achieved.

Independent modelling has been carried out to explore uncertainties identified in the document review. Furthermore, the recipient (also called the biosphere dose object or LDO – landscape dose object) for dose calculations has been identified using site-descriptive material obtained during this assignment. The independent radiological risk assessment is performed by following ISAM and BIOMASS methodology that are described below.

2.2 ISAM methodology

IAEA Safety Guide SSG-23 (IAEA 2012) recommends the ISAM methodology be used in the safety assessment not only for near surface disposal facilities but also for other types of disposal facilities. Thus, the ISAM methodology for radiological risk assessment is adapted for the assignment. The ISAM project primarily focused on developing a consensus on the methodological aspects of safety assessment (shown in Fig. 2-1), especially:

- i) specification of the assessment context,
- ii) description of the waste disposal system,
- iii) development and justification of scenarios,
- iv) formulation and implementation of models and
- v) analysis of results and building confidence.

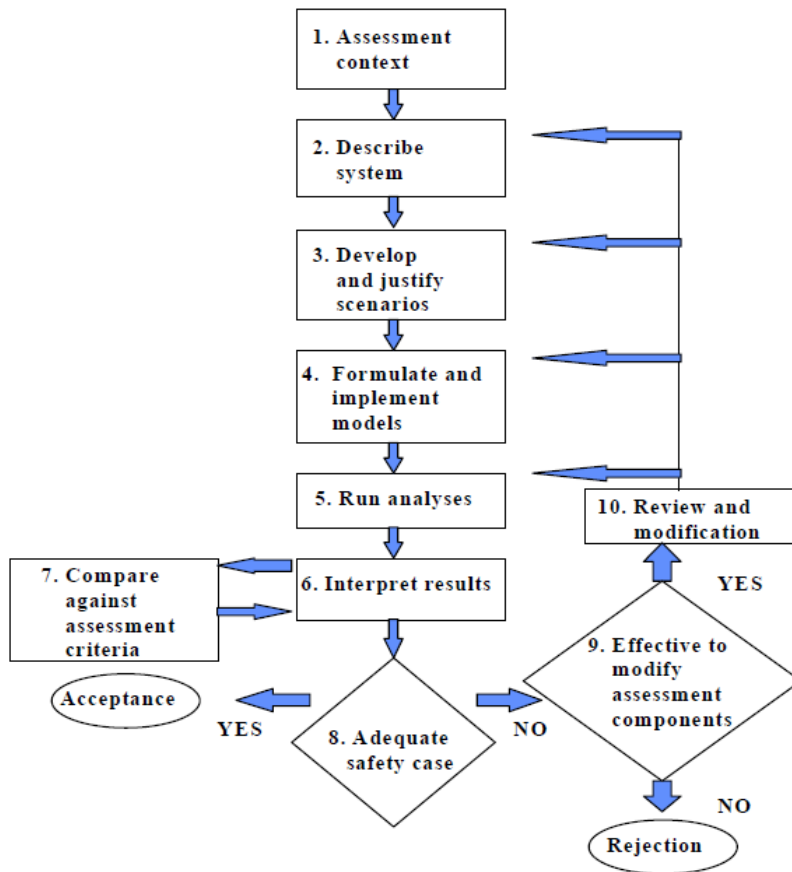


Fig. 2-1 The ISAM project methodology (IAEA 2004a).

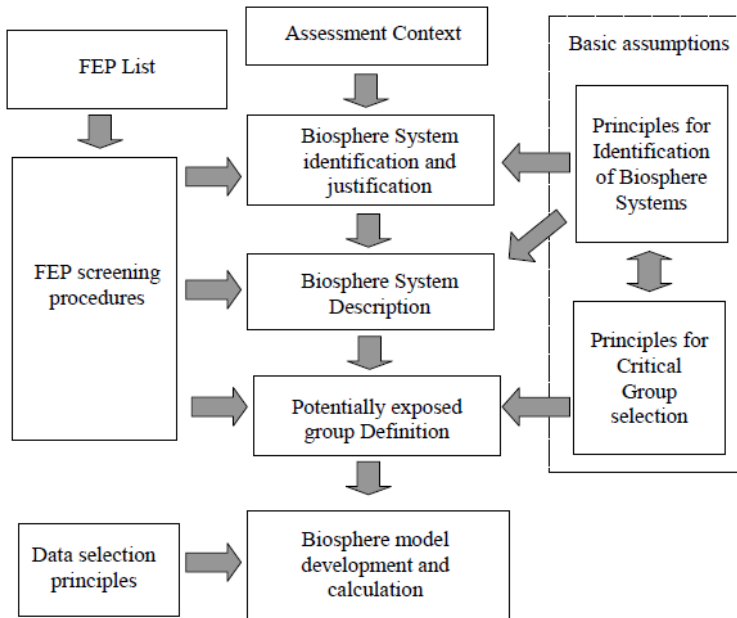


Fig. 2-2 Schematic illustration of the BIOMASS Methodology including BIOMASS supplementary guidance (after IAEA 2003a, figure A2).

The ISAM reports (IAEA 2004ab) document the assessment of several hypothetical facilities, among others the trench is similar in concept to the existing facility at Norrtorp, which simplifies the identification of scenarios and mathematical models applied here.

2.3 Methodology for biosphere assessment

The IAEA Biosphere Modelling and Assessment (BIOMASS) project, which ran from 1996 to 2001, developed the reference biosphere methodology, drawing on experience of its application and through development of several illustrative examples (IAEA 2003a). The BIOMASS Methodology is based on a staged approach in which each stage introduces further detail so that a coherent biosphere system description and corresponding conceptual, mathematical and numerical models can be constructed. The Methodology, summarised in Fig. 2-2, includes:

- A high-level approach, emphasising the importance of clarity regarding the assessment context as a foundation for identifying the biosphere(s) to be represented and subsequent model development.
- An explanation and description of steps of the methodology that could be undertaken, including detailed tables of biosphere characteristics and classification schemes.
- An updated biosphere FEP list.

Subsequent development of the methodology within IAEA MODARIA³ program is being published (IAEA, 2020) and key features of the revised methodology (e.g., Guerfi et al., 2019; Xu et al., 2022) are also applied in this assignment.

³ MODARIA (Modelling and Data for Radiological Impact Assessments) was an IAEA program in 2012 - 2019. The MODARIA program comprised seven Working Groups (WG), in which WG 6 had the objective of enhancing the BIOMASS methodology.

3. Site description of the Fortum landfill at Norrtorp

3.1 Methodology

In the mid-1990s the BIOMOVs II project determined that a set of generic *reference biosphere models* for waste disposal assessments was not practical because the local *specific* characteristics of each site would dominate uncertainties. A methodology was developed (BIOMOVs II, 1996) and further refined in the BIOMASS programme (IAEA, 2003) that allows the identification and justification of site characteristics to be systematically defined when constructing a dose assessment model. The approach has recently been updated in the IAEA's MODARIA II program (Thorne et al. 2020).

The current state-of-the-art in dose assessment modelling has been used to characterise the salient features of the Norrtorp site for the dose assessment here, in particular the use of the available datasets held by various national organisations is central to the progressive refinement of the biosphere description from regional to local to site scale and finally to the identification and justification of the structure and data of the dose assessment model itself.

For waste disposal safety assessments, the development of detailed site-descriptive databases has been promoted by SKB in Sweden (SKB 2011) and POSIVA in Finland (POSIVA 2013) and the use of such data – particularly in geographic information systems (GIS) formats – indicated how to construct dose assessment models with a high degree of site-specific information.

To characterise the model for Fortum's Norrtorp site for assessments beyond the operational and institutional control periods (after which maintenance and knowledge of the site can no longer be assumed) data have been accessed from

- Lantmäteriet – The Swedish Mapping, Cadastral and Land Registration Authority
- Swedish Meteorological and Hydrologic Institute (SMHI), and
- Swedish Geologic Survey (SGU)

Via a request from SSM, Lantmäteriet provided a detailed (1 m resolution) digital elevation model (DEM) of the region centred on the Norrtorp site (20 km from north to south and 17.5 m east to west). In addition, a high resolution orthophoto of the area was also delivered the same area, as well as numerous mappable shapefiles that delineate roads and communications. The locations of infrastructure (buildings) at the site were also useful in providing information in respect of industrial and disposal activities at the site. Landuse for the present-day was provided and the recorded locations of surface water drainage system and lakes were also included as shapefiles.

The surface drainage system is a prime mover of material in the biosphere. Net precipitation is collected in catchments and transported downstream in sub-surface flows or as accumulations in streams, drainage ditches, rivers and lakes. The SMHI website [Vattenwebb.se](http://vattenwebb.se) was the source of background material defining watersheds in the region.

The Norrortorp site has an interesting industrial history (Kemakta AR 2014-21) and has been much studied in the context of other operations at the site. The SGU online [map viewer](#) allows the user highly detailed, searchable maps that provide information on the overburden and bedrock as well as wells and aquifers. This material allowed the geological description of the site to be completed.

Altogether these three sources of information provided a high proportion of the material required to characterise the biosphere dose model for this assessment. Details from earlier assessments (Kemakta AR 2005-01; Kemakta AR 2020-02) were also incorporated into the extensive existing database and this was reviewed in a staged approach to define relevant details for the contaminant transport in the model. A final step added the representation of the behaviour of the potentially exposed groups so as to define the final form of the dose assessment model.

3.2 Regional scale

The Norrortorp facility is in the Kumla District south of the city of Örebro (Fig 3-1). The overall topographic gradients are low with several small settlements in the area around the site. There are three catchments associated with the site (Fig 3-2). These carry net precipitation northwards; #63571 to the west and #63573 to the east, with the boundary running through the site. Surface drainage combines in the smaller #63574 where it enters the *Kvismare Kanal*, then flowing to the east before reaching *Mellanfjärden*.

The catchment map is the starting point for the site description. The water divide between #63571 and #63573 is important because it reflects the natural features of the regional topography that influence drainage from the site in the presumed absence of human control in the period after institutional control has ended (300 year post-closure of the facility).

Currently there is a water treatment plant that processes infiltrating water within the site boundaries and discharges it to the west towards two large lakes in #63571. SMHI understand that this surface drainage system flows to the north, although the details of the surface drainage system in the Lantmäteriet dataset indicate that this is not a continuous *surface* drainage system to the west of the site. As a managed drainage system it is likely that a series of culverts is involved. As discussed in the following section, the DEM provides a way of estimating the *natural* drainage pattern. Comparing the existing and natural (topographic) drainage confirms the effects of human actions on the present-day landscape to the extent that some of the drainage channels actually are maintained along the local ridgelines between the assessed subcatchments.

The main drainage channel in #63573 is close to another lake that is close to the eastern site boundary. Assuming that the managed water processing within the boundary is no longer functional in the medium to long-term the shorter path length to site boundary becomes the main concern for dose assessment modelling. Details at the site scale are clearly important, such as the location of the landfill operations within the facility boundary.

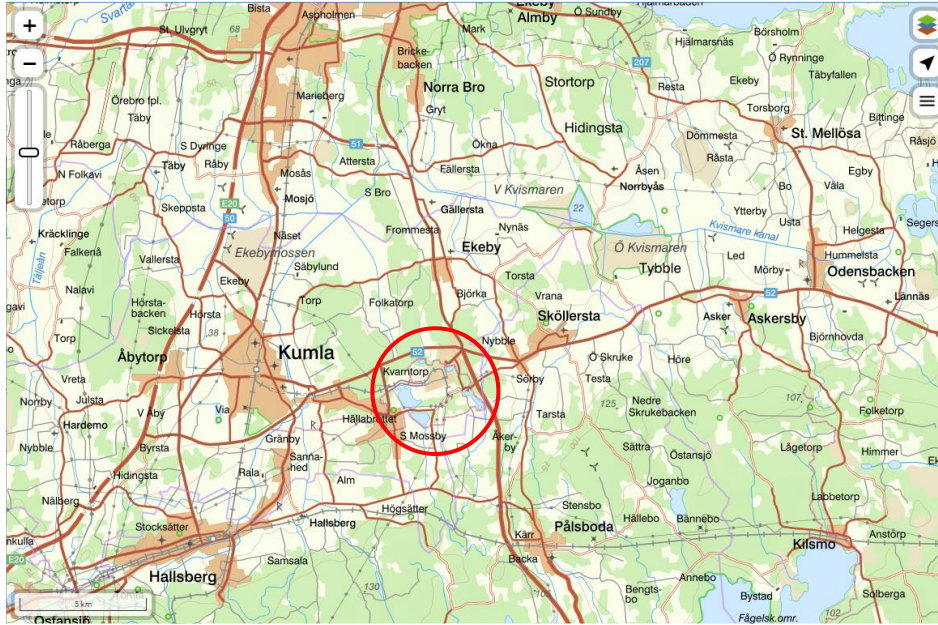


Fig. 3-1 The region around Fortum’s Norrtorp facility. The site (ringed) is in the Kumla district close to the Kvarntorp tumulus, a prominent legacy of the industrial history of Norrtorp. Accessed from <https://www.lantmateriet.se/sv/Kartor-och-geografisk-information/Kartor/>.

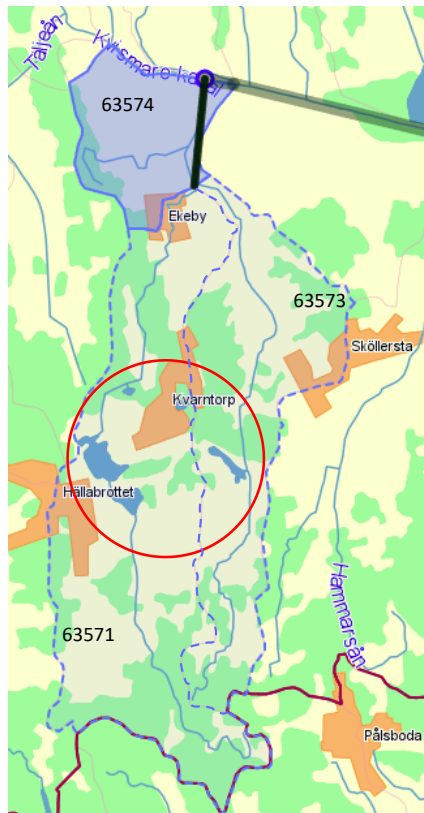


Fig. 3-2 Vattenwebb catchments #63571, #63573 and #63574. Surface drainage flows northwards the *Kvismare Kanal*. The boundary between #63571 and ~63574 runs south to north through the site. Accessed from <https://www.smhi.se/data/hydrologi/vattenwebb>.

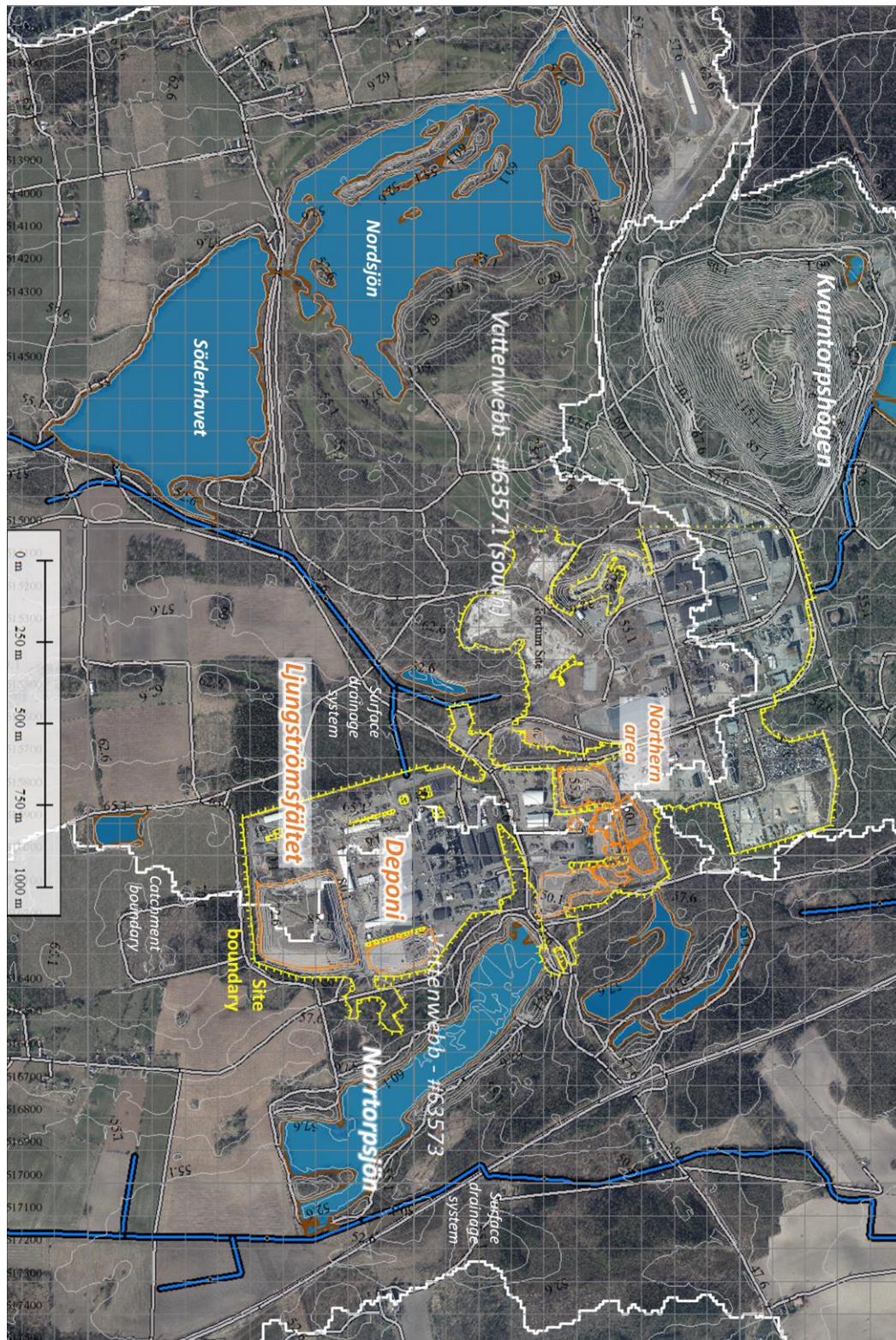


Fig. 3-3 Augmented orthophoto of the area around Fortum's Norrtorp facility. Features from the digital elevation model, DEM, are shown: catchment boundaries (white), site boundary (yellow) and potential landfill locations (orange) indicate the places of interest. 5 m contours are mapped and the water bodies (blue areas) and the surface drainage channels are by blue lines.

3.3 Site scale

The digital elevation model (DEM) combined with the orthophoto together provide a great deal of information covering the site. The map in Fig 3-3 is a composite of the Lantmäteriet digital elevation model and the orthophoto with the site boundary, surface water channels and roads, also from the Lantmäteriet dataset. The GIS mapping software [Global Mapper 22.1](#) has been used to highlight other features of the site. Closed contours in the DEM have been used to determine the positions of water bodies and the overall relief of the area is indicated by the 5 m contour lines.

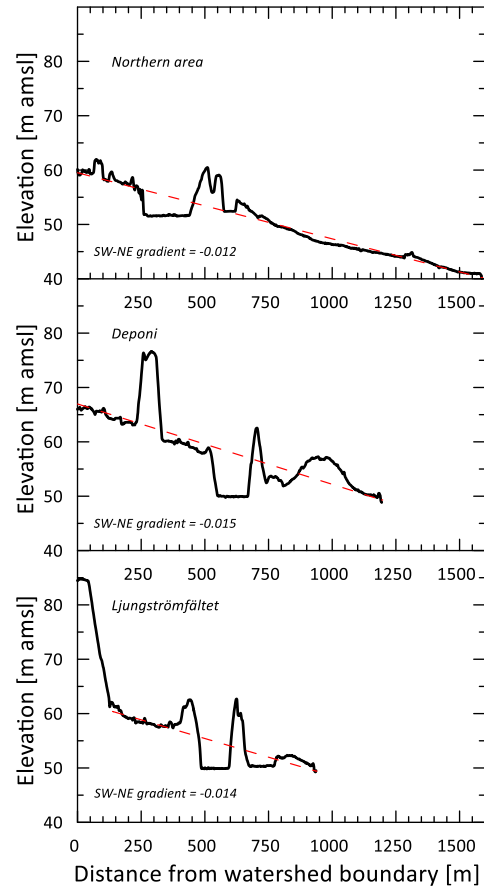
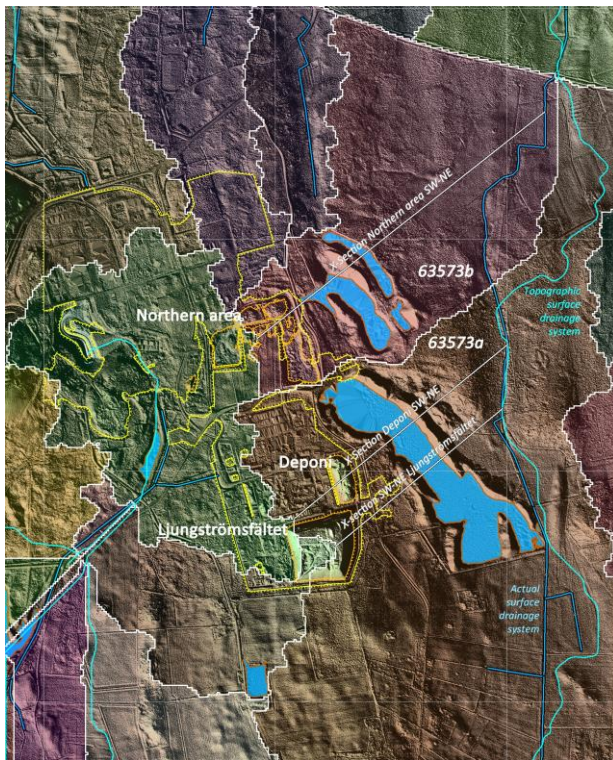
The area is fairly flat but with the *Kvarntorpshögen*, the old slag hill, dominating the landscape. This mound rises over 100 m above the surrounding landscape and is the site where ash was deposited after oil shale had been processed to extract hydrocarbons during the middle part of the 20th century (Kemakta AR 2014-21). The human impact of industrial activities is also seen in the large lakes in the map. To the west, *Nordsjön* and *Söderhavet* were excavated for mineral extraction as was *Norrtorpsjön* to the east of the site. In fact there are no natural lakes in the map (though there are some small areas of peat formation to the north of *Kvarntorpshögen*).

During this project information as to the location of landfill operations at the site were not available. From the orthophoto it is apparent that some activity was in progress at the location labelled *Ljungströmsfältet* near the southern site boundary. This area is a relatively high mound (around 25 m above the surrounds) which was identified in a dose assessment report from Kemakta (Elert *et al.* 2014). The *Deponi* mound was also cited therein. Analysis of the topography within the site boundary also indicated that there are some mounds and ongoing excavations around 500 m north of *Deponi*, also in the eastern (#63576) catchment. This focuses attention on the southeastern parts of the site, land outside the site boundary and the *Norrtorpsjön* lake. This lake – an excavated quarry for alum shale – is adjacent to the main surface drainage channel in catchment #63573 and so is expected to be involved in the drainage of the site in the post-closure period.

Global Mapper has been used to analyse the DEM so as to determine the watershed areas with the corresponding natural (ie, topographic) surface flow system. Watershed boundaries are identified as ridgelines delineating hydrologic units. There is generally a good agreement with the Vattenwebb catchments where #63573 is identified but #63571 is indicated as having northern and southern portions. The confluence of the two Vattenwebb areas #63574, which flows into the *Kvismare Kanal* is also identified but with differences in the boundary locations. Overall the areas are similar but not exact.

The watershed analysis uses an 8-point pour algorithm to determine accumulations of particles dropped onto the topographic surface so some deviation from the hydrologic boundaries described by SMHI is to be expected. The watershed analysis indicates that the natural drainage system is in the lower parts of the topography. The detail supplied by Lantmäteriet shows that the engineered and emplaced present-day drainage system differs markedly from the natural state (illustrated in Fig 3-4). This human influence is needed to provide adequate drainage for cultivation in the farmed areas and to provide suitable conditions for the construction and maintenance of housing in the landscape.

Fig 3-4 shows a refined watershed analysis of the landscape to the east of the site boundary. The *northern area* is linked to the northern subcatchment and the southern subcatchment contains both *Deponi* and *Ljungströmsfältet*. Each area has an upstream area and one or more lakes with a further area of land before the drainage channel. Conceptually,



a. Relief map of the candidate areas for the landscape dose objects with disposals considered for the northern area, Deponi and Ljungströmsfältet

b. Elevation profile in sections away from the watershed boundary

Fig. 3-4 Identification of landscape dose objects. Watersheds defined using a cell-count criterion of 10000 show a distinction between the northern and southern sub areas of catchment #63573. Areas to the east of the #63573 catchment with landfill activity are identified and the topographic gradients from the catchment boundary to the #63573 drainage channel are plotted. For reference the topographic drainage stream is shown in light blue. Its location differs from the managed drainage system in the present-day landscape.

therefore the potential dose objects have the same structure, albeit with differing data descriptions.

The watersheds indicate the prevalent direction of groundwater movement. The sections shown in Fig 3-4, drawn to cut across the lake systems towards the main drainage channel, show that the landscape in the region slopes toward the lakes with a similar gradients (0.012 to 0.015, i.e., ~1.3 m in 100 m, or 0.75°). It is therefore reasonable to consider the area immediately between the site boundary and the lakes as candidate areas for the dose assessment model. Furthermore, the transverse slopes in the area around the southeastern boundary the prevailing direction is directly toward the lake and, beyond that, the drainage stream. For this reason it is possible to delineate the boundaries for the landscape dose objects as shown in Figure 3-5.

The landscape around and south of Norrtorpsjön is cultivated at present, with mixed forest to the northern side of the road that crosses the area. The northern area outside the site boundary is similarly mixed forest. There are no signs of surface drainage streams in the two areas and the lakes. This indicates that the lakes – as excavated areas – are depressions where the aquifer is at the surface. It is reasonable to take the water level in the lakes as the level of the aquifer in the area. At the southeastern edge of the southern lake a channel is visible on the orthophoto but it is dry in the image. This is confirmed in the 1 m resolution DEM and is clearly used as an outlet of the lake to the main drainage channel at times of higher groundwater table. A number of ostensibly dry channels are also visible in the DEM relief map. These are understood to be part of the managed drainage system used by local farmers. Some of these are shown in the Lantmäteriet database but most are not.

The water surface (the lower level of the DEM in water bodies, as indicated in the flat regions of the sections in Fig 3-4b) is at around 50 m amsl (Norrtorpsjön) to 51 m amsl (Lake 1) and this is 7 m below the LDO south and 8 m below the LDO north land surfaces. The relatively tall banks of the lakes indicate that spoil was piled at the edges of the pits during the excavation.

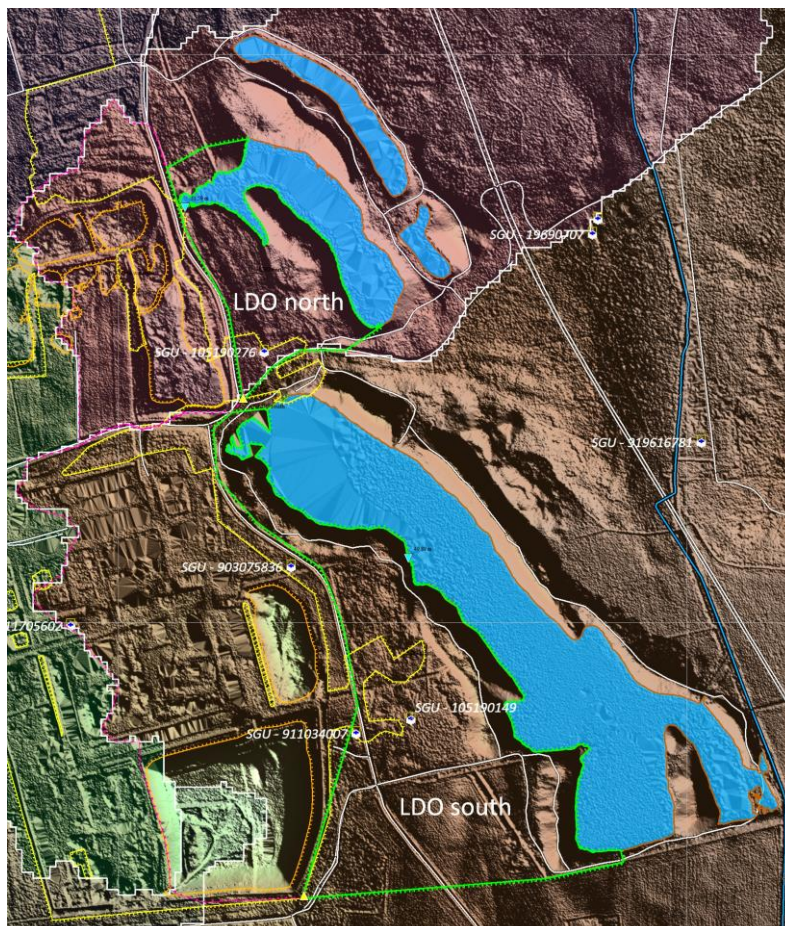
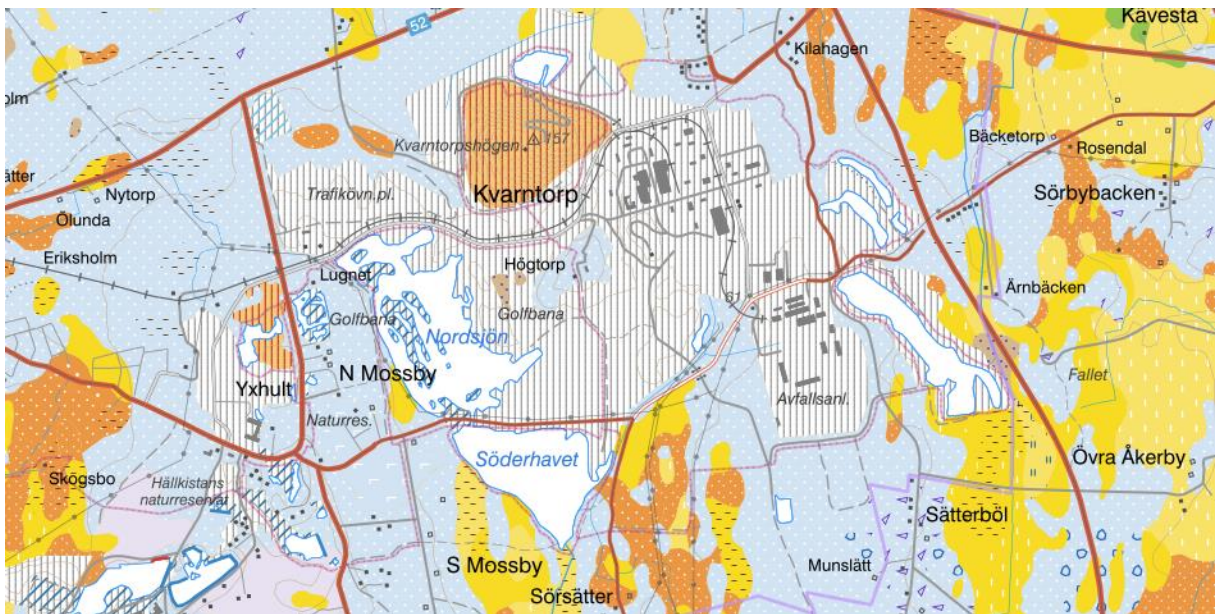
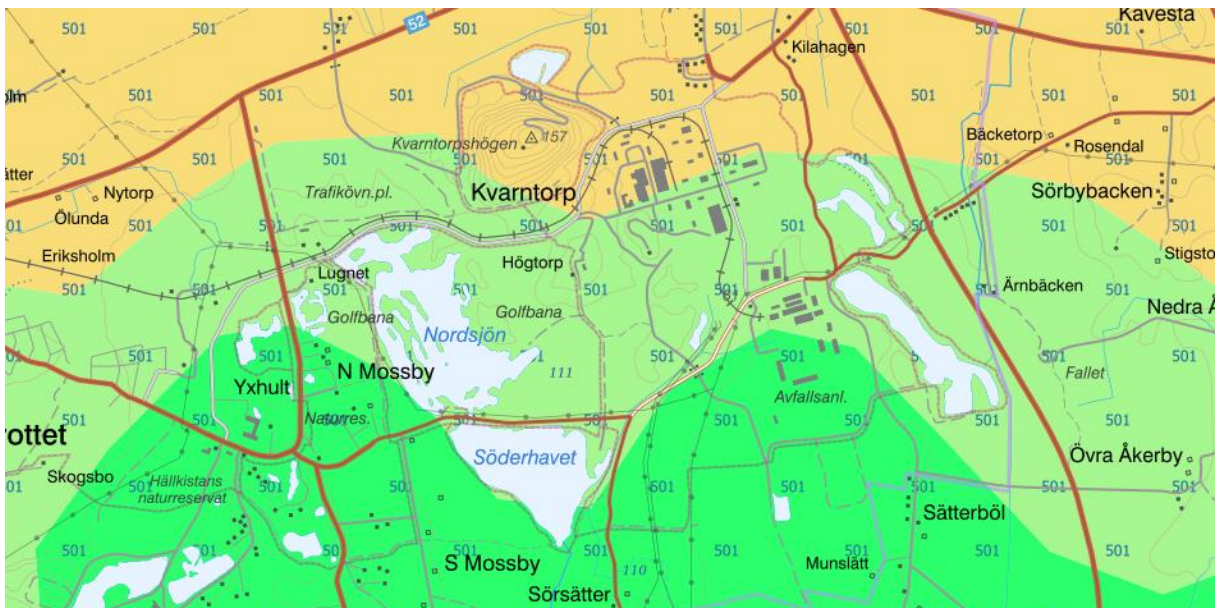


Fig 3-5 Definition of landscape dose objects (LDOs). Objects are bordered in green in each of the northern and southern watersheds. Locations of wells in the SGU database are indicated.



- a. Soil type at surface. In-fill material (*fyllning*) is the predominant type at the site (vertical stripes), surrounded by morane material (mostly sandy – light blue with white dots). Yellow denotes glacial clays and orange glacial silts and postglacial sands. There are some isolated areas of peat indicating infilled small lakes and wetlands. The material at *Kvarntorpshögen* (orange with stripes) is industrial ash from shale-oil production.



- b. Bedrock type. The northern bedrock band (yellow) is sandstone, conglomerate, siltstone and shale, pale green is bituminous shale (alum shale) and subordinate limestone and the bright green is Limestone.

Fig 3-6 Soil and bedrock types. Data from SGU map creator ([SGUs Kartvisare](https://kartvisare.sgu.se/)). Details of the maps are obtained online by clicking on the different shadings.

The conceptual understanding of the site that emerges from Fig 3-5 is of waste deposited in the higher elevations of the landscape to the east of the #63573 catchment boundary. Infiltrating rainwater will migrate through the landfill material and, in the post institutional control period, will enter the underlying groundwater with flow towards the lakes and so to the drainage channel. Details from the SGU database have been used to characterise the overburden, aquifer, groundwater and wells in the modelled area. Fig 3-6a is a map of the surface material and the bedrock is shown in Fig 3-6b. The predominant surface material in the area around the landscape dose objects is *fyllning* (in-fill) derived from the industrial activities at the site.

The SGU database for wells around the site have been accessed. These data include the total depth of the well, the depth of the water table, soil thickness as well as the soil type, local landuse and bedrock. The collected data for the area east of the #63573 boundary are shown in Table 3-1. From this a practical stratigraphy of the landscape dose objects in Fig 3-5 is as shown in Fig 3-7 for the three subareas – upper catchment, lower catchment and lake.

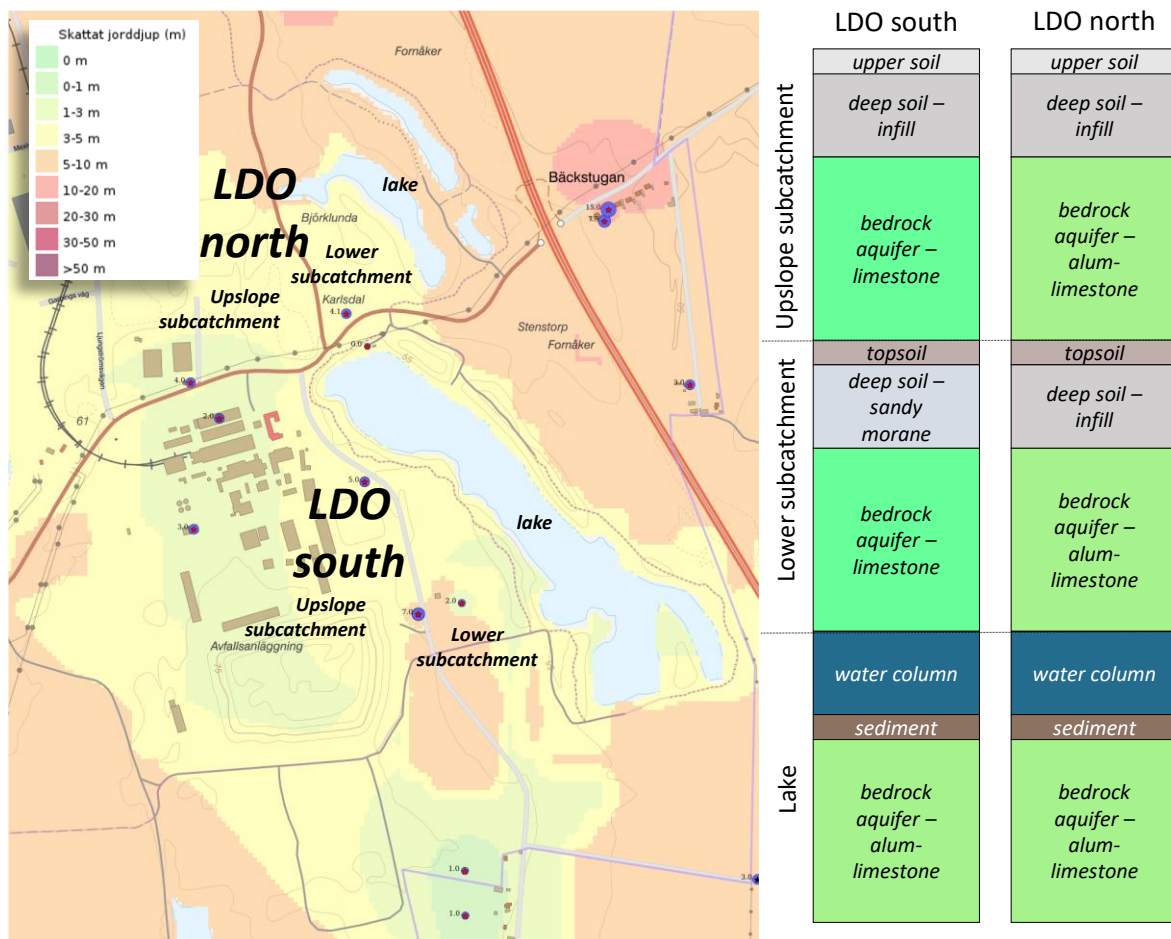


Fig 3-7 Soil depth information from the SGU online map viewer and generalised stratigraphy of areas in the northern and southern candidate landscape dose objects, based on details in Fig 3-6.

Table 3-1. Details of local maps from the SGU dataset (file: underlag_brunnar.gpkg downloaded from SGU.se 2022-01-16). Details of well use and local conditions from SGUs online Map Viewer. Wells relevant to the characterisation of the biosphere dose objects are unshaded. Bold indicates wells used to characterise the biosphere dose objects. Figure in parentheses are land surface elevation above Norrtorpsjön water level.

| Well ID | Total Depth [m] | Soil Depth [m] | Flow Rate [litre hour ⁻¹] | Waterable depth m | Land use | Soil type | Bedrock |
|-----------------|-----------------|----------------|---------------------------------------|-------------------|-------------------|------------------------------|--------------------------------|
| SGU - 19690707 | 40 | 7.5 | - | 13.6 (3) | garden | sandy morane | Mudstone, claystone, siltstone |
| SGU - 20140922 | 210 | 15 | 600 | - (3) | domestic heatpump | sandy morane | Mudstone, claystone, siltstone |
| SGU - 105100472 | 67 | 1 | 600 | 25 | domestic heatpump | sandy morane | Limestone |
| SGU - 105100484 | 39 | 12 | 4000 | 5 | farmland | sandy morane | Mudstone, claystone, siltstone |
| SGU - 105100652 | 136 | 4 | 360 | - | domestic | glacial clay | Limestone |
| SGU - 105190004 | 61.5 | 1 | 4500 | 32 | farmland | sandy morane | Limestone |
| SGU - 105190005 | 60 | 1 | 4500 | 31 | farmland | sandy morane | Slate |
| SGU - 105190006 | 67 | 1 | 4500 | 32 | farmland | sandy morane | Limestone |
| SGU - 105190007 | 60 | 1 | 4500 | 31 | farmland | sandy morane | Limestone |
| SGU - 105190008 | 60 | 1 | 4500 | 31 | farmland | sandy morane | Limestone |
| SGU - 105190149 | 57 | 2 | - | 19.3 (7) | mixed forest | sandy morane | Limestone |
| SGU - 105190264 | 9 | 9 | 3600 | 67 | farm | postglacial fine sand | Limestone |
| SGU - 105190276 | 54 | 4.1 | 2900 | 29 (7) | mixed forest | sandy morane | Slate |
| SGU - 105190325 | 88.8 | 19.6 | 1000 | 12.5 | Industry (site) | infill | Mudstone, claystone, siltstone |
| SGU - 105190462 | 52 | 4 | 5400 | 2 (11) | Industry (site) | infill | Limestone |
| SGU - 105190477 | 65 | 2 | 2400 | 22.8 | farm | sandy morane | Limestone |
| SGU - 903075836 | 27 | 5 | 900 | - (11) | mixed forest | infill | Limestone |
| SGU - 90755231 | 81 | 50 | 12000 | 10 | domestic | sandy morane | Limestone |
| SGU - 911034007 | 30 | 7 | 500 | 10 (9) | mixed forest | sandy morane | Limestone |
| SGU - 911034015 | 37 | 7 | 30 | 10 | mixed forest | sandy morane | Limestone |
| SGU - 911034023 | 30 | 7 | 30 | 10 | mixed forest | sandy morane | Limestone |
| SGU - 911705602 | 9 | 3 | - | - | Industry (site) | infill | Limestone |
| SGU - 913534742 | 25 | 2 | 0 | 9 (12) | Industry (site) | infill | Limestone |
| SGU - 914073056 | 66 | 2 | 3600 | - | farm | sandy morane | Limestone |
| SGU - 916516801 | 190 | 6 | 15000 | 4 | domestic heatpump | sandy morane | Mudstone, claystone, siltstone |
| SGU - 919616781 | 50 | 3 | 5000 | 6 (0.75) | farm | Clay (glacial/ post glacial) | Slate |
| SGU - 920602776 | 202 | 22 | 500 | - | domestic heatpump | sandy morane | Mudstone, claystone, siltstone |

3.4 Dose assessment model

The previous section has compiled relevant information describing the parts of the Norrtorp site that are relevant to dose assessment modelling. This detail provides the basis for defining the dose assessment model specific to the site (Table 3-2). There are a number of practical assumptions that are necessary to turn the site description into a model for dose assessment. However, not least of which are the interpretation of the activities of the potentially exposed population group that is assumed to inhabit the contaminated area.

Around the site much of the area is given over to cultivation, with arable land being much in evidence. This level of agribusiness is not appropriate for dose assessment purposes, where the traditional model for population behaviour is the *subsistence farmer*. Water resources are available because the aquifers are close to the surface and, as the data in the SGU online dataset shows (Table 3-1) the flow rates are suitable for cultivation. A variant on the subsistence farmer exposure group is adopted here. Data from Löfgren (2010) suggests that an area of 2×10^4 m² is sufficient to supply the dietary requirements of a group of four adults, including cereals, root and green vegetables as well as livestock.

Currently, crop cultivation is seen in the orthophoto close to the southeastern corner of the site though, at present, there is an area of natural forest between the site boundary and

Table 3-2 Basic numerical data for the components of the biosphere dose objects at Norrtorp.

| | LDO north | Lake 1 | material | BE | lower | upper |
|----------------------|-----------|-----------------|------------------|---------|---------|---------|
| upslope subcatchment | area | | | 1.4E+05 | 4.6E+04 | 1.4E+05 |
| | thickness | upper soil | weathered infill | 0.3 | 0.1 | 0.5 |
| | | deep soil | infill | 3 | 1 | 5 |
| | | bedrock aquifer | alum-limestone | 50 | 30 | 70 |
| lower subcatchment | area | | | 7.0E+04 | 2E+04 | 7.0E+04 |
| | thickness | cultivated soil | cultivated soil | 0.3 | 0.1 | 0.5 |
| | | deep soil | infill | 5 | 1 | 10 |
| | | bedrock aquifer | alum-limestone | 50 | 30 | 70 |
| Lake | area | | | 4.0E+04 | 1.0E+00 | 1.7E+04 |
| | thickness | water column | water | 25 | 20 | 30 |
| | | sediment | alum-limestone | 0.3 | 0.1 | 0.5 |
| | | bedrock aquifer | alum-limestone | 10 | 1 | 50 |
| | | | | | | |
| | LDO south | Norrtorpssjön | material | BE | lower | upper |
| upslope subcatchment | area | | | 3.1E+05 | 1.0E+05 | 3.1E+05 |
| | thickness | upper soil | weathered infill | 0.3 | 0.1 | 0.5 |
| | | deep soil | infill | 3 | 1 | 5 |
| | | bedrock aquifer | limestone | 50 | 30 | 70 |
| lower subcatchment | area | | | 2.2E+05 | 1.0E+05 | 2.2E+05 |
| | thickness | cultivated soil | cultivated soil | 0.3 | 0.1 | 0.5 |
| | | deep soil | sandy morane | 5 | 1 | 10 |
| | | bedrock aquifer | limestone | 50 | 30 | 70 |
| Lake | area | | | 1.8E+05 | 1.8E+05 | 1.8E+05 |
| | thickness | water column | water | 25 | 20 | 30 |
| | | sediment | alum-limestone | 0.3 | 0.1 | 0.5 |
| | | bedrock aquifer | alum-limestone | 10 | 1 | 50 |
| | | | | | | |

Norrtröpsjön. This relatively flat area of land could readily be cleared and used for cultivation by the 4-person group advocated here. This is the area considered for the location of the farm. It is directly downstream from the *Ljungströmsfältet* mound with a short path length to the location of the well. Similar considerations apply to the *Deponi* disposal mound and also to the area beyond the site boundary in the northern area.

The dose assessment model is an abstraction of reality but based on the site-specific information described above. A conceptual sketch of the organisation of the model is shown in Fig 3-8. As well as the areas identified in Table 3-2, the size and location of the cultivated area within the lower subcatchment must be defined because this determines the dilution in the local aquifer (well) that is the source of the domestic and agricultural water supplies.

Water balance for the LDO suggests that all the water collected within the boundaries flows to the lake. However, the size of the disposal area is less than that of the whole upstream catchment and the cultivated area is not necessarily the same as the area of the lower subcatchment. As shown the area of contaminated aquifer affected by leaching from the disposal area is taken to be delineated by the size of the disposal mound and the cultivated area is assumed to be in a direct line in the direction of the aquifer flow. In the context of the *Deponi* and *Ljungströmsfältet* disposal areas, the configuration is shown in Fig 3-9. For *Deponi*, the location of the cultivated area is constrained but for the *Ljungströmsfältet* disposal there is a small range in the locations to be considered. The numerical data for the two options are listed in Table 3-3.

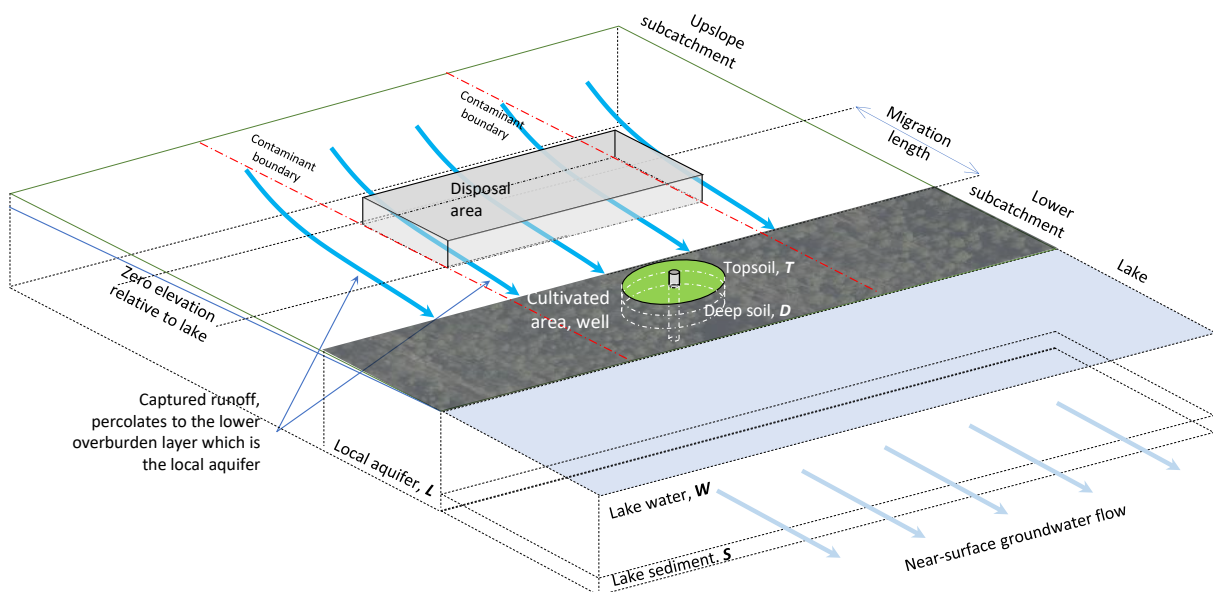


Fig 3-8 Location of cultivated area in the context of the upslope, and lower subcatchments. Near surface drainage is directed towards the lake. The contaminant plume in the aquifer downstream from the disposal location spreads as it migrates. The contaminant boundary represents a conservative low-dilution boundary condition. The high-dilution boundary conditions assumes contaminant mixing in the full area of the lower catchment.

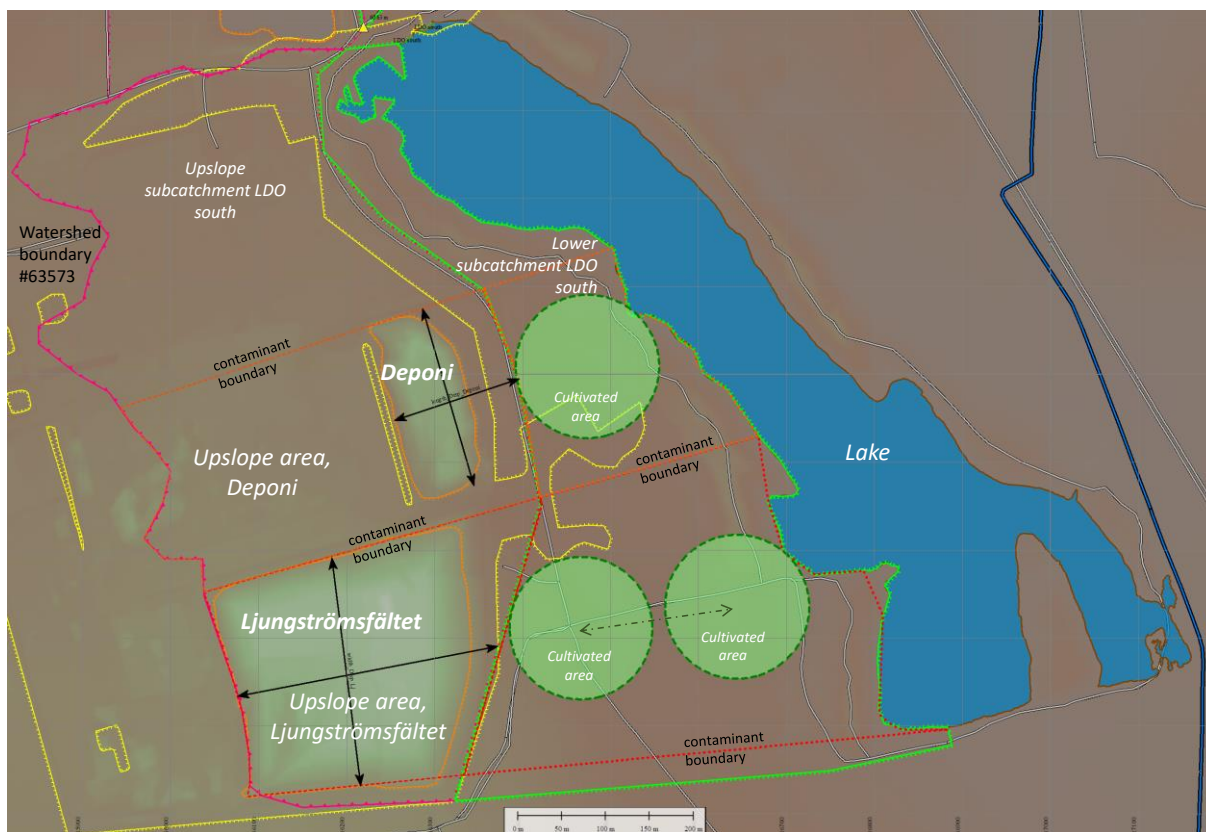


Fig 3-9 Cultivated areas in the dose assessment model of LDO south. A well is the assumed source of domestic and agricultural water, at the centre of the areas.

Table 3-3 Biosphere compartment dimensions.

| | Area m ² | minimum dilution | maximum dilution | extreme low dilution |
|-------------------|--------------------------|------------------|---------------------|----------------------|
| Ljungströmsfältet | upslope subcatchment | 1.47E+05 | 1.53E+05 | 20E+04 |
| | lower subcatchment | 1.39E+05 | (not used in model) | |
| | geosphere path length, m | 250 | 500 | 250 |
| Deponi | upslope subcatchment | 1.00E+05 | 1.69E+05 | 20E+04 |
| | lower subcatchment | 4.79E+04 | (not used in model) | |
| | geosphere path length, m | 100 | 300 | 150 |
| | Lake | 1.80E+05 | | |
| | Cultivated area | 20E+04 | | |
| compartment | | depth, m | | |
| | Topsoil, T | 3.00E-01 | | |
| | Deep soil, D | 5.00E-01 | | |
| | Local aquifer, L | 2.50E+01 | | |
| | Lake Water, W | 2.50E+01 | | |
| | Lake sediment, S | 5.00E-01 | | |

Dilution in the well compartment (the *local* aquifer) is a key determinant of the dose in the biosphere so there is scope for different assumptions concerning the volumetric flow of water entering the well. These denotes as

- Maximum dilution – where the full area in the upslope subcatchment to the boundary of the cultivated area is used for the water flow in the biosphere model aquifer
- Minimum dilution – the area is only the area of the disposal mound
- Extreme minimum dilution – the flow in the well is assumed to be the same as the irrigation demand so that water is abstracted from the well and returned to the well. This extreme case is useful as a limiting dilution.

These data, being derived from site-specific considerations are also used to define the ranges in the probabilistic modelling discussed in Section 4.3.

4. Preparation of independent risk assessment

4.1 Description of the assessment based on ISAM methodology

4.1.1 Assessment context

The objective of this radiological risk assessment is to provide a basis for supporting SSM's investigation with a holistic view of all cases of applications for conditional clearance for landfill disposal at Norrtorp. The assessment is not only based on the Kemakta's site description but includes the development of a site-specific biosphere model for the landfill site. The assessment endpoints are annual effective doses to the assumed human inhabitants of the selected biosphere locations and environmental concentrations used to assess the potential radiological impact on non-human biota.

Only post-closure safety is assessed, operational safety case is not considered. An institutional control period of 300 years is assumed. No time cut-off for calculations is assumed and the peak dose for each radionuclide is evaluated irrespective of when it occurs.

4.1.2 Description of the disposal system

Kemakta AR 2014-12 states

The landfill for hazardous waste is located in the southeastern part of Sakab's area in Norrtorp. In 2011, Sakab received permission to expand the landfill. When the landfill is filled, the total volume of waste in the landfill will be just over 2,000,000 m³, which corresponds to approximately 3,000,000 tonnes of waste. The final height of the landfill is estimated to be about 30 m. The landfill is located on a silty sandy moraine. Under the landfill there is a bottom seal and after the landfill is completed, coverage will be carried out so that the landfill more than meets the requirements for a landfill for hazardous waste, which means that the leachate formation must be less than 5 l/m², year. According to the dimensioning for the landfill in question, the infiltration, even with the conservative assumption that the HDPE membrane in the surface cover has broken down, will be 0.8 l/m², year (VBB Viak 2001).

and

The area of the entire landfill for hazardous waste is 160,000 m².

Descriptions of disposal systems for three cases mentioned above are almost identical in Kemakta's documents (Kemakta AR 2014-21, AR 2015-42 and AR 2020-02) except the operator of the landfill for hazardous waste, which was changed from Sakab to Ekokem and finally Fortum Waste Solutions AB and the total volume of waste in the landfill is increased from 2×10^6 m³ to 4×10^6 m³.

The case for Ranstad waste (Kemakta AR 2014-21)

The amount of waste from Ranstad has been estimated to be approximately one per mil of the total amount of waste in the landfill. Because the waste is not emplaced, waste from Ranstad can be assumed to be anywhere within a relatively large area. The calculations assume that waste from Ranstad can occupy 1% of the landfill area. The surface has been assumed to be largely square with a length in the flow direction of 40 m. The total amount of waste in the landfill is 2.8×10^6 tonnes.

The case for Westinghouse Electric Sweden AB (WSE) waste (Kemakta AR 2015-42)

The area of the entire landfill for hazardous waste is 160,000 m². The landfill is planned to be operational in 15 years. The total amount of waste in the landfill is about 3 million tons. The amount of waste from WSE has been estimated to be less than one per mil of the total amount of waste in the landfill. As the waste is not emplaced in specific locations, waste from the WSE can end up within a relatively large area. In the calculations. It has been assumed that WSE waste is present within 1% of the landfill area. The surface has been assumed to be largely square with a length in the flow direction of 40 m.

The case for Cyclife waste (Kemakta AR 2020-02)

No corresponding description of the Cyclife waste in the landfill is currently available, However, the parameter values used in radiological assessment for the landfill with Cyclife waste given in Kemakta AR 2020-02 are almost identical to the values for the cases of Ranstad and WSE (see Table 4-1).

In Kemakta AR 2014-21 a derivation of the transport time for the leachate is given. A sketch of definition of transport times is shown in Fig. 4-1, in which transport times regarding to the transport through the bottom seal, the vertical transport to the groundwater surface and the horizontal transport with the groundwater to a recipient such as a well.

Table 4-1 Hydrological parameters for Fortum Waste Solution AB (FWS) at the Norrtorp site, taken from Kemakta AR 2020-02

| Landfill Parameter | Value | Unit |
|--|-------------------|--------------------------------|
| Landfill area in which Cyclife waste is deposited | 1600* | m ² |
| Length of landfill in the direction of groundwater flow | 40 | m |
| Leachate formation after closure | 5 | l/m ² /a |
| Transport time for leachate between the landfill and well | 200 | a |
| Distance to the well | 500 | m |
| Hydraulic gradient | 0.003 | m/m |
| Aquifer thickness | 10 | m |
| Net infiltration in the area downstream of the landfill | 300 | l/m ² /a |
| Bulk density of the geological barrier | 1700 | kg/m ³ |
| Porosity of the geological barrier | 0.3 | m ³ /m ³ |
| Hydraulic conductivity in the aquifer | $5 \cdot 10^{-6}$ | m/s |
| Dimensionless number for the relationship advection/dispersion (Peclet) | 10 | |
| Width of the landfill perpendicular to the direction of groundwater flow | 40 | m |
| Increase in the width of the plume in the mixing zone | 57.1 | m |
| Thickness of the mixing zone | 10 | m |
| Dilution in the well | 1914 | |

Table 4-2 Kemakta's calculation of transport time from landfill for hazardous waste at SA-KAB to recipient (after Kemakta AR 2014-21).

| | Value | Unit |
|-----------------------------|---------------------|-------------|
| Vertical transport | | |
| Total thickness | 10.5 | m |
| Efficient hydraulic cond. | $22 \cdot 10^{-9}$ | m/s |
| Effective porosity | 0.098 | - |
| Gradient | 1 | m/m |
| Vertical transport time | 161 | year |
| Horizontal transport | | |
| Length | 500 | m |
| Efficient hydraulic cond. | $5.0 \cdot 10^{-6}$ | m/s |
| Effective porosity | 0.1 | - |
| Gradient | 0.003 | m/m |
| Horizontal transport time | 106 | year |
| Total transport time | 267 | year |

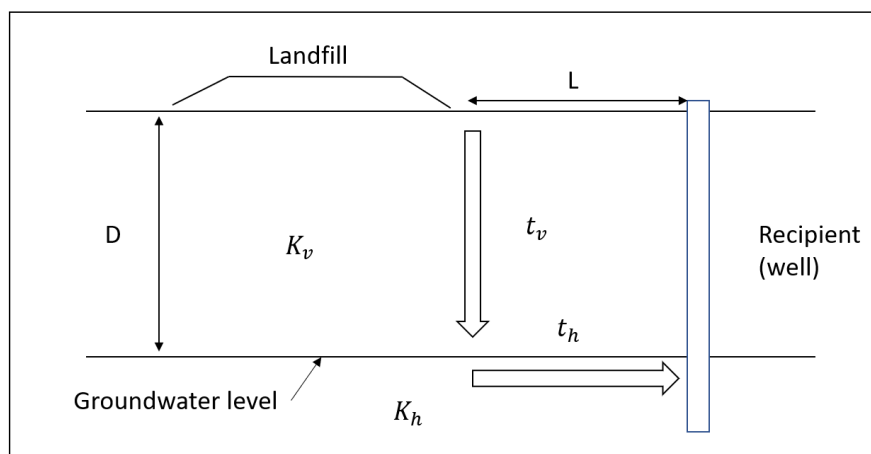


Fig. 4-1 Conceptual sketch for calculation of transport time from landfill (Kemakta AR 2014-21).

Table 4-2 shows Kemakta's results for the vertical and the horizontal transport times. The calculations indicate that the total transport time exceeds the 200 years assumed in the dose calculations.

On behalf of the Swedish Geological Survey (SGU) Kemakta Konsult AB carried out an investigation of groundwater conditions in the bedrock in Kvarntorp in Kumla municipality (Kemakta AR 2005-01). Within the investigation area, *Ljungströmsfältet* is the area where oil was extracted *in situ* from the kerogen-rich alum shale using the Ljungström method from the early 1940s into the 1950s. The method involved using electric heating elements drilled into the alum shale to gasify volatile hydrocarbons. In separate holes, the gases were collected and piped to a condensing plant. The depth of the boreholes varied from 18-20 m in the northern part of the field to 30-35 m in the southern part depending on the slope of the slate rock to the south. Due to the extensive drilling and heating to

Table 4-3 Calibrated parameter values for numerical groundwater modelling

| Layer | Geological unit | K_h (m/s) | K_z (m/s) |
|---------|----------------------------------|---------------------|---------------------|
| 1 – 4 | Top layer | $5 \cdot 10^{-6}$ | $5 \cdot 10^{-6}$ |
| 5 – 8 | Alum shale | $7.5 \cdot 10^{-7}$ | $1.5 \cdot 10^{-7}$ |
| | Ljungström field | $1 \cdot 10^{-5}$ | $2 \cdot 10^{-6}$ |
| | Top layer | $5 \cdot 10^{-6}$ | $5 \cdot 10^{-6}$ |
| | Superficial slate clay | $1 \cdot 10^{-8}$ | $1.1 \cdot 10^{-9}$ |
| 9 – 12 | Slate clay | $1 \cdot 10^{-9}$ | $1 \cdot 10^{-10}$ |
| | Superficial slate clay | $1 \cdot 10^{-8}$ | $1 \cdot 10^{-9}$ |
| 13 | Sandstone glauconite phosphorite | $1 \cdot 10^{-8}$ | $1 \cdot 10^{-9}$ |
| 14 – 16 | Sandstone Lingulide | $1 \cdot 10^{-6}$ | $1 \cdot 10^{-7}$ |
| 17 – 18 | Sandstone Wickwiza | $5 \cdot 10^{-9}$ | $1 \cdot 10^{-9}$ |
| 19 – 20 | Akvifer | $1 \cdot 10^{-5}$ | $1 \cdot 10^{-5}$ |
| 5 - 20 | Crystalline bedrock | $1 \cdot 10^{-8}$ | $1 \cdot 10^{-8}$ |

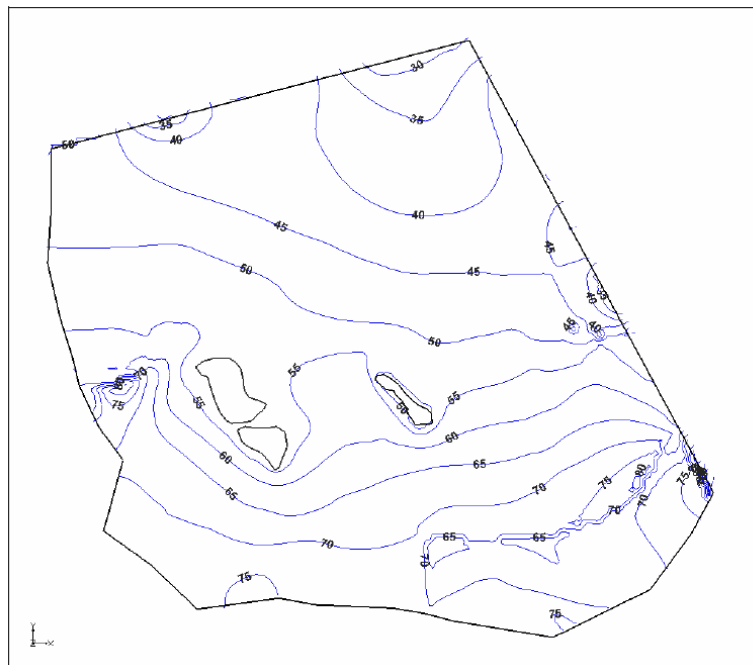


Fig. 4-2 Overview of calculated groundwater pressures in the alum shale for the current situation shown with 5 m equidistance (After Kemakta AR 2005-01).

which the alum shale was subjected, the hydraulic permeability has increased significantly in relation to the surrounding alum shale (Gustafson, 1978). Large parts of the land above *Ljungströmsfältet* are currently used for after-treatment and disposal of waste within Sydkraft SAKAB AB's operations, i.e., the current Fortum Waste Solutions AB.

Hydrogeological modelling was performed, based on a developed conceptual model, new data from rock boreholes and previous investigations, the geometry of the numerical model is defined as follows. The model consists of about 150,000 elements distributed

over 20 layers. The cell size is 100 x 100 meters (1 ha). Table 4-2 shows calibrated parameters used for the simulations performed. The modelling results show a drainage of the alum shale reservoir towards Norrtorpsjön (see Fig. 4-2).

As can be seen the hydraulic conductivity of top layer (quaternary deposits and limestone formation) is $5 \cdot 10^{-6}$ m/s (Table 4-3) and the hydraulic gradient is about $5\text{m}/100\text{m} = 0.05$, using a pessimistic assumption of a distance of 100 m based on Fig. 4-3. It is not clear how the values used by Kemakta in the assessments were derived, for example the hydraulic conductivity as $22 \cdot 10^{-9}$ m/s for the vertical transport and the gradient as 0.003 for the horizontal transport. Uncertainties of these parameter values is part of the analysis in our independent modelling assessment.

Surprisingly, the earlier reports did not specify the spatial locations where the landfill operations take place. In the assessment here it is assumed that the wastes are either deposited at the location of *Ljungströmsfältet* or *Deponi*, as discussed in Chapter 3.

4.1.3 Generation of scenarios and calculation cases

Generally, a scenario can be considered as a hypothetical sequence of processes and events leading to human exposure and is one of a set devised for the purposes of illustrating the range of future behaviours, for the purposes of evaluating a safety assessment. Scenarios are intended to portray alternative future states of the system. Scenarios can be classified according to the IAEA (2004a, 2011a, 2012, 2014):

- The base scenario - also called the ‘reference scenario’, ‘expected evolution’, ‘normal evolution’ or ‘undisturbed performance’
- Alternative scenarios - scenarios that may deviate the reference evolution for the long-term safety of the disposal facility or rare event scenario
- Human intrusion scenarios - that carried out on the basis of ‘stylized’ scenarios, which have been agreed with the regulatory body and meet the criteria set out by the regulator
- *What-if scenarios* – often intended to illustrate the specific properties of one or more of the natural or engineered barriers

In the context of radioactive waste disposal, scenario formulation is usually divided into so called ‘top down’ and ‘bottom-up’ approaches (e.g. NEA 2012). The bottom-up approach is based on forming a comprehensive list of relevant features, events and processes (FEPs). Then the interactions between the FEPs and key factors are identified and irrelevant FEPs are screened out from the process. The remaining FEPs are combined to form scenarios. In the top-down approach, the most safety relevant safety functions are first identified and then a combination of FEPs that can jeopardise their performance are identified.

The ISAM approach is mainly a bottom-up approach. The ISAM FEP list consisting of high level FEPs that could influence the behaviour of a near surface disposal system is considered to be a useful tool when generating scenarios and comparing FEPs lists for specific safety case. It is important to use a systematic approach for scenario development and justification that clearly identifies and documents the underlying assumptions. This helps to make the scenario generation process transparent and facilitates its review. In this

way, the ISAM approach provides an assurance that the assessment has effectively addressed all the potentially relevant FEPs and the interactions between them and to produce an appropriate range of scenarios. The systematic approach also provides the setting for demonstrating how uncertainties associated with the future evolution of the disposal system have been addressed and assimilated into the safety case. A formal approach to developing a set of generic post-closure scenarios for near-surface disposal facilities has been developed (shown in Fig. 4-3). We adopt the generic scenarios developed in ISAM, which helps us relatively easy to generate scenarios for a safety assessment of a landfill by combining with specific site information.

Based on FEPs screening general scenarios are divided into three groups: undisturbed performance, naturally disturbed performance and inadvertent intrusion. All these cases should in general be considered for both on-site and off-site human residence. Combining these scenarios with required FEPs produces a list of general scenarios as shown in Fig. 4-3. This greatly simplifies the procedure of generation of scenarios in this assignment, i.e., combining site specific conditions we are able to select scenarios for the assessment of this risk assessment. Calculation cases included in the scenario are defined to assess uncertainties. Descriptions of selection of scenarios and calculation cases are given below. In this case we have not assessed *What-if* cases.

Base scenario

The base scenario (ISAM SCE1, also called *reference evolution*) is based on the probable evolution of the system in respect of *external* conditions combined with realistic or, where justified, pessimistic assumptions with respect to *internal* conditions. According to the description of Kemakta AR 2014-21 the engineered barriers for the landfill are the bottom seal (bentonite) and the cover. It is assumed that climate remains as present-day conditions, thus, temporal evolution of the system is expected for the safety-related features. It is assumed that the engineered functions, the bottom seal and the cover, are successively broken down after the institutional control period i.e., even if the bottom of the bentonite remains intact the cover will be degraded. Infiltrating water will flow out from the edge of the bottom and migrate downwards to the local water table.

As described in Chapter 3 from the disposition of cultivated land in the region and the low topographic gradients it may be assumed that cultivation could be reasonably expected to occur anywhere adjacent to the site boundary. The identified biosphere object is an area that is used for cultivation of crops located in the southeast corner of the site between the present-day site boundary and *Norrtorpsjön*.

Alternative scenarios

Scenarios that may deviate from the reference evolution for the long-term safety of the disposal facility are selected as alternative scenarios. Because the main safety function for the existing facility is the bottom seal and the cover, the potential failure of the cover (top liner) of the landfill, could lead to a greater inflow of water to the waste than can be carried downwards through the bottom seal/liner. It is assumed that the resulting contaminated soil beside the landfill is used to cultivate vegetables. Hence, the two alternative scenarios here are also known as a *Bathtubbing* scenario and *Garden* scenario.

Human intrusion scenarios

Two human intrusion scenarios are selected based on Fig. 4-3 to assess the disturbed evolution of the disposal facility and potential harm to humans directly excavating the waste after institutional control: SCE6 – on-site residence and SCE7 –road construction (SCE7).

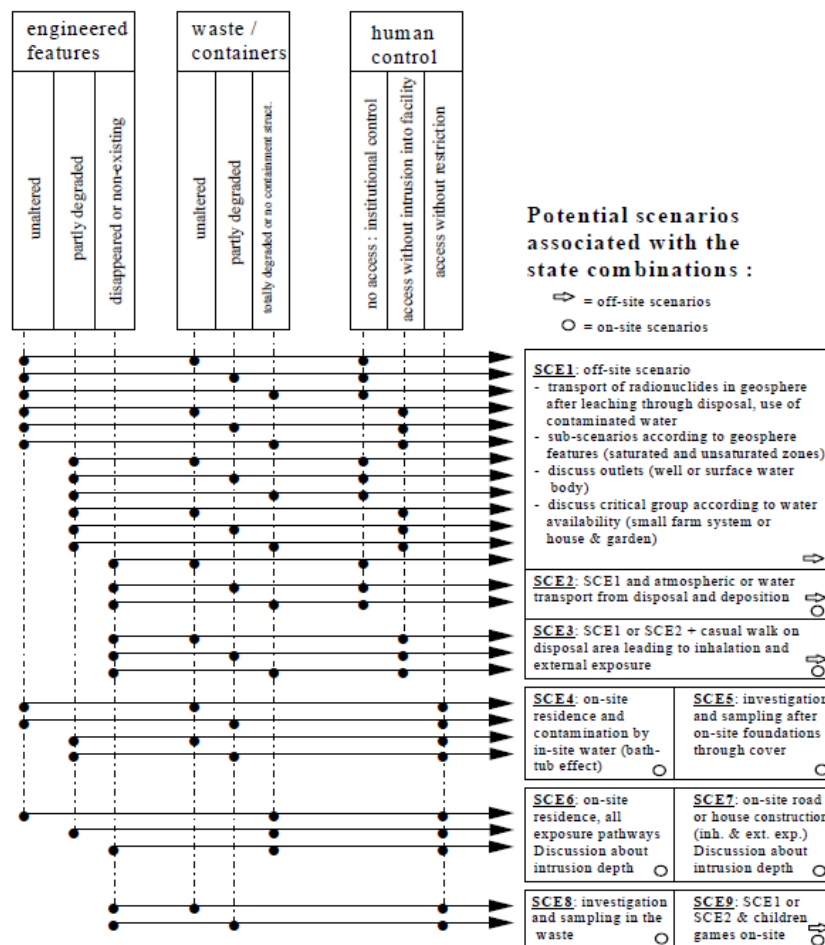


Fig. 4-3 Generation of a Set of Scenarios (SCE) According to Various States of the Disposal and Human Behaviour Components (IAEA 2004b).

4.2 Formulation of models

The test cases in ISAM (IAEA 2004b) uses an interaction matrix to express the conceptual model for the site. The interaction matrix is a convenient and compact technique for developing models because it promotes the screening of interactions for specific applications. Furthermore, Klos and Thorne (2020) have illustrated how interaction matrices can be used to define compartmental mathematical models and we adopt this method here.

Fig. 4-4 is an interaction matrix based on the original ISAM (IAEA 2004a) generic description but processed to include four levels of screening, including those in the IAEA (2004b) documentation. Aggregation and nesting has been used to define the matrix for development into mathematical models for the assessment. We identify the landfill and geosphere submodel as distinct from the biosphere submodel. As shown, many interactions are ruled out by generic considerations and other from the description in the ISAM example documentation. Site specific considerations are used to rule out the interactions as a final stage before translation into mathematical form. Thus, we assume no interaction (in terms of radionuclides transport) from the aquifer back to the unsaturated

| vault and geosphere submodel | | | biosphere sub-model | | | | | | | | | | |
|------------------------------|-------------------|----------------------------|----------------------------|-----------------|----------------------|---------------------|-------------------|-------------------|---------------------------|---------------------------|--------------------|-------------------------------|----------------------------|
| | | | GBI | soil submodel | | | | exposure submodel | | | | | |
| vault and geosphere submodel | EBS | source term from vaults | | | | | | | | | | | |
| | | unsat zone | infiltration & percolation | | | | | | | | | | |
| | | limited - (depth of soils) | geosphere aquifer | discharge | | | | | | | | | |
| biosphere sub-model | GBI | | no connection | conservative bc | local aquifer (well) | no connection | irrigation | no connection | groundwater flow | irrigation - interception | drinking water | drinking water | outflow to drainage system |
| | | | | | drainage | lower soil (unsat.) | capillary rise | no connection | no connection | no connection | no connection | no connection | no connection |
| | soil submodel | | | | no direct connection | drainage | rooting zone soil | no connection | no connection | | | | |
| | | | | | no flow | no connection | no connection | lake water | diffusion | | | | |
| | | | | | no flow | no connection | no connection | diffusion | lake sediment | root uptake | direct soil intake | irradiation & dust inhalation | conservative bc |
| | exposure submodel | | | | no access | | | | weathering (not modelled) | plants | ingestion | ingestion | conservative bc |
| | | | no access | no access | no access | | | | excretion (not modelled) | | animals | ingestion | conservative bc |
| | | | | | extraction only | | | | no transfer | | | humans | conservative bc |
| | | | | | | | | | | | | | sink |

| | | | | | |
|---------------------|-------------------------|-------------|---|--------------------------|---------------------------|
| dynamic compartment | equilibrium compartment | active FEPS | Ruled out by site specific considerations | ruled out in ISAM Vol. 2 | Ruled out by generic ISAM |
|---------------------|-------------------------|-------------|---|--------------------------|---------------------------|

Fig. 4-4 Site specific IM, describing radionuclide transfers used for model definition, based on the site descriptive information in Chapter 3. Different submodels are identified for vault and geosphere and for the biosphere. These share a common element – the aquifer /well feature that forms the geosphere-biosphere interface (GBI). Within the biosphere sub-system we distinguish the soils from those elements that are affected by the radiation content of water and soils. Influence from each leading diagonal element on the others is read as the clockwise off-diagonal elements. White shaded elements are treated as dynamic (time varying) compartments and blue as in equilibrium. Details for each model are given in the main text.

zone and, similarly, that the aquifer is not in contact with the lower soils. Contamination reaches them only via irrigation of the rooting zone soils. Drainage from the system is via the local aquifer. In this form the mathematical models for the landfill and geosphere and for the biosphere are defined.

In the following we describe the models that are adapted from ISAM test case to reproduce results of Kemakta's assessment (see section 4.2.1) and the models that are used in our independent modelling assessment based on our understanding of the site-specific information described in Chapter 3 (see section 4.2.2).

4.2.1 Descriptions of ISAM models

We adapted so called Little's model, compartment model approach, in ISAM test case (IAEA 2004b) mainly to represent the entire disposal system (landfill, unsaturated zone, saturated zone, and biosphere) and calculate doses. The model structure is shown in Fig. 4-5.

The compartmental model equation is used for dynamic compartments:

$$\frac{dN_i}{dt} = S_i(t) + \lambda_N M_i + \sum_{j \neq i} \lambda_{ji} N_j - \left(\lambda_N + \sum_{i \neq j} \lambda_{ij} \right) N_i \quad \text{Eq. (4-1)}$$

where the external time-dependent source term to the i^{th} compartment is $S_i(t)$ Bq/y, in-growth from precursor radionuclide (in the decay chain) is $\lambda_N M_i$ Bq/y, and the transfers to the i^{th} compartment from the other compartments is denoted by $\sum_{j \neq i} \lambda_{ji} N_j$ Bq/y, representing the sum of fractional transfers from the other (j) compartments. Losses are by radioactive decay $\lambda_N N_i$ Bq/y, and the sum of all transfers to the other compartments including the sink compartment, $\sum_{j \neq i} \lambda_{ij} N_i$ Bq/year. The elements λ_{ij} of the transfer matrix can be linked to the off-diagonal elements of the interaction matrix (Kłos & Thorne 2020).

Compartment modelling is an approximation because it is a discretisation of continuous transport process. Increasing the number of compartments increases accuracy but at the cost of model run-time and model complexity. Based on the guidance of Kirchner (1998) and Xu et al. (2007) the optimal number of compartments can be determined. As shown in Fig. 4-5, the waste form is modelled by a single compartment, the unsaturated zone by three and the aquifer downstream from the disposal facility by five compartments.

The transfer coefficient $\lambda_{leach,barrier}$ [1/y] is expressed as:

$$\lambda_{leach,barrier} = \frac{q_{in}}{\theta_w DR} \quad \text{Eq. (4-2)}$$

where q_{in} is the infiltration [m/y]; θ_w is water filled porosity of the landfill [-]; D is depth of the landfill through which the radionuclide is transported and R is the retardation factor (-),

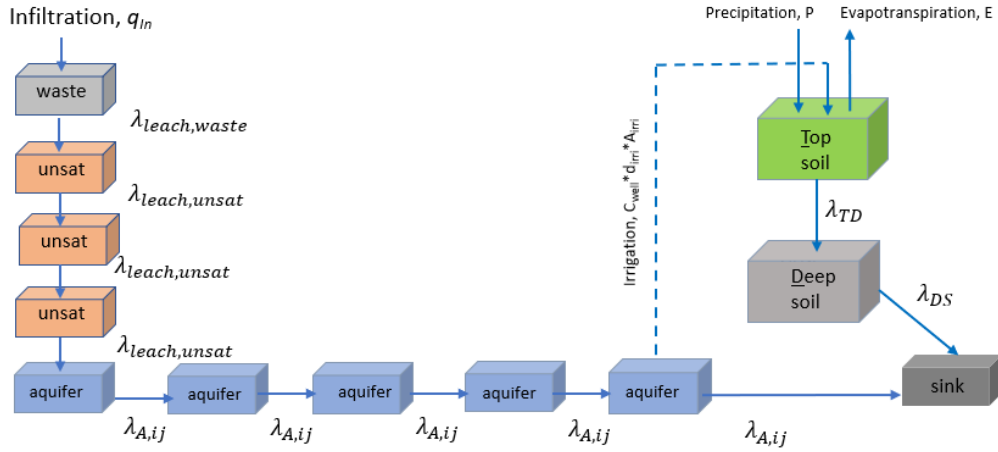


Fig. 4-5 Compartment model of radionuclide transport disaggregated from the interaction matrix in Fig. 4-4 and used for reproducing Kemakta's results.

$$R = 1 + \frac{\rho(1 - \theta)K_d}{\theta_w} \quad \text{Eq. (4-3)}$$

where ρ is the density of the waste material [kg/m^3]; K_d is the sorption coefficient of the waste [m^3/kg]. The overall porosity is θ , so that $\theta_w \leq \theta$.

The quantities q_{in} and K_d can be time dependent. The transfer coefficient $\lambda_{leach,unsat}$ [$1/\text{y}$] is expressed in a similar way to Eq. (4-3) as:

$$\lambda_{leach,unsat} = \frac{q_{in}}{\theta_w D_{unsat} R_{unsat}} \quad \text{Eq. (4-4)}$$

Transport of solute in the aquifer in general is described by an advection-dispersion partial equation. The compartment model can be used to approximate the solution of this solute transport problem. Xu et al., (2007) show that discretisation of a transport path into a few number of compartments results in a solution that is still close to the analytical solution, and the amount of numerical dispersion is similar to the amount of physical dispersion. The rule of thumb is the number of compartments required should exceed $Pe/2$, where Pe is the Peclet number. As can be seen in Fig. 4-5, five compartments are used in the modelling. The transfer coefficient $\lambda_{A,ij}$ [$1/\text{y}$] is expressed as

$$\lambda_{A,ij} = \frac{q}{L/n \theta_w R_w} \quad \text{Eq. (4-5)}$$

where L is the total transport length [m]; n is a number of compartments [-]; θ_w is the porosity of the medium [-]; R is the retardation coefficient of the medium [-]; q is Darcy velocity [m/y] given by

$$q = -K \frac{\partial H}{\partial x} \quad \text{Eq. (4-6)}$$

where K is the hydraulic conductivity of the medium [m/y]; $\partial H/\partial x$ is the hydraulic gradient [-].

The model to represent dynamic transfers in the biosphere shown in Fig. 4-5 can be described as follows. The irrigation rate to the top soil is expressed as:

$$\text{Irrigation rate} = C_{well} \cdot A_{irri} \cdot d_{irri} \quad \text{Eq. (4-7)}$$

in which A_{irri} is the area of the biosphere object [m²] and d_{irri} is the irrigation demand [m/y] and the activity concentration of well water C_{well} is further expressed as:

$$C_{well} = DF_{well} \cdot C_{geo} \quad \text{Eq. (4-8)}$$

where DF_{well} is dilution factor and the value of DF_{well} is given in Table 4-1 for the case of reproducing. C_{geo} is the concentration of the radionuclide along a one-dimensional stream tube along which dispersion occurs. As mentioned above the transport of the radionuclide in the aquifer can be approximated by the compartment model shown in Fig. 4-5. Thus this C_{geo} is given as:

$$C_{geo} = \frac{\text{Inventory}_{aqu,5}}{A_{aqu} \cdot \text{Length}_{aqu} \cdot \text{Porosity}_{aqu} \cdot R_{aqu}} \quad \text{Eq. (4-9)}$$

where $\text{Inventory}_{aqu,5}$ is the amount of the radionuclide in the compartment of aquifer No.5 [Bq] (see Fig. 4-5), A_{aqu} [m²] is the cross-section area of the stream tube which is assumed as 1 m². Length_{aqu} is the length of the compartment aquifer No. 5, which is the same as $\frac{L}{n}$ in Eq. (4-5). It is assigned as 100 m for the distance from the disposal facility to the well as 500 m. Porosity_{aqu} is the porosity of the aquifer which is the same as θ_w in Eq. (4-5). R_{aqu} is the retardation coefficient of the aquifer which is the same as the R_w in Eq. (4-5).

The transfer coefficients λ_{TD} and λ_{DS} are expressed as:

$$\lambda_{TD} = \frac{(P - E + d_{irri})}{s_T \varepsilon_T R_T z_T} \quad \text{Eq. (4-10)}$$

$$\lambda_{DS} = \frac{(P - E + d_{irri})}{s_D \varepsilon_D R_D z_D} \quad \text{Eq. (4-11)}$$

where P is the annual precipitation [m/y], E is the evapotranspiration [m/y], s_T and s_D are the volumetric moisture contents for top soil and deep soil [-], ε_T and ε_D are the porosities of top soil and deep soil [-], R_T and R_D are the retardation factor for top soil and deep soil [-] and z_T and z_D are the depths of top soil and deep soil [m], respectively.

Doses to the human exposed group are evaluated as a linear sum over the exposure from all pathways arising from water and soil via the different exposure routes and can be expressed as:

$$Dose = Dose_{inh} + Dose_{ext} + Dose_{ing} \quad \text{Eq. (4-12)}$$

where $Dose_{inh}$, $Dose_{ext}$ and $Dose_{ing}$ are the doses due to the inhalation, external exposure and the ingestion pathways [Sv/y].

The dose due to inhalation is expressed as:

$$Dose_{inh} = C_{soil} \cdot b_r \cdot 8766 \cdot [dust_{act} \%_{occup} + dust_{norm}(1 - \%_{occup})] DF_{inh} \quad \text{Eq. (4-13)}$$

Where b_r is the breathing rate [m^3/h]; 8766 are the hours in a year [h/y]; $dust_{act}$ and $dust_{norm}$ are the dust concentrations during ploughing and non-ploughing activities [kg/m^3]; $\%_{occup}$ is the occupancy factor for ploughing activities [-]; DF_{inh} is the dose factor for inhalation [Sv/Bq].

The dose due to external exposure is expressed as

$$Dose_{ext} = C_{soil} \cdot 8766 \cdot DF_{ext} \quad \text{Eq. (4-14)}$$

where DF_{ext} is the external exposure dose factor [Sv/h per Bq/kg].

The dose due to ingestion is expressed as:

$$Dose_{ing} = Dose_{ing_water} + Dose_{ing_crop} + Dose_{ing_animal} \quad \text{Eq. (4-15)}$$

where $Dose_{ing_water}$ is the dose due to water ingestion [Sv/y]

$$Dose_{ing_water} = Ing_{wat} \cdot C_{well} \cdot DF_{ing} \quad \text{Eq. (4-16)}$$

where Ing_{wat} is the individual ingestion rate of freshwater [m^3/y]; and DF_{ing} is the dose coefficient for ingestion [Sv/Bq]. The water is assumed to be consumed unfiltered so that any particulates are included in the calculation.

$$Dose_{ing_crop} = \sum_{root, green, grain} [Ing_{crop}(C_{soil} \cdot TF_{crop})DF_{ing}] \quad \text{Eq. (4-17)}$$

where Ing_{crop} is the consumption rate of crop including root vegetables, green vegetables and grain [kg/y]; TF_{crop} is the soil to plant concentration factor for the crop including root vegetables, green vegetables and grain [Bq/kg fresh weight per Bq/kg dry soil].

The dose due to animal product consumption is expressed as

$$Dose_{ing_animal} = \sum_{beef, milk} [Ing_{animal}(q_{water}C_{well} + q_{soil}C_{soil} + q_{pasture}C_{soil}TF_{pasture}) \times TF_{animal}DF_{ing}] \quad \text{Eq. (4-18)}$$

where Ing_{animal} is the annual animal product consumption rate (beef or milk) [kg/y]; q_{water} is the daily animal water intake [m³/day]; q_{soil} is the daily animal soil intake [kg/day]; $q_{pasture}$ is the daily animal pasture intake [kg/day]; $TF_{pasture}$ is the soil to plant concentration factor for the pasture [Bq/kg fresh weight per Bq/kg dry soil]; TF_{animal} is the transfer coefficient to the animal product [day/kg].

The activity concentration of well water, C_{well} is expressed in Eq. (4-8) and the activity concentration of soil, C_{soil} , is expressed as:

$$C_{soil} = \frac{Inventory_{top\ soil}}{A_{irri} \cdot z_T \cdot \varepsilon_T \cdot R_T} \quad \text{Eq. (4-19)}$$

4.2.2 Site-specific biosphere models

The development of the biosphere model is relatively straightforward following the system identification and justification phase discussed in Chapter 3. Based on the structure in the site specific interaction matrix (Fig 4-4) compartments and transfers coefficients of the biosphere model are as shown in Fig 4-6.

The “lake” is treated as the top part of the aquifer. Water fluxes from the contaminated disposal areas flow into the Local aquifer which is used as a well and irrigation water percolates through the Top and Deep soil returning to the Local aquifer, with net precipitation (rainfall – evapotranspiration). Given the relatively flat topography and it is assumed that the evapotranspiration flux from soil to atmosphere includes a flow from the Deep soil to the Top soil compartment.

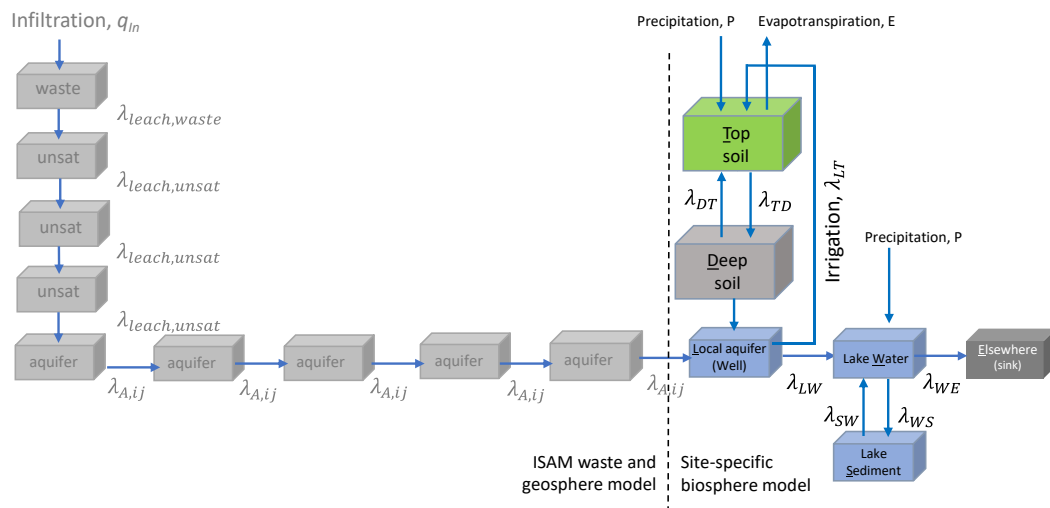


Fig. 4-6 The compartment model structure of radionuclide transport with focus on the site-specific biosphere models. The waste and geosphere model is unchanged with respect to Fig 4-5.

Drainage from the upslope and lower subcatchment enters the lake with the water flux that has passed through the biosphere dose object. Flow from the lake Water column continues downslope towards the regional drainage system of catchment #63573. Diffusion between the lake Water and lake Sediment allows accumulation of radionuclides in the lake bed.

Based on Kłos & Thorne (2020), when no solid material transfers are included, the generic form of the transfer coefficients from compartment i to compartment j in the biosphere is

$$\lambda_{ij} = \frac{F_{ij} + \frac{A_{ij}^{liq} D_e}{L_{ij}^{diff}}}{R_i V_i} \quad \text{Eq. (4-20)}$$

taking into account water fluxes F_{ij} , the physical volume of the compartment, V_i , in which the retardation coefficient is R_i (cf. Eqn. 4.3). Diffusion is in the water filled volume across the contiguous boundary between the compartments A_{ij}^{liq} , with an effective diffusion coefficient D_e and the /diffusion length is the distance between the centroids of the two compartments, $L_{ij}^{diff} = \frac{1}{2}(z_i + z_j)$. The compartment indices are $i, j = L, D, T, W, S, E$. In practice the expressions are similar to those in Eqns. 4-10 and 4-11.

Diffusion takes place from the water column to the lake bed and all advective fluxes in the biosphere model are described in Appendix B.

A single “soil” k_d value is used for all of the biosphere compartments as the solid material in the lake (suspended sediment and bed sediment) is derived from the soils. Additionally the soils in the area around the site are predominantly the infill material (Fig 3-6a). The area where the cultivation is assumed to be sandy moraine but for the present assessment the values obtained from the Kemakta documentation are adopted.

4.2.3 Models for the alternative and human intrusion scenarios

Models for the alternative scenario - bathtubting

The model used for the bathtubting scenario is adapted from the ISAM RADON test cases, which is an analytical expression to describe radionuclides in the overflowing leachate. The analytical solution of the concentration of radionuclides in the overflowing leachate C_{disp} [Bq/m³] used in evaluation of the bathtubting scenario is expressed as:

$$C_{disp}(t) = e^{-\lambda t} \frac{A_{mi}}{V_{dispunit}(\omega_{ed} + \rho_{bd} K d_d)} \quad \text{Eq. (4-21)}$$

where $e^{-\lambda t}$ is the radioactive decay before the scenario [-]; A_{mi} is the initial activity in the disposal unit [Bq]; $V_{dispunit}$ is the volume of the disposal unit [m³]; ω_{ed} is the moisture content of the disposal unit [-]; ρ_{bd} is the dry bulk density in the disposal unit [kg/m³]; $K d_d$ is the radionuclide distribution coefficient in the disposal unit [m³/kg].

The dose due to “bath-tub” effect is a sum of external dose ($Dose_{ext}$), inhalation dose ($Dose_{inh}$) and ingestion dose ($Dose_{ing}$).

$$Dose_{ext} = \frac{OF}{\rho_{soil} \cdot Th_{soil}} C_{disp}(sf \cdot t_{in} + t_{out})DF_{ext} \quad \text{Eq. (4-22)}$$

where OF is the water overflow to the garden in one year [m]; ρ_{soil} is the soil dry bulk density of the soil [kg/m^3]; Th_{soil} is the soil thickness [m]; C_{disp} is the concentration of radionuclides in overflowing leachate [Bq/m^3]; sf is the shielding factor [-]; t_{in} is the time spent indoors [h/y]; t_{out} is the time spent outdoors [h/y]; DF_{ext} is the external exposure dose factor [Sv/h per Bq/kg].

$$Dose_{inh} = \frac{OF}{\rho_{soil} \cdot Th_{soil}} C_{disp}(dust_{in}br_{in}t_{in} + dust_{out}br_{out}t_{out})DF_{inh} \quad \text{Eq. (4-23)}$$

where $dust_{in}$, $dust_{out}$ are the indoor and outdoor dust levels [kg/m^3]; br_{in} , br_{out} are the indoor and outdoor breathing rates [m^3/h]; DF_{inh} is the dose factor for inhalation [Sv/Bq].

$$Dose_{ing} = \frac{OF}{\rho_{soil} \cdot Th_{soil}} C_{disp}(TF_{vegt}Q_{vegt} + TF_{root}Q_{root} + Q_{soil})DF_{ing} \quad \text{Eq. (4-24)}$$

where TF_{vegt} and TF_{root} are the soil to plant concentration factor for the leafy green and root vegetables [Bq/kg fresh weight per Bq/kg dry soil], respectively; Q_{vegt} and Q_{root} are the leafy green and root vegetable consumption rate [kg/y]; Q_{soil} is the inadvertent soil ingestion rate [kg/y]; DF_{ing} is the dose factor for ingestion [Sv/Bq].

Models for the human intrusion scenarios

On-site residence scenario

The analytical expression of activity to which the on-site resident is exposed, A_{res} [Bq/kg of waste], is given by:

$$A_{res} = A_m e^{-\lambda t_1} \cdot dil \quad \text{Eq. (4-25)}$$

where A_m is the initial concentration of the radionuclide disposed waste [Bq/kg]; λ is the radioactive decay constant [1/y]; t_1 is the time before exposure starts [y]; dil is the dilution factor [-].

The dose due to on-site residence is a sum of external dose ($Dose_{ext}$), inhalation dose ($Dose_{inh}$) and ingestion dose ($Dose_{ing}$).

$$Dose_{ext} = A_{res}(sf \cdot t_{in} + t_{out})DF_{ext} \quad \text{Eq. (4-26)}$$

$$Dose_{inh} = A_{res}(dust_{in}br_{in}t_{in} + dust_{out}br_{out}t_{out})DF_{inh} \quad \text{Eq. (4-27)}$$

$$Dose_{ing} = A_{res}(TF_{vegt}Q_{vegt} + TF_{root}Q_{root} + Q_{soil})DF_{ing} \quad \text{Eq. (4-28)}$$

Road construction scenario (SCE7)

The analytical solution of the activity concentration to which the intruder is similar to the Eq. (4-25) and is expressed as A_{int} [Bq/kg of waste], which is given by

$$A_{int} = A_m e^{-\lambda t_1} \cdot dil \tag{Eq. (4-29)}$$

where A_m is the initial concentration of the radionuclide disposed [Bq/kg of waste]

The dose due the road construction scenario can be expressed as (in [Sv/y]):

$$Dose = A_{int} (Q_{soil} DF_{ing} + DF_{ext} + b_r \cdot dust \cdot DF_{inh}) t_2 \tag{Eq. (4-30)}$$

where A_{int} is the activity to which the intruder is exposed [Bq/kg of waste]; Q_{soil} is the inadvertent soil ingestion rate of the intruder [kg/h]; DF_{ing} is the dose factor for ingestion [Sv/Bq]; DF_{ext} is the external exposure dose factor [Sv/h per Bq/kg]; b_r is the breathing rate of the intruder [m³/h]; $dust$ is the dust level experienced by the intruder [kg/m³]; DF_{inh} is the dose factor for inhalation [Sv/Bq]; t_2 is the exposure duration [h].

4.2.4 Non-human biota dose rate calculations

Calculations of doses with respect to non-human biota are based on the ERICA assessment approach (Brown et al., 2008, Beresford et al., 2008). In brief, the ERICA Tool estimates absorbed dose rates from both external irradiation resulting from radionuclides in environmental media (soil, sediment, water) and internal irradiation from the incorporation of radionuclides within the organism. Because radionuclides are expected to be discharged into the Norrtorpsjön (described in section 4.2.2), environmental media at the exposure locations in natural ecosystems were identified in the assessment (Table 4-4).

The ERICA models used to calculate doses to other biota are described by Saetre et al., (2013). Weighted internal dose rates [$\mu\text{Gy h}^{-1}$] for biota in all ecosystems are calculated by weighting all dose conversion coefficients by radiation type before multiplying with the radionuclide activity concentration inside the organism:

$$DoseRate_{int,j} = (w_{low\beta} DCC_{int,low\beta,j} + w_{\beta\gamma} DCC_{int,\beta\gamma,j} + w_{\alpha} DCC_{int,\alpha,j}) AC_j \tag{Eq. (4-31)}$$

Table 4-4 Exposure pathways from source to potentially exposed populations of non-human biota.

| Ecosystem | Source type | Exposure point | Exposure route | | Exposure population (Repr. Organism.) |
|-----------|-----------------------|----------------------|----------------------|----------------------|---------------------------------------|
| | | | Environmental medium | Internal irradiation | |
| Lake | Groundwater discharge | Lake water /sediment | × | × | Pelagic and benthic limnic organisms |

where

- $w_{low\beta}$ is the weighting factor of internal low energy β -radiation [unitless],
- $w_{\beta\gamma}$ is the weighting factor of internal (high energy) β - and γ -radiation [unitless],
- w_{α} is the weighting factor of internal α -radiation [unitless],
- $DCC_{int,low\beta,j}$ is the dose conversion coefficient of internal low beta radiation for organism j [$\mu\text{Gy h}^{-1}$ per Bq kg fw $^{-1}$],
- $DCC_{int,\beta,j}$ is the dose conversion coefficient of internal beta gamma radiation for organism j [$\mu\text{Gy h}^{-1}$ per Bq kg fw $^{-1}$],
- $DCC_{int,\alpha,j}$ is the dose conversion coefficient of internal alpha radiation for organism j [$\mu\text{Gy h}^{-1}$ per Bq kg fw $^{-1}$], and
- AC_j is the radionuclide activity concentration in the organism j whole body [Bq kg fw $^{-1}$],

The internal whole body activity concentration, AC_j [Bq kg fw $^{-1}$], of aquatic organism j is:

$$AC_j = CR_j AC_{water} \quad \text{Eq. (4-32)}$$

where

- CR_j is the concentration ratio of radionuclide x for organism j [$\text{m}^3 \text{kg fw}^{-1}$], and
- AC_{water} is the activity concentration of the dissolved radionuclide in water [Bq m $^{-3}$]

The weighted external dose rate for biota in aquatic ecosystem can be calculated as:

$$DoseRate_{ext,j}^{aqu} = 0.001(w_{low\beta}DCC_{ext,low\beta,j} + w_{\beta\gamma}DCC_{ext,\beta\gamma,j})AC_{occup,j} \quad \text{Eq. (4-33)}$$

where

- 0.001 is a unit transformation factor [$\text{m}^3 \text{l}^{-1}$],
- $w_{low\beta}$ is the weighting factor of external low energy beta radiation [unitless],
- $w_{\beta\gamma}$ is the weighting factor of external beta gamma radiation [unitless],
- $DCC_{ext,low\beta,j}$ is the dose conversion coefficient of external low beta radiation for organism j [$\mu\text{Gy h}^{-1}$ per Bq l $^{-1}$],
- $DCC_{ext,\beta\gamma,j}$ is the dose conversion coefficient of external beta gamma radiation for organism j [$\mu\text{Gy h}^{-1}$ per Bq l $^{-1}$],
- $AC_{occup,j}$ is the occupancy corrected activity concentration for organism type j [Bq m $^{-3}$]

The occupancy activity concentration is a weighted average of the activity concentration in water and in sediments by using occupancy factor. The parameter occupancy factor to describe which habitat each considered organism is given in Grolander (2013).

5. Analysis of results

5.1 Reproducing results of Kemakta's assessment

As mentioned previously reproducing Kemakta's assessment results is included in our assessment method. The purpose is to understand and build confidence in Kemakta's risk assessment. To achieve this, we implement ISAM models given in section 4.2.1 for the landfill used for disposal of waste in a suitable compartment modelling code by using Ecolego 6.5 (Ecolego 2018). The model structure shown in Fig. 4-5 was used for the reproducing calculations. The ISAM models are broadly similar to Kemakta's models for radionuclide transport from landfill to the recipient except the release for release of radionuclides from waste matrix. The former uses a so-called K_d concept model and later uses a leaching model to describe the release of radionuclides from waste matrix with two key parameters, *leaching fraction* (quantity of waste released) and a leaching parameter κ (leaching rate). More details about descriptions of these two models can be found in Xu and Kłos (2022). Reproducing results of Kemakta's assessment were obtained for three cases: Ranstad, WSE and Cyclife..

5.1.1 Ranstad waste disposal case

All the data used in describing the landfill are adapted from Kemakta AR 2014-21, among others in Table 4-1. The initial waste inventory was calculated based on Table 3-2, 3-3 and 3-4 in AR 2014-21 (see Table 5-1). Because of differences of waste properties, the waste is treated simply as two categories. One category is treated as cementitious material. K_d values for cement (SKB 2014) are assigned to this category waste, which means sorption of radionuclides on cement material is taken into account. The second category assumes the radionuclides to be fully soluble in water, which means that no retardation is

Table 5-1 Initial activity inventories of Ranstad with different waste properties

| Radionuclide | Cement type waste (Bq) | Soluble type waste (Bq) |
|-------------------|------------------------|-------------------------|
| ²³⁸ U | 4.51E+09 | 6.00E+07 |
| ²³⁴ Th | 4.51E+09 | 6.00E+07 |
| ²³⁴ U | 4.94E+09 | 6.00E+07 |
| ²³⁰ Th | 2.94E+09 | 6.00E+07 |
| ²²⁶ Ra | 2.94E+09 | 6.00E+07 |
| ²³⁵ U | 2.25E+08 | 2.81E+06 |
| ²³¹ Pa | 1.43E+08 | 2.81E+06 |
| ²²⁷ Ac | 1.43E+08 | 2.81E+06 |
| ²³² Th | 7.66E+07 | 5.61E+05 |
| ²²⁸ Ra | 7.66E+07 | 5.61E+05 |
| ²²⁸ Th | 7.66E+07 | 5.61E+05 |
| ⁴⁰ K | 9.71E+08 | 2.00E+07 |

taken into account for the waste matrix but it is for the backfill material. This category includes loose objects, filter cakes and rags. Except the initial inventory and landfill parameter values shown in Table 4-1 and 5-1, other parameter values used in the simulation are given in Appendix B. The decay chains considered in the assessment is as follows:

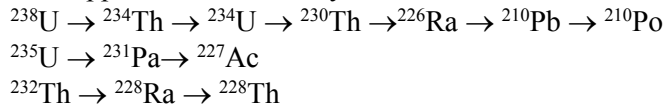


Fig. 5-1 shows comparison of reproduced result (solid line) versus Kemakta's result (dashed line). Fig. 5-2 shows calculated doses as a function of time for various radionuclides from reproducing. As can be seen there are two peaks of calculated total annual doses for both simulations (Fig. 5-1). The first peak occurs after ca. a few hundred years because of release of ^{40}K (see also Fig. 5-2). The second peak occurs after ca. 100 000 years caused by the release from uranium-thorium chain with ^{226}Ra and its daughter nuclides that dominate the doses (see Fig. 5-2). This behaviour (double peaks and dominated radionuclides) are similar for both simulations and the second peak values are similar too. However, the first peak from the reproducing is significantly higher than that of Kemakta's with a factor about 10. The reason might be the selected K_d value of cement for ^{40}K is almost zero while the leaching fraction of ^{40}K in Kemakta's assessment is ca. 10%, which means 90% of ^{40}K in the waste will never be released. The values of second peak are similar for both calculations but the timing of the second peak is different. The difference might be attributed to the effect of retardation due to backfill material.

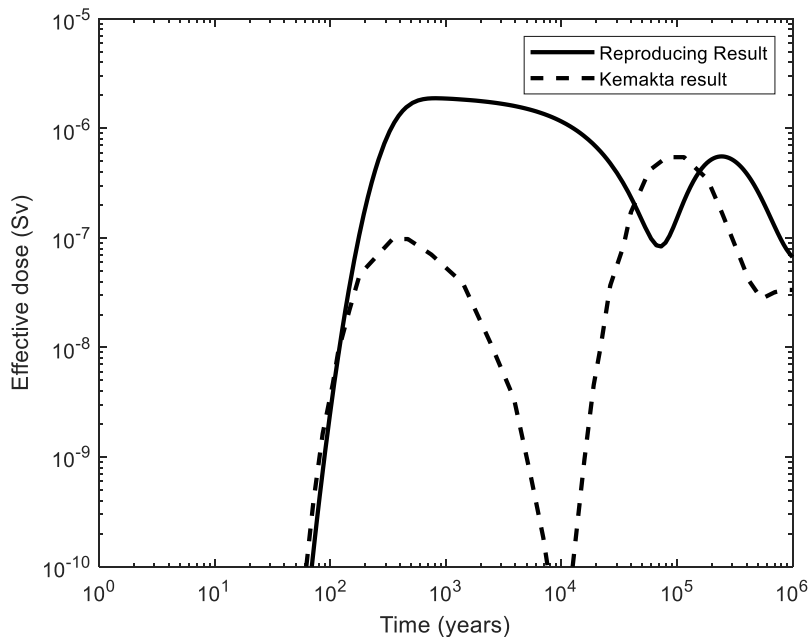


Fig. 5-1 Comparison of calculated results between reproducing and Kemakta's assessment for the case of Ranstad waste.

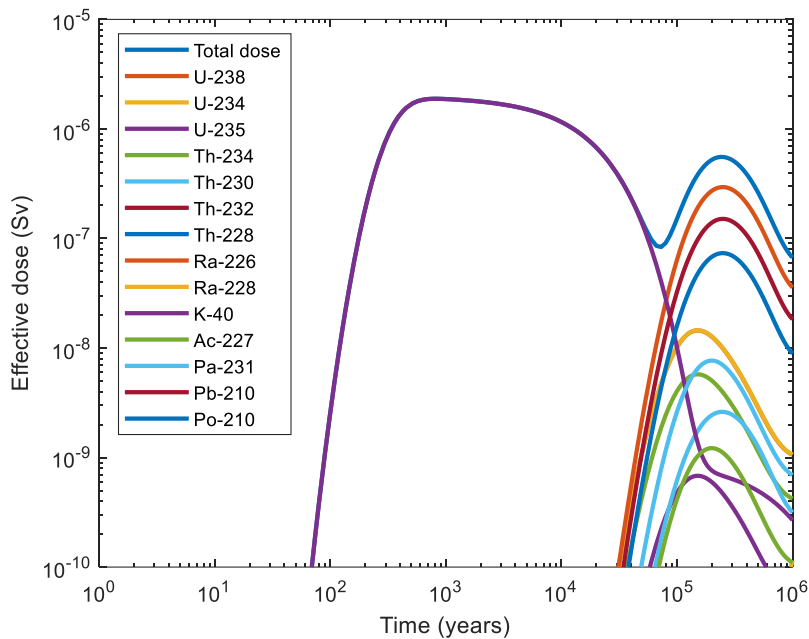


Fig. 5-2 Calculated effective doses as a function of time for different radionuclides from reproducing.

5.1.2 WSE waste disposal case

In the simulation of reproducing results for the case of WSE waste disposal the data used in describing landfill are the same as for the case of Ranstad waste disposal, i.e., the data shown in Table 4-1. The initial waste inventory was calculated based on Table 3-6, 3-7 and 3-13 in AR 2015-42. The initial waste inventory used in the calculation is shown in Table 5-2. Other parameter values used in the simulation are given in Appendix #A#.

WSE waste consists of various types of waste. However, in AR 2015-42 it says that “*All of these types of waste are planned to be incinerated by Ekokem AB after which the ash is deposited at the landfill at Norrtorp.*”. Thus, it is treated as no retardation of waste matrix itself but the backfill material. K_d values for soil are assigned to the backfill material. The decay chain considered in the assessment is as follows:

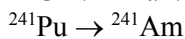
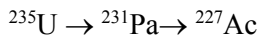
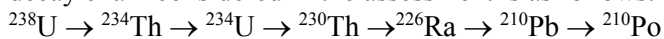


Fig. 5-3 shows comparison of reproduced result (solid line) versus Kemakta’s result (dashed line). As can be seen the peak values from both calculations are in the same order of magnitude ($< 10 \mu\text{Sv}$). The timing of the peak from reproducing occurs much later than that of Kemakta’s. This might be explained by using the K_d concept model due to the retardation effect on radionuclide migration. Fig. 5-4 shows calculated doses as a function of time for various radionuclides from reproducing. ^{226}Ra dominates the dose which is in

agreement with Kemakta's calculation. One should bear in mind that this peak dose occurs ca. 100 000 years after the closure according to the simulation therefore the results are with a great uncertainty.

Table 5-2 Initial activity inventories of WSE waste

| Radionuclide | Waste (Bq) | Radionuclide | Waste (Bq) |
|-------------------|------------|-------------------|------------|
| ²²⁷ Ac | 5.73E+07 | ²²⁶ Ra | 6.88E+07 |
| ²⁴¹ Am | 9.55E+07 | ²²⁸ Ra | 0.0 |
| ⁶⁰ Co | 7.86E+06 | ²²⁸ Th | 3.68E+08 |
| ²³¹ Pa | 1.87E+08 | ²³⁰ Th | 1.97E+09 |
| ²¹⁰ Pb | 0.00E+00 | ²³² Th | 0.00E+00 |
| ²¹⁰ Po | 0.00E+00 | ²³⁴ Th | 7.97E+09 |
| ²³⁸ Pu | 5.70E+07 | ²³² U | 4.27E+06 |
| ²³⁹ Pu | 1.34E+07 | ²³⁴ U | 1.22E+10 |
| ²⁴⁰ Pu | 1.76E+07 | ²³⁵ U | 4.95E+08 |
| ²⁴¹ Pu | 1.75E+09 | ²³⁶ U | 4.51E+07 |
| | | ²³⁸ U | 2.62E+09 |

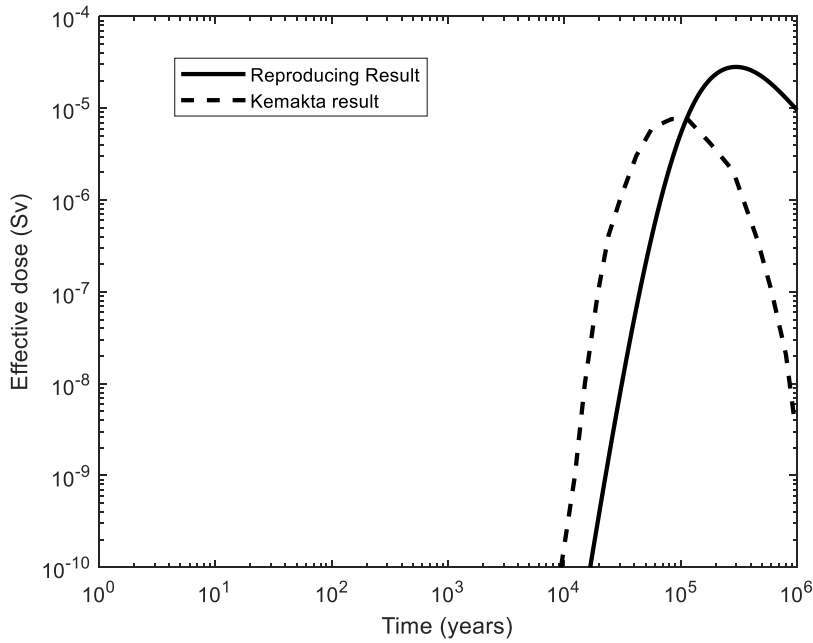


Fig. 5-3 Comparison of calculated results between reproducing and Kemakta's assessment for the case for WSE waste.

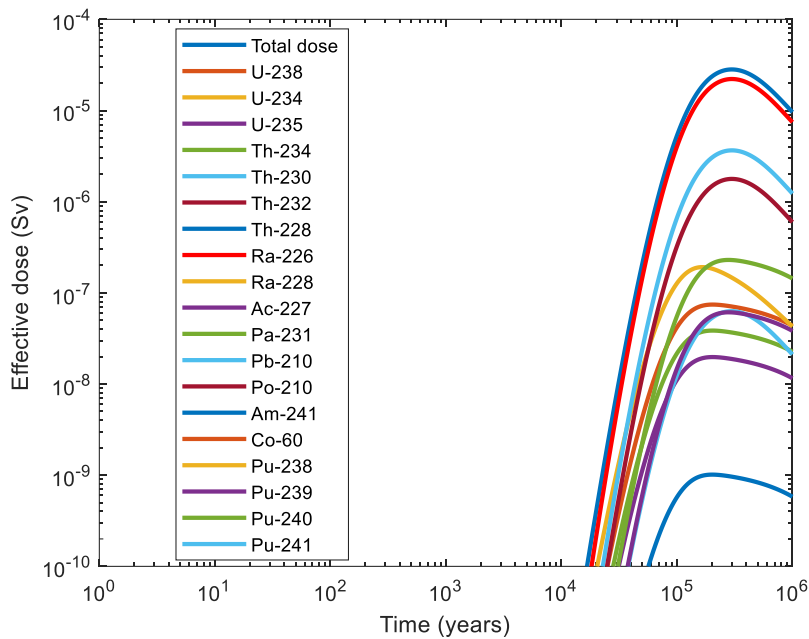
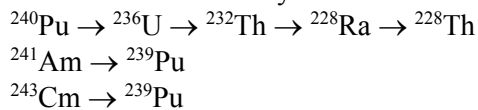


Fig. 5-4 Calculated effective doses as a function of time for different radionuclides from reproducing for the WSE waste.

5.1.3 Cyclife waste disposal case

The data used in describing landfill and transport are the same as for the case for Ranstad and WSE waste disposal. The initial waste inventory was calculated for disposal of 200 t/y over 25 years based on estimated annual average concentration (Bq/g) and estimated mass of each type of slag and melting furnace refractory given in Table 2-2 and 2-3 in AR 2020-02, respectively. The initial waste inventory used in the calculation is shown in Table 5-3. Cyclife waste consists of five types of slag and melting furnace refractory. However, no fraction of each type of waste was explicitly given in AR 2020-02. For simplicity, no retardation of waste matrix is considered. K_d values for soil are assigned to the backfill material. The decay chain considered in the assessment is as follows:



Reproduction of the base case scenario, a drinking water scenario, was performed. Fig. 5-5 shows the calculated annual effective dose as a function of time for Cyclife case. There is no calculated dose as a function of time given in AR 2020-02. The available information are calculated doses for various scenarios tabulated for different radionuclides. The maximum total dose for drinking water scenario is $4.2\text{E-}11$ [μSv] in Table 5-1 of AR 2020-02. Comparing with our calculated maximum dose shown in Fig. 5-5 (which is $1.7\text{E-}7$ [μSv]) it is almost four orders of magnitude difference. The reason for why the results deviates so much is not clear, although we use the same code as used for calculations for WSE waste case. All parameter values used in both cases are the same except the initial inventory.

Table 5-3 Initial activity inventories of Cyclife waste

| Radionuclide | Waste (Bq) | Radionuclide | Waste (Bq) |
|--------------|------------|--------------|------------|
| Co-60 | 7.90E+09 | Pu-238 | 5.47E+06 |
| Fe-55 | 3.94E+09 | Pu-239 | 5.77E+05 |
| Ni-63 | 1.55E+10 | Pu-240 | 5.20E+06 |
| Sr-90 | 9.59E+08 | Pu-241 | 1.03E+09 |
| Cs-137 | 3.93E+09 | Am-241 | 5.47E+06 |
| Mn-54 | 8.58E+07 | Am-243 | 5.47E+05 |
| Sb-125 | 3.95E+07 | Cm-242 | 1.02E+07 |
| Zn-65 | 3.89E+08 | Cm-243 | 3.08E+06 |
| | | Cm-244 | 3.08E+06 |

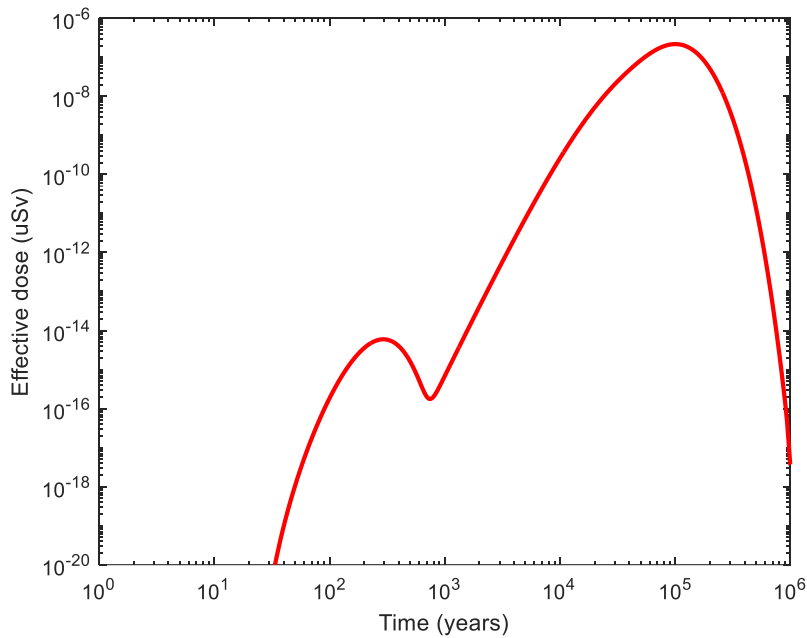


Fig. 5-5 Calculated effective doses as a function of time for Cyclife case

As a summary, based on document review and reproduction of Kemakta's results, the following uncertainties are identified:

- Selection of parameter values such as infiltration rate and groundwater flow rate
- Identification of biosphere object (distance from landfill to the well)
- Well water dilution factor
- The use of a leaching model vs a K_d -concept model

The next sections investigate the impact of these uncertainties by means of independent modelling.

5.2 Independent dose risk assessment

The model structure (Fig. 4-6) with associated models described in the previous chapter are used in independent radiological risk assessment. The models are implemented in software Ecolego. The scenarios formulated in section 4.1, with various calculation cases are shown in Table 5-4. As can be seen there are twenty calculation cases for the main scenario. Nineteen calculation cases are a combination of various waste sources, selected parameter values and different disposal locations. These are deterministic calculations to explore the effect of respective combination of parameters or assumptions on the final dose, for instance the uncertainties identified in the previous section. The last case is to perform probabilistic calculations and sensitivity analysis. Three waste sources are used in the calculations: i) Ranstad waste (denoted as R), ii) Cyclife waste (denoted as C), iii) Total waste deposited at Norrtrorp (denoted as T).

One of the objectives for this assignment is to perform a risk assessment taken into account all deposited waste at the landfill that has been approved by SSM and have a holistic view of radiological risk for such waste disposed at Norrtrorp. A best estimation of those deposited waste is shown in Table 5-5 (SSM 2021), in which the inventory of ^{14}C and ^3H can be reduced dramatically due to combustion of the waste (Stark, 2022). The assessment is performed by assuming 1% of the initial inventories ^{14}C and ^3H remained in the waste. A sensitivity analysis with full initial inventory is also performed.

The total waste used in the assessment is a sum of the waste of Ranstad (Table 5-1), WSE (Table 5-2) and already disposed at Norrtrorp (Table 5-5). The waste from Cyclife is neglected in the total waste because the radiotoxicity of Cyclife waste is much lower than that of other waste at Norrtrorp (see Fig. 5-6). However, a bathtubting scenario for Cyclife waste is included based on the request of SSM.

Lacking details of the exact location of the existing disposed waste, we assume that all the waste was either deposited at *Deponi* or *Ljungströmsfältet* (Figs. 3-3 and 3-9). This is because the size of the landscape dose object in each of these locations differ slightly.

Finally, four calculation cases for alternative scenario and human intrusion scenario are presented, as well as an estimate of dose rates to non-human biota for the main scenario.

Data used in simulations of the different scenarios and calculation cases are found in the Appendix B. Data obtained from the site investigation are noted as site data. The remaining data used in simulations are adapted from Kemakta's reports, IAEA technical document 1380 (IAEA 2003b) and SKB's reports (Grolander 2013, Tröjbom et al., 2013).

5.2.1 Main scenario

In Kemakta's modelling a key parameter is the well dilution factor, DF_{well} in Eqn. 4-8. In such assessments this is often an uncertain parameter with conservative values used in the absence of local information. Xu et al. (2022) have developed an approach that allows the value to be bounded and this is described in Section 3.4 for the Norrtrorp site. Three cases are defined to describe dilution in well water based on site-specific considerations, namely cases for maximum dilution, minimum dilution, and extreme low dilution.

Table 5-4 Summary of formulated scenarios and calculation cases, in column Waste, R denotes Ranstad waste, C denotes Cyclife waste, and T denotes Total waste deposited at Norrtorp.

| No. | Scenarios/Calculation cases | ID | Waste | Near-field | Geosphere | | Bios. |
|---------------------------------|---|---------------------|-------|---|----------------------|----------------------|--------------------------------|
| | | | | Infiltration rate (l/m ² /y) | Darcy velocity (m/y) | Transport length (m) | Upslope area (m ²) |
| Main Scenario | | | | | | | |
| 1 | Extreme low dilution, constant infiltration and low advection velocity | BC_EXD_CI_LV | R | 5 | 0.47 | 250 | 2E+4 |
| 2 | Minimum dilution, constant infiltration and low advection velocity | BC_MID_CI_LV | R | 5 | 0.47 | 250 | 8.36E4 |
| 3 | Maximum dilution, constant infiltration and low advection velocity | BC_MAD_CI_LV | R | 5 | 0.47 | 500 | 1.72E5 |
| 4 | Extreme low dilution, variation infiltration and high advection velocity | BC_EXD_VI_LV | R | 5 - 300 | 0.47 | 250 | 2E4 |
| 5 | Extreme low dilution, variation infiltration and high advection velocity | BC_EXD_VI_HV | R | 5 - 300 | 4.7 | 250 | 2E4 |
| 6 | Minimum dilution, variation infiltration and high advection velocity | BC_MID_VI_HV | R | 5 - 300 | 4.7 | 250 | 8.36E4 |
| 7 | Maximum dilution, variation infiltration and high advection velocity | BC_MAD_VI_HV | R | 5 - 300 | 4.7 | 500 | 1.72E5 |
| 8 | Extreme low dilution, variation infiltration and high advection velocity | BC_EXD_VI_HV_T | T | 5 - 300 | 4.7 | 250 | 2E4 |
| 9 | Minimum dilution, variation infiltration and high advection velocity | BC_MID_VI_HV_T | T | 5 - 300 | 4.7 | 250 | 8.36E4 |
| 10 | Maximum dilution, variation infiltration and high advection velocity | BC_MAD_VI_HV_T | T | 5 - 300 | 4.7 | 500 | 1.72E5 |
| 11 | Extreme low dilution, constant infiltration and high advection velocity | BC_EXD_CI_LV_T | T | 5 | 0.47 | 250 | 2E4 |
| 12 | Extreme low dilution, constant infiltration and low advection velocity | BC_VC-EXD-VI | R | 5 - 300 | 4.7 | 150 | 2E+4 |
| 13 | Minimum dilution, constant infiltration and low advection velocity | BC_VC_MID_VI | R | 5 - 300 | 4.7 | 150 | 3.15E4 |
| 14 | Maximum dilution, constant infiltration and low advection velocity | BC_VC_MAD_VI | R | 5 - 300 | 4.7 | 150 | 1E5 |
| 15 | Extreme low dilution, variation infiltration and high advection velocity | BC_VC_EXD_VI_T | T | 5 - 300 | 4.7 | 150 | 2E4 |
| 16 | Minimum dilution, variation infiltration and high advection velocity | BC_VC_MID_VI_T | T | 5 - 300 | 4.7 | 150 | 3.15E4 |
| 17 | Maximum dilution, variation infiltration and high advection velocity | BC_VC_MAD_VI_T | T | 5 - 300 | 4.7 | 150 | 1E5 |
| 18 | Minimum dilution, variation infiltration and high advection velocity and 10% of C-14 INV | BC_VC_MID_VI_T_10p | T | 5 - 300 | 4.7 | 150 | 3.15E4 |
| 19 | Minimum dilution, variation infiltration and high advection velocity and 100% of C-14 INV | BC_VC_MID_VI_T_100p | T | 5 - 300 | 4.7 | 150 | 3.15E4 |
| 20 | Probabilistic simulation (based on No.9 - BC_MAD_VI_HV_T) | BC_PRO_T | T | | | | |
| Alternative Scenario | | | | | | | |
| 21 | Bathtubbing | LP_BATH_TUB_R | R | | | | |
| 22 | Bathtubbing | LP_BATH_TUB_C | C | | | | |
| Human Intrusion Scenario | | | | | | | |
| 23 | On-site residence | RE_ON_SITE_HI | R | | | | |
| 24 | Road construction | RE_ROAD_CONS | R | | | | |

Table 5-5 Estimated total activity inventory of all the waste that has been approved by SSM to be deposited at Norrtorp except for wastes in Table 4-3, 4-4 and 4-5.

| Radionuclides | Waste amount (Bq) | Waste origin | Waste type | Treatment |
|---------------|-------------------|------------------------|------------------------------|-------------------------|
| U-238 | 5.74E+07 | WSE | Leached ion exchange carrier | combustion |
| U-238 | 3.73E+06 | WSE | Leached ion exchange carrier | combustion |
| H-3 | 5.93E+11 | AstraZeneca | Organic material | combustion |
| C-14 | 2.45E+11 | AstraZeneca | | |
| Am-241 | 3.55E+07 | Outokumpu Stainless AB | Dust | conditioned |
| Th-232 | 5.14E+08 | Försvarsmakten | Scrapped engine parts | Combustion and disposal |
| U-238 | 2.61E+09 | Ranstad | * | Combustion and disposal |
| Th-234 | 1.92E+09 | | | |
| Pa-234m | 2.12E+09 | | | |
| U-234 | 3.44E+09 | | | |
| Th-230 | 1.74E+09 | | | |
| Ra-226 | 7.53E+08 | | | |
| Pb-214 | 4.22E+08 | | | |
| Bi-214 | 4.21E+08 | | | |
| Pb-210 | 1.16E+09 | | | |
| U-235 | 1.63E+08 | | | |
| Pa-231 | 1.42E+08 | | | |
| Ac-227 | 7.00E+07 | | | |
| Th-227 | 5.10E+07 | | | |
| Ra-223 | 4.96E+07 | | | |
| Rn-219 | 5.38E+07 | | | |
| Pb-211 | 8.49E+07 | | | |
| Bi-211 | 4.99E+07 | | | |
| Th-232 | 3.69E+07 | | | |
| Ac-228 | 2.79E+07 | | | |
| Pb-212 | 2.46E+07 | | | |
| Tl-208 | 2.61E+07 | | | |
| K-40 | 5.28E+08 | | | |
| Co-60 | 4.14E+06 | | | |
| Cs-137 | 5.51E+06 | | | |
| Am-241 | 3.11E+07 | | | |

* Materials from leachate basins (gravel, sludge, bricks), metal components, electrical components, process equipment

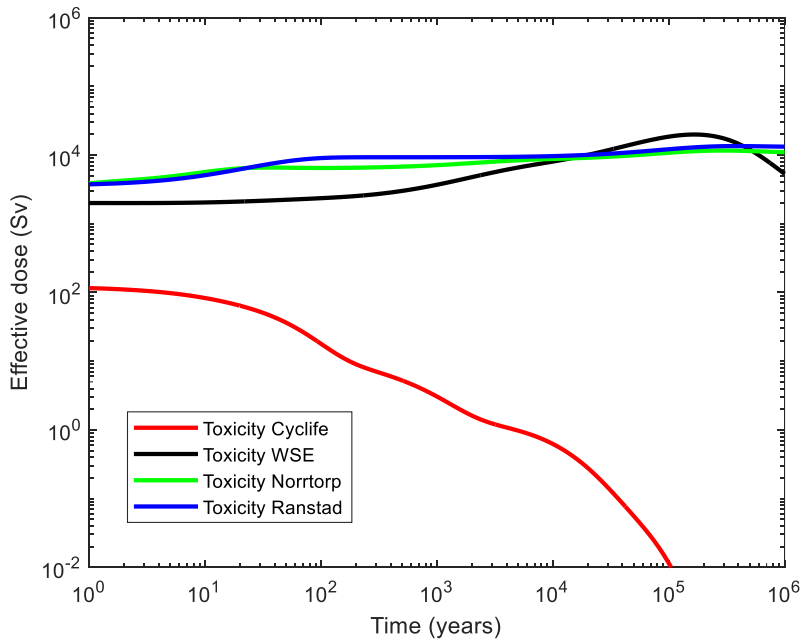


Fig. 5-6 The total radiotoxicity as a function of time for the wastes of Ranstad, WSE, Cyclife and all earlier deposited waste at Norrtorp.

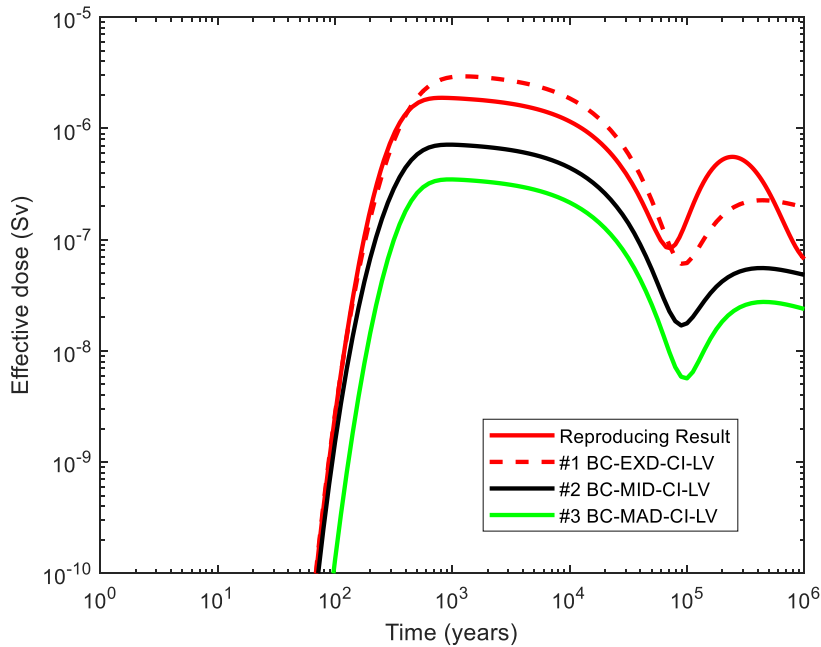


Fig. 5-7 Calculated effective doses for the cases of No.1 to 3 (disposal location of *Ljungströmsfältet*, Ranstad waste and constant infiltration rate as well as low groundwater velocity).

Calculation cases No.1 to 3 in Table 5-4 are deterministic sensitivity analysis to explore the uncertainties of defined upslope sub-catchment area (see Fig. 5-7). The infiltration rate and groundwater velocity in aquifer are constant, which are the same values used by Kemakta. As can be seen the ratio of maximum dose to minimum is around a factor of 8 and this is close to the inverse ratio of the limits of the overall dilution factor, i.e., the ratio of upslope of sub-catchment area for extreme dilution and maximum dilution (see Table 5-4). In addition, the reproduced result shown in Fig. 5-1 is used as a reference to compare with the calculated results of the case No. 1 to 3. As can be seen the reproduced result taken from Fig. 5-1 is close to the result of the extreme dilution case (the first peak is lower than that of the extreme dilution case but the second peak higher than that of the extreme dilution case). This means the dilution factor derived in Kemakta's assessment at a distance of 500 m does not underestimate the well concentration. In other words the dilution factor used in Kemakta's assessment is conservative, which was concerned by a comparison in the early study (Xu and Kłos, 2022).

Based on the description of the disposal system given by Kemakta (section 4.1.2) the infiltration rate into the landfill is constant throughout the whole assessment period, i.e., 5 l/m²/y and the horizontal groundwater transport velocity (Darcy velocity) is 0.471 m/y. The 5 l/m²/y value is taken from the maximum permissible infiltration rate for landfills containing hazardous waste (Section 31 Deponeringsförrordningen, 2001:512). However the ordinance is formulated for the period for which the landfill should be under some form of institutional control. This should be at least 30 years or longer if required. Typically in dose assessment a period of 300 years is assumed (e.g., IAEA 2004b).

It is implausible that the landfill cap would remain intact for one million years. When the engineered barriers of the landfill is degraded the infiltration can reach about 300 l/m²/y based on the site-specific information, precipitation and run-off. This value is assumed for the unmanaged state of the landfill, in its natural state. Assuming an earlier failure of the cap leads to a more conservative calculational case.

The horizontal groundwater Darcy velocity could be around 4.71 m/y based on Fig. 4-2. These uncertainties are investigated in the calculation cases No. 5 to 7, in which it is assumed that the groundwater Darcy velocity is 4.71 m/y and infiltration rate is from 5 l/m²/y after the closure increasing linearly to 300 l/m²/y at 300 years and thereafter constant throughout the assessment period. Fig. 5-8 shows the simulated results with three cases related to dilution factors. Comparing with the case using constant infiltration and low groundwater Darcy velocity a significant effect on the calculated dose can be seen due to increasing of infiltration and low groundwater velocity in aquifer.

Fig. 5-9 shows comparison of effect of low groundwater velocity versus high groundwater velocity assumed in the calculation on the calculated doses, i.e., Case No. 1 (dashed red line) versus No. 4 (black solid line). As can be seen the low groundwater velocity leads to a low second peak and delaying of the timing of the second peak compared with the high velocity case. With high infiltration rate and even low velocity (black solid line) both the first and second peak are higher than that of with constant infiltration and velocity case (the red solid line).

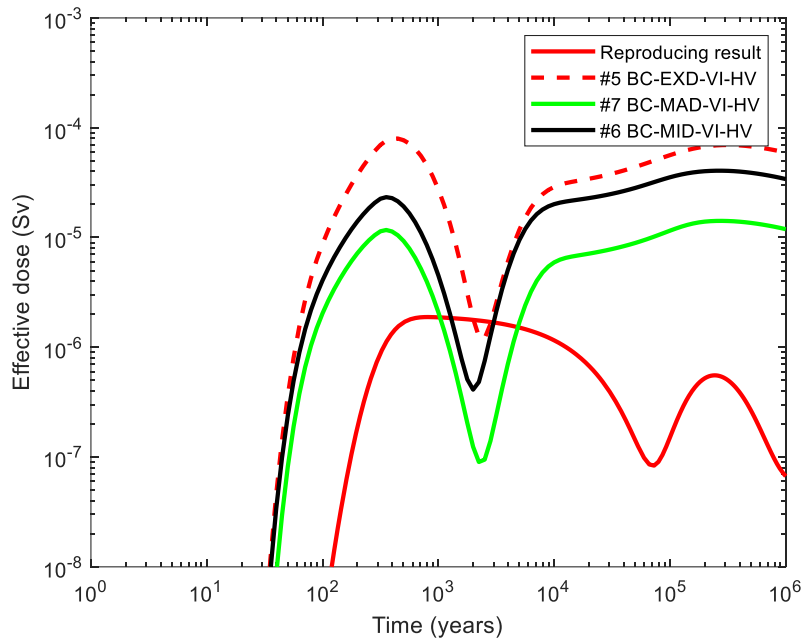


Fig. 5-8 Calculated effective doses for the cases of No.5 to 7 (disposal location of *Ljungströmsfältet*, Ranstad waste and increasing infiltration rate as well as high groundwater velocity).

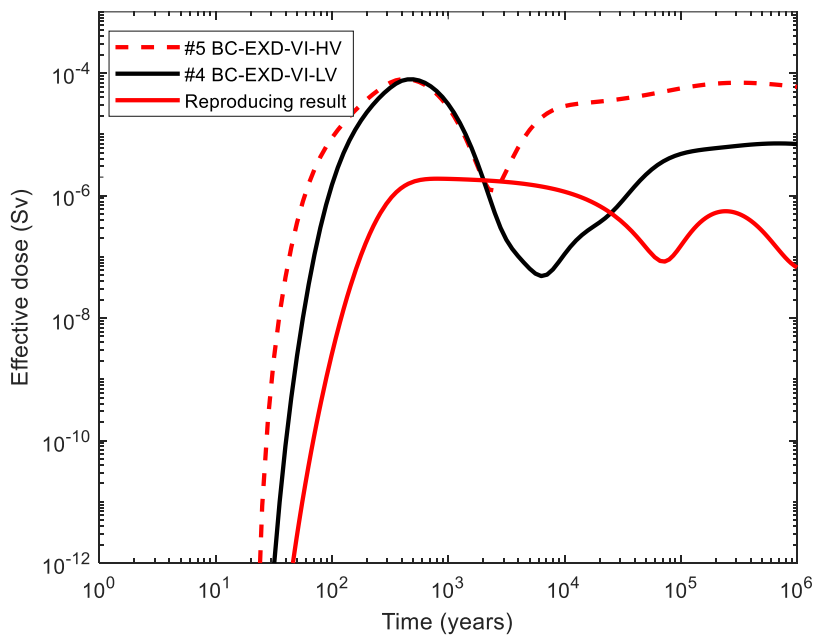


Fig. 5-9 Effects of infiltration rate and groundwater velocity on the calculated effective doses (Case No. 4, 5 and the case in Fig. 5-2).

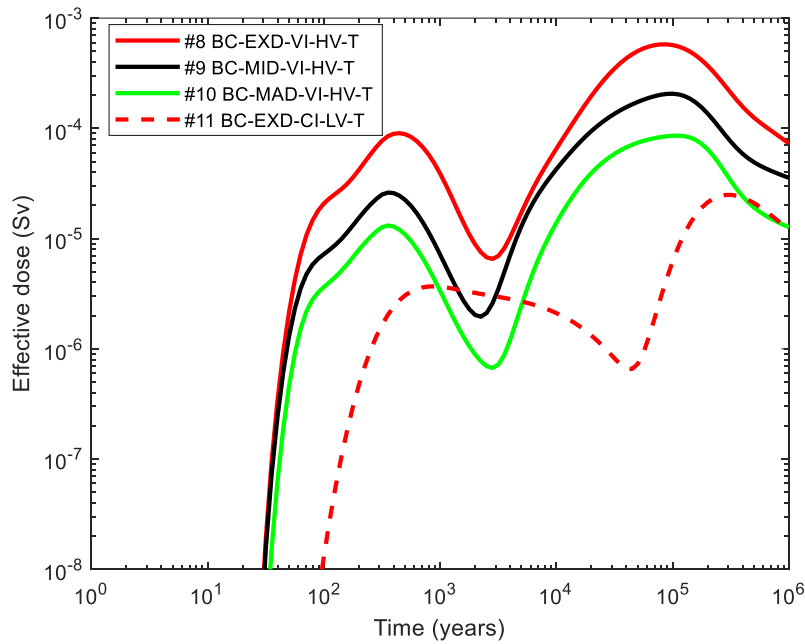


Fig. 5-10 Calculated effective doses for the cases of No. 8 to 11 (disposal location of *Ljungströmsfältet*, Total waste at Norrtorp and increasing infiltration rate as well as high groundwater velocity).

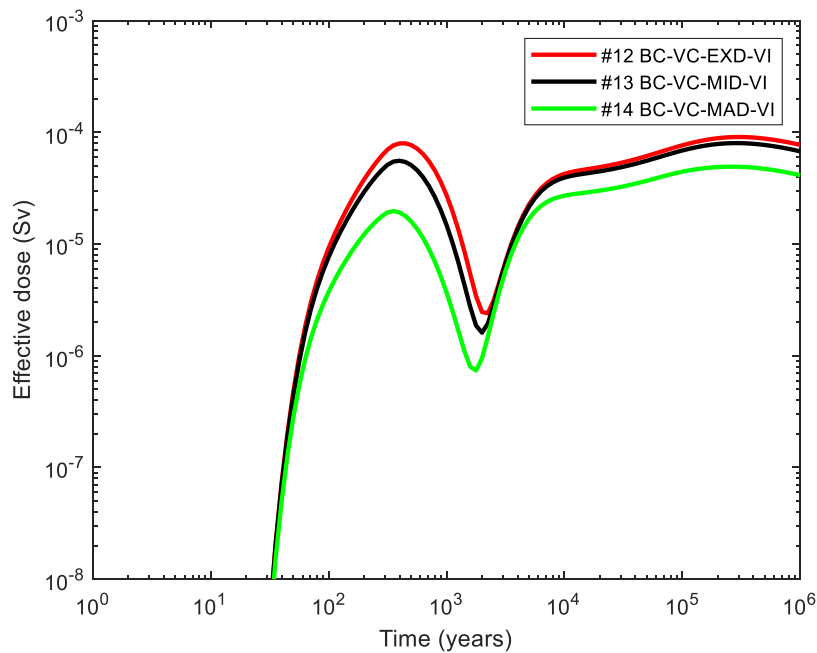


Fig. 5-11 Calculated effective doses for the cases of No.12 to 14 (disposal location of *Deponi*, Ranstad waste and increasing infiltration rate as well as high groundwater velocity).

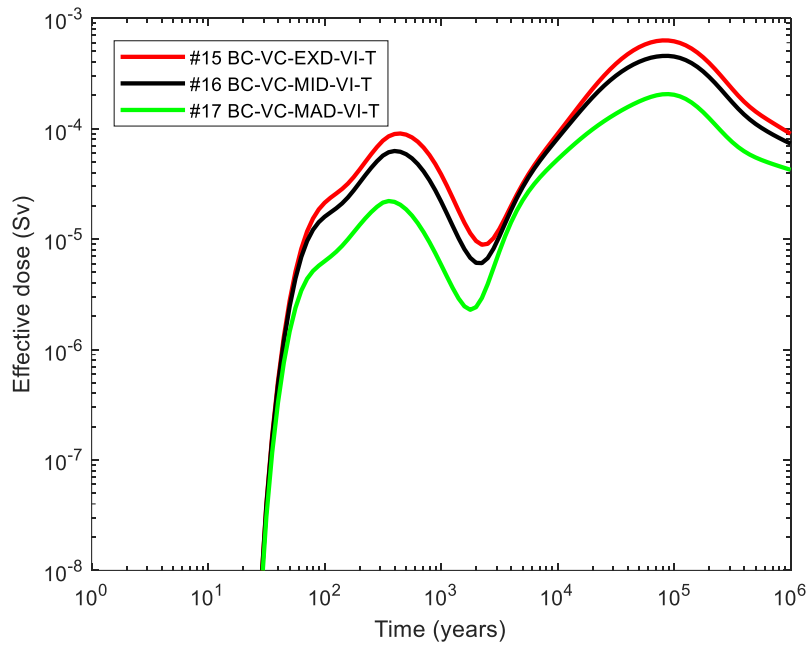


Fig. 5-12 Calculated effective doses for the cases of No.15 to 17 (disposal location of *Deponi*, Total waste at Norrtorp and increasing infiltration rate as well as high groundwater velocity).

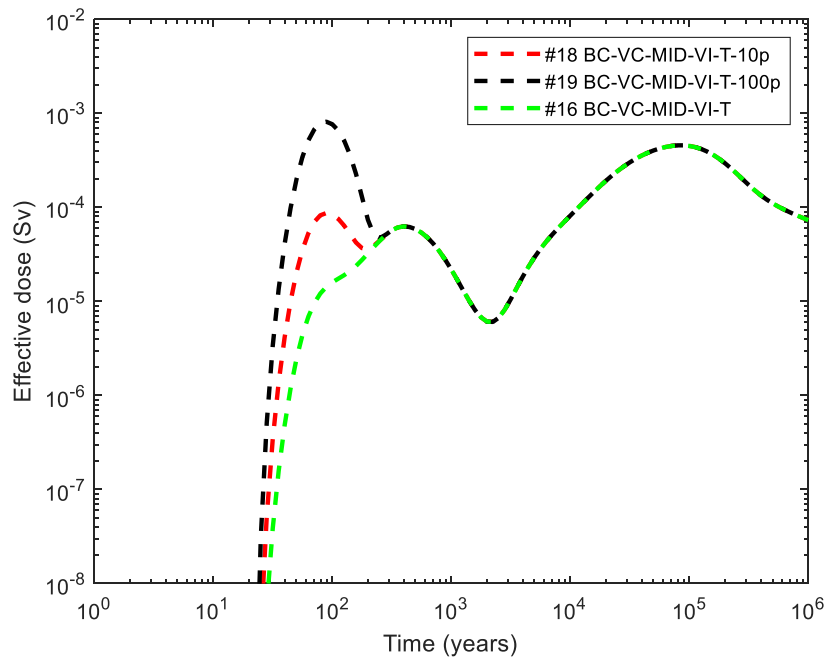


Fig. 5-13 Comparison of calculated effective doses for assuming 1%, 10% and 100% of initial inventories of ^{14}C and ^3H remained in the waste (Case No. 16, 18 and 19).

To have a holistic view of the potential radiological impact of all the waste that has been disposed and to be disposed at Norrtorp simulations were performed using all initial inventories of the wastes given in Table 5-1, 5-2 and 5-5. The disposal location is assumed at *Ljungströmsfältet*. The simulated results are shown in Fig. 5-11 for the calculation cases No. 8 to 11 (red, black and green solid lines). Similar to the results shown in Fig. 5-7 the ratio of maximum dose to minimum is around a factor of 8. In Fig. 5-11 the dashed red line shows the result calculated with all wastes but constant infiltration rate and low groundwater velocity. As can be seen even using extreme low dilution assumption the calculated peak doses are lower than that of using the assumption of increasing infiltration rate and high groundwater cases, which indicates again the effect of infiltration and horizontal groundwater velocity on the calculated doses.

Assessment of the case for the wastes being deposited in the *Deponi* area have also been undertaken (cases 12 to 17) with the results plotted in Fig. 5-12 and 5-13 show the simulated results for the Ranstad waste and Total waste, respectively. Comparing Fig. 5-12 with Fig. 5-8 and Fig. 5-13 with Fig. 5-10 shows no significant difference. This means that even the areas of upslope sub-catchment and transport distances are slightly different for these two biosphere objects but the differences of the calculated doses are small.

As discussed, we have assumed that only 1% of the initial inventories of ^{14}C and ^3H remained in the waste. Fig. 5-13 compares calculated effective doses assuming 1%, 10% and 100% of initial inventories of ^{14}C and ^3H remained in the waste. As can be seen the calculated dose exceeds the regulatory dose constraint when 100% of ^{14}C and ^3H is assumed to remain in the waste. However, it is unlikely that 100% of ^{14}C and ^3H is remained in the waste after the incineration because the waste is organic material. When the waste is incinerated, all C is oxidized to CO_2 , i.e., ^{14}C becomes $^{14}\text{CO}_2$ and ^3H are oxidized to tritiated water (Stark 2022).

The probabilistic calculations includes parameters from near-field, geosphere and biosphere models so as to understand the key parameters affecting dose. Additionally, some indication of the overall uncertainty associated with the doses is calculated although the assumed probability distribution functions (pdfs) are better suited to the sensitivity study.

Appendix B gives the numerical values of the parameters varied:

- Upslope subcatchment area (uniform, 2×10^4 , 1×10^5) m^2
- Infiltration (uniform, 5×10^{-3} , 0.3) $\text{m}^3 \text{m}^{-2} \text{year}^{-1}$
- Geosphere pathlength (uniform, 100, 500) m (+0.95 correlation to upslope area)
- K_d -values for waste form 1 and wasteform 2, geosphere aquifer and soil (log-normal, with geometric mean taken to be the best estimate values and geometric standard deviation = 2 in all cases).

The case uses the total waste inventory and the sampled infiltration applies throughout the simulation period as a constant. The base model is therefore case No. 9 (BC-MID—VI-HC-T).

1000 LHS samples were run and the maximum dose summed over all radionuclides was analysed. Output from the Ecolego model was taken as a geometric series from 100 years to 10^6 years with 41 equispaced timepoints. The time evolution of the 5th, 50th (median) and 95th percentiles are plotted in Fig 5-14, together with the geometric and arithmetic mean values. The deterministic case on which probabilistic case is based is also plotted.

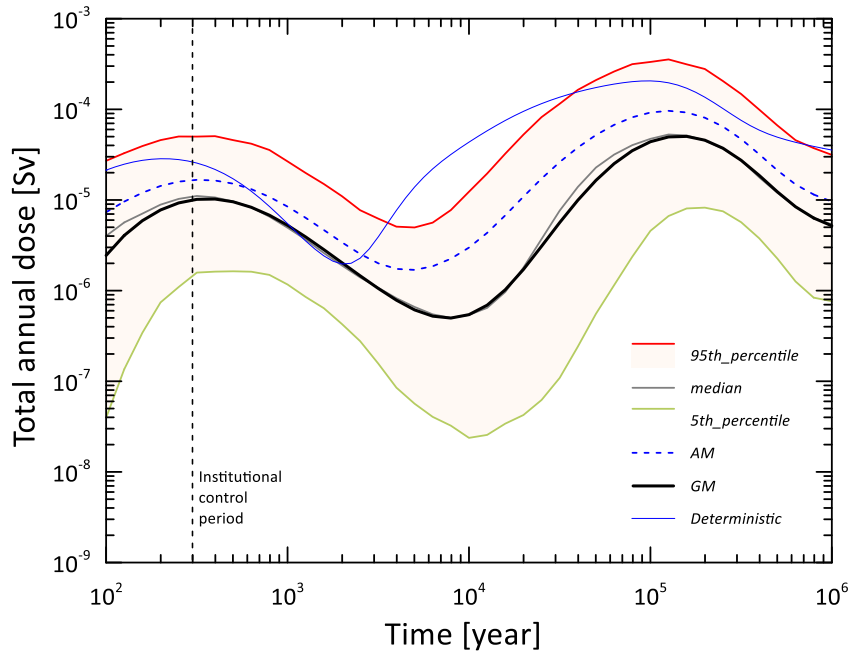


Fig. 5-14 Time evolution of statistical quantities for total dose in the probabilistic uncertainty and sensitivity analysis.

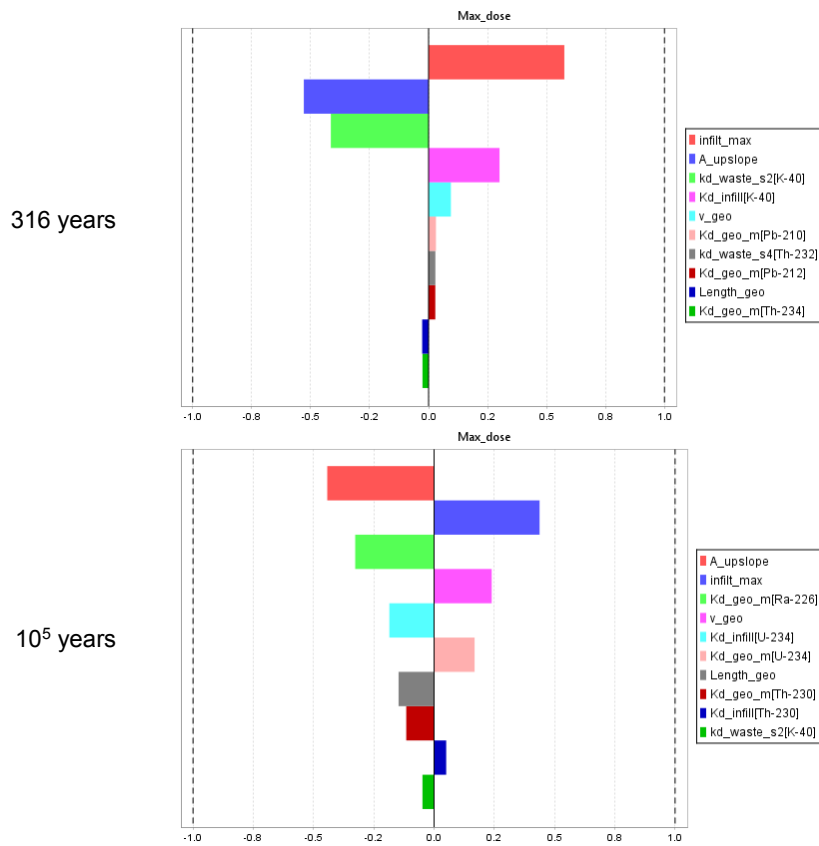


Fig. 5-15 Tornado charts of standardise rank regression coefficients (SRRC) expressing the parameters having the most influence on total dose.

Sensitivity was determined using the standardised rank regression coefficients as calculated in the Ecolego sensitivity analysis options. Results for total dose at 316 years (just after the end of the institutional control period) and at 10^5 years. These times corresponding to the peak effects of ^{40}K and ^{226}Ra respectively. Fig 5-15 shows the tornado plots.

Overall, the uncertainty analysis shows a range of less than 2 orders of magnitude. However, it should be understood that the selection of pdfs for the probabilistic modelling is rather crude and is better suited to sensitivity rather than to uncertainty analysis. The median and geometric mean are similar with 3 to 10 times lower than the deterministic values, but this is largely due to the assumed pdfs being symmetric around the best estimate values. Nevertheless, these results reflect where the potential uncertainty might be reduced with improved focus on those FEPs identified as important in the sensitivity analysis.

Around the timepoint 300 years the parameters having most influence on the dose are the infiltration rate through the waste (positive correlation) and the dilution in the well (upslope subcatchment, negative) is also important. In this k_d -model the availability of ^{40}K in the waste is also negatively correlated but retention in the soil (positive correlation of K_d_{infil} , the soil k_d here) is also an important influence. There is also a smaller correlation of the geosphere Darcy velocity with high doses. The remaining SRRC values are small and relate to radionuclides of less significance. The length of the geosphere path is at a similar level of importance.

The later dose peak is due to ^{226}Ra in the well. Water fluxes are the two dominant parameters, albeit with different sense – Higher dilution in the well (upslope catchment area) means lower doses and higher infiltration through the waste transfers more of the ^{226}Ra to the well. Similarly, retention of ^{226}Ra in the geosphere (negative influence) is countered by higher transfers through the geosphere (Darcy velocity). Retention of ^{226}Ra 's grandparent (^{234}U) has a small positive correlation but a longer path length act to lower doses, as does the retention of the immediate parent ^{230}Th .

Overall the geometric factors have a greater influence on doses than the k_d s but the k_d database used here is from earlier assessments and might benefit from review.

5.2.2 Alternative scenarios

From section 4.1.3 an alternative scenario was selected to assess the deviation of the reference evolution for the long-term safety of the landfill: the Bathtubbing and Garden scenario. ISAM models for bathtubbing scenario given in section 4.2.3 are used in the risk assessment. Two calculation cases are performed, one for Ranstad waste and one for Cyclife waste. Ranstad waste is believed as a representative waste at Norrortorp because all the disposed waste is distributed over the disposal location of *Ljungströmsfältet* or *Deponi* or both. The Cyclife waste is special in the sense that the initial activity concentration is in excess of the clearance level but includes radionuclides with relatively short half-life times.

Fig. 5-16 shows the calculated total effective annual dose due to bathtubbing scenario during the whole assessment period for the Cyclife waste. Bathtubbing scenario means that leaching of radionuclides from the waste and subsequent overflow into nearby cultivated soil from 300 years after the closure. The calculated effective annual dose at 300

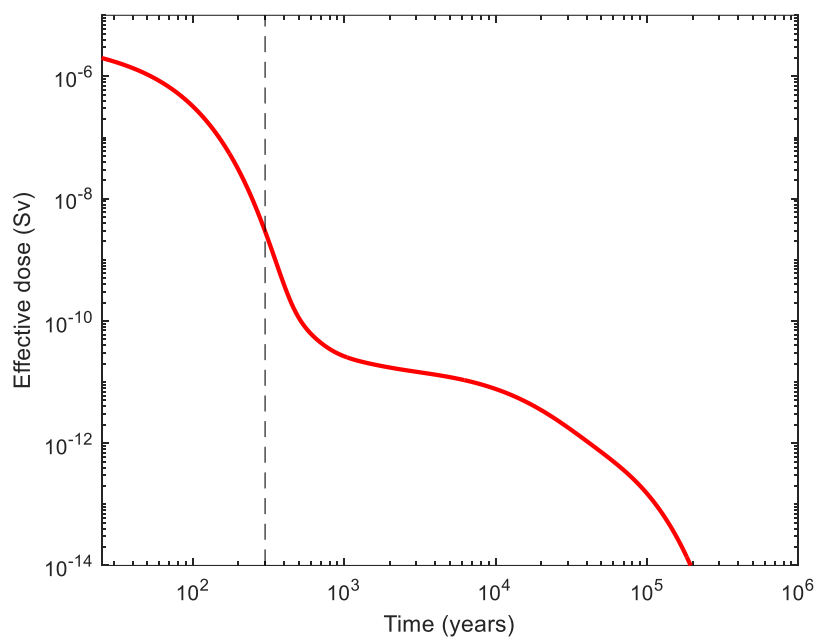


Fig. 5-16 Total effective annual dose for releases from the landfill for Cyclife waste due to the bathtubting event of the alternative scenario (Case No. 22).

years after the closure is $2.9\text{E-}3 \mu\text{Sv}$ which is higher than $6.9\text{E-}5 \mu\text{Sv}$ obtained by Kemakta (AR 2020-02). The reason could be that we used a conservative value for the volume of the disposal unit, i.e., the volume of the deposited waste was assumed to be smaller.

The calculated total effective annual dose due to bathtubting scenario during the whole assessment period for the Ranstad waste is rather constant, i.e., $4.2 \mu\text{Sv}$. The total dose is dominated by ^{40}K .

5.2.3 Human intrusion scenarios

Two human-intrusion scenarios are selected; *onsite residence* and *road construction*. The on-site residence scenario assumes that the engineered barriers of the disposal facility as well as the waste are totally degraded. The exposed residents in this scenario are assumed to live in a house built directly on top of the facility. Because of the distribution of waste material, the soil around the house is expected to be contaminated which is equal to the specific activity of the waste divided by a dilution factor. Residents grow vegetables in the garden for their own consumption.

The road construction scenario anticipates that the engineered barriers of the disposal facility as well as the waste are totally degraded. A road construction is directly across the disposal facility. The situation is considered as very unlikely to occur but, were it to do so, potentially important radiological impacts could arise.

According to Kemakta AR 2014-21 the total amount of the waste is about 5000 tonnes. Assuming the density of the waste is 1600 kg/m^3 the amount of the waste volume is about 3000 m^3 . The area for the disposal is 1600 m^2 (Table 4-1) the depth of the waste disposal is ca. 2 m. The whole landfill depth with backfill materials is 30 m. The dilution factor is 15. We use a factor of 10 in our calculation. As mentioned in section 4.1.2 in practice this dilution factor could be much higher than that we chose depending on the actual distribution of the waste in the entire landfill.

Fig. 5-17 shows the total effective annual dose for these two scenarios. The calculated total dose at 300 years after the closure is 0.23 mSv for the on-site residence scenario. The total dose is dominated by ^{226}Ra . The calculated total effective annual dose at 300 years after the closure is $4.9 \text{ }\mu\text{Sv}$ for the road construction scenario. The total dose is dominated by ^{226}Ra . Kemakta calculated total effective annual doses for on-site residence and road construction scenarios for Ranstad waste are $11 \text{ }\mu\text{Sv}$ and $1.3 \text{ }\mu\text{Sv}$, respectively. Our calculated doses are higher than that of theirs. The main reason is the conservative dilution factor we selected in the calculation.

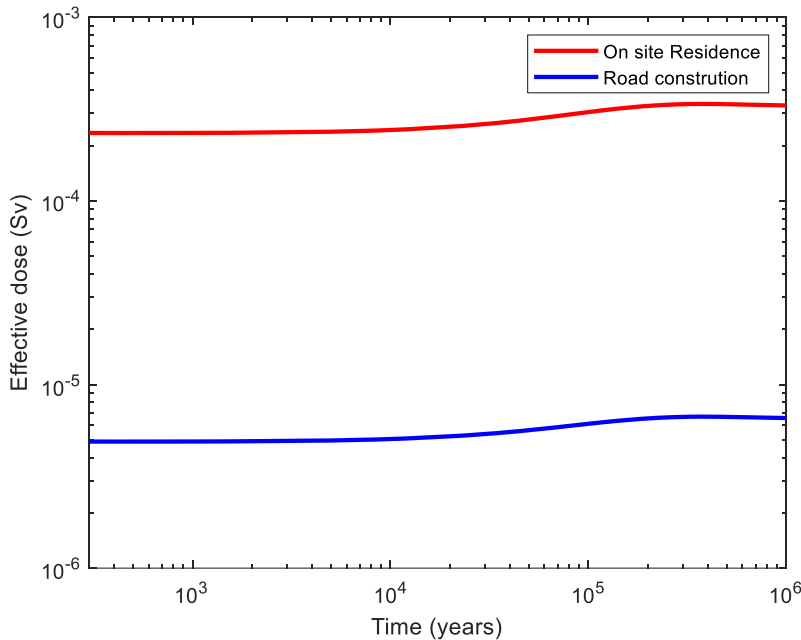


Fig. 5-17 Total annual effective dose for the on-site residence scenario and road construction scenario (Case No. 23 and 24).

5.2.4 Non-human biota

Exposures of non-human biota to ionising radiation from radionuclides originating from the landfill have been estimated by calculating absorbed dose rates, based on the ERICA assessment approach (Brown et al., 2008, Beresford et al., 2008) with the models in Saetre et al. (2013).

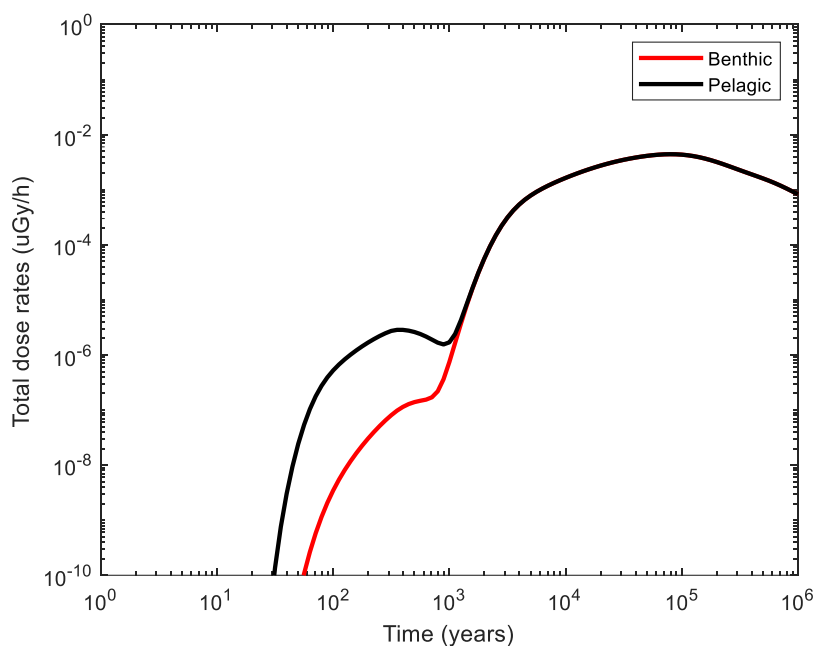


Fig. 5-18 Dose rates to non-human biota in the freshwater ecosystem, in the calculation case No.15 of the Main scenario.

The natural ecosystem included in the assessment is Norrtorpsjön. Reference organisms from the ERICA tool selected for this assessment are freshwater organisms: benthic and pelagic fish (see Table 4-4). Dose rates to the reference organisms are estimated for the main scenario case No. 15 which is the case for the total waste at the location of *Deponi*.

Fig. 5-18 shows calculated dose rates to benthic and pelagic fish as a function of time. The maximum dose rates are about 4.4E-3 $\mu\text{Gy/h}$, which is well below the screening value of 10 $\mu\text{Gy/h}$. In the dose assessment dose rates to the reference organisms from activity concentrations of the background was not included.

The landfill in Norrtorp is located in an area with alum shale, which is described as a high-risk area for radon (AR 2014-21). A research study financed by SSM indicates that “For water in the Kvarntorp area, the highest activity concentrations were found mainly in Surpölen because of its acidity, second highest in Norrtorpsjön and lowest in the Serpentine ponds.... In the water, ²¹⁰Po was not in equilibrium with the U-isotopes due to differences in solubility.... The radiological risk to biota at Kvarntorpshögen, the Serpentine ponds, Surpölen and Norrtorpsjön cannot be concluded as being of negligible concern.” (Hultqvist 2020).

5.2.5 Dose conversion factors (DCF)

During the period of the performance of this assignment four meetings between consultants and SSM’s staff have been conducted. SSM expressed desire for a general calculation for all radionuclides included in the current risk assessment so that such results can

Table 5-6 Comparison of site-specific DCF (Sv/Bq) in different modelling studies

| Radionuclide | SR-Site | SR-97 | Independent modelling in this study* | | |
|--------------|-----------------|--------------|--------------------------------------|----------|----------|
| | Landscape model | Aberg (well) | EXD | MID | MAD |
| C-14 | 5.4E-12 | 2.4E-13 | 4.28E-13 | 1.02E-13 | 4.98E-14 |
| Ra-226 | 3.8 E-12 | 1.2E-10 | 2.21E-08 | 7.54E-09 | 3.47E-09 |
| Th-230 | 1.3 E-11 | 2.1E-10 | 1.03E-10 | 4.58E-11 | 2.62E-11 |
| U-238 | 1.9 E-12 | 1.6E-11 | 3.04E-11 | 7.26E-12 | 3.53E-12 |
| Pu-239 | 1.9 E-12 | 2.2E-10 | 25E-11 | 1.40E-11 | 9.76E-12 |
| Pu-240 | 1.9 E-12 | 1.8 E-10 | 5.68E-12 | 4.98E-12 | 4.24E-12 |
| Am-241 | 1.5 E-12 | 6.8E-11 | 2.31E-13 | 2.28E-13 | 2.25E-13 |

* Here, EXD denotes extreme low dilution, MID denotes minimum dilution, MAD denotes maximum dilution (see Table 3-3).

be used to scale up until the dose criterion to approximate how much activity can be deposited at the landfill.

Site-specific dose conversion factor (DCF) may partly meet SSM's requirements. DCF concept has been used in various safety assessments, such as SR-97, SFR, SR-Can and SR-Site (Lindgren and Lindström, 1999, Karlsson et al., 2001, SKB 2006, SKB 2011). The DCFs are derived on a continuous release of 1 Bq/year to a specific biosphere object of interest during 10 000 to 100 000 years of assessment period for each radionuclide. The assessment period depends on calculated DCF values that reach equilibrium. If the flux of release through landfill and geosphere (aquifer) is known the effective dose for certain radionuclide can be calculated by multiplying the flux with DCF for that radionuclide.

As an example DCF may be used in a scoping calculation. If we assume disposed waste will be released within 300 years the dose can be estimated by dividing initial waste inventory of certain radionuclide with 300 years and then multiplying corresponding DCF. The total doses are the sum of all calculated doses for each radionuclide. This can be expressed as:

$$Dose_{total} = \sum_{i=1}^n \frac{Inventory_i}{300} \cdot DCF_i \quad \text{Eq. (5-1)}$$

where i denotes radionuclide i .

Site-specific DCFs are derived based on the biosphere object identified in section 3.4. For a few radionuclides the calculated DCFs reach equilibrium within 10 000 years. For most of radionuclides the calculated DCFs reach equilibrium at 100 000 years. Calculated DCFs are compared with the earlier DCF values with common radionuclides used in SR-97 and SR-Site by SKB (shown in Table 5-6). As can be seen most of the values are in the same order of magnitude. DCFs for SR-97 are derived for the well case but for SR-Site derived for the landscape models.

6. Discussion and conclusions

In this radiological risk assessment, a number of scenarios and calculation cases have been formulated. We used extreme conditions and assumptions to explore uncertainties both using deterministic and probabilistic calculations. The purpose is to highlight key factors that may have significant effects on the calculated doses and suggest SSM focusing on these key factors in coming reviews of conditional clearance applications. Calculated doses for the estimated inventory of all the waste deposited at Norrtorp (Fig 5-10), with a combination of extreme low dilution and a constant infiltration rate (red dashed line) remain below the criterion of 10 μSv per year upto around 100 kyear post closure. However, the criterion is breached for the combination of minimum and extreme low dilution with varying infiltration cases after a few hundred years post closure. The maximum dilution case approaches the 10 μSv limit after around 200 years and exceeds it, again after 10 kyear. As noted, the probabilistic uncertainty analysis reflects the deterministic results at the 95th percentile level throughout the simulation but this result should not be taken as a definitive statement since the probability distribution functions assumed for the parameters are intended for use in the probabilistic sensitivity study, used to identify the key model parameters affecting dose. They should not be taken to mean that the disposal at the site are unsafe. However the results do indicate some important properties of the assessment. The geometric mean dose in the probabilistic analysis is lower than the deterministic value, by a factor 3 to 10. This reflects the symmetry in the assumed pdfs and the fact that the deterministic values for the upslope area that controls dilution in the well are defined to be conservative whereas the probabilistic value varies over a factor of five which, when combined with the other sampled values produces the overall range in the probabilistic results.

Firstly, the exceedance is associated with the *extreme* low dilution case where the water flow in the well is just sufficient to meet irrigation demand for the cultivated land in the dose model. This is a highly restrictive case and does not take into account the site descriptive material outlined in Chapter 3 of this report, where two alternative interpretations of site-specific but still conservative formulations of the well dilution are defined. The minimum dilution case assumes that only the net infiltration on the waste disposal area itself contributes to the water flux in the well aquifer, whereas the site context clearly defines that there is a larger upslope area that would contribute to dilution in the well, particularly for the disposal area *Ljungströmsfältet*. The situation is closer to the minimum dilution case for assumed disposal in the *Deponi* area. Even so, the conceptual model (Fig 3-8) shows that the imposition of *contaminant boundaries* defined by the dimensions of the disposal areas is also a conservative modelling convenience. The Maximum Dilution formulation is most reliable in this case. Kemakta's biosphere model gives similar results to the extreme low dilution case here, though based on a less well justified well dilution factor. The distance to the well – 500 m – is also conservative.

A second point concerns the simplifying assumptions used to describe the aquifer in the dose assessment model. The conservative assumption here is that the contaminant plume downstream from the disposal mound is restricted laterally to the width of the landfill area. A lower boundary condition is that there is no mixing in the aquifer below the level defined by the deepest part of the lake, because this former quarry is not a natural lake in the landscape with no permanent surface drainage system. This maximises the concentration of contaminants in the lake and the aquifer used for well water extraction. The site

characterisation here has used available resources to provide a relatively detailed site-specific biosphere model. Should it be necessary, a more detailed characterisation of the near surface aquifers downstream from the disposal area should be produced. This would mean details both under present-day conditions with active human maintenance and in their natural (future) states when human action may not be assumed.

Thirdly, there is increasing uncertainty over time, not least because the constant biosphere conditions assumed here are clearly unrealistic beyond a 1 to 10 kyear. Doses at the later peak, around 100 kyear, are due the ^{226}Ra disposed and ingrown post-closure. There is known to be a significant ^{238}U content of materials at the site (Kemakta AR 2014-21), including the *fyllning* that forms much of the upper overburden at the site (Fig 3-6a). The issue is that ^{226}Ra transported from the waste material appears to accumulate in the well aquifer and so, being relatively immobile, will be available into the far future should a well be sunk into the contaminant plume. The rather simplistic assumption of continued cultivation means that accumulations in the rooting zone soil are high over the whole period from a few thousand years to the end of the simulations at 1 Myear. However, because the ^{226}Ra accumulates in the aquifer – not the soil if there were no well – it is still a potential hazard at any time that cultivation might occur. A case where cultivation did not occur until 100 kyear gives similar results to the constant cultivation case because as soon as the well starts depositing contaminated irrigation water at the surface the ^{226}Ra accumulates in the soil.

Turning to the characterisation of the radionuclides in the wasteform itself, it is clear that there are major conceptual differences between Kemakta's *leaching model* and the k_d -concept used here. It is likely that the water processing facility, to the west of the two disposal areas assumed here, monitors for radionuclides in the collected leachate. It would be of interest to have more information in this respect. Results might be able to be used to better formulate details of the potential releases from the waste, particularly for ^{40}K that is expected to give rise to doses at early times post-closure. Analysis of the collected throughflow from the waste would also inform how the release and transport through the disposal mound material should be understood. Is it possible to verify the following:

- Infiltration rate through the membranes and within the landfill itself, as well as below the deposited landfill material
- Groundwater velocities in the geosphere material
- K_d -values in the landfill and geosphere
- k_{ds} in the soils within and outside the site boundary

Finally, we have compared the dose conversion factors (DCFs) for this site with those elsewhere. There is a good degree of commonality between the values. It would be possible to use the DCF approach to assess this site but to obtain site-specific DCF values requires at least as much site-specific understanding as has been used here so that all the necessary information is available to define the biosphere model. The use of such a biosphere model is required to define the site-specific DCFs and it requires few additional resources to attach the biosphere model to the waste and geosphere model. DCF values are more suited to scoping studies whereas this is a real site with specific features. As such it is better to address the local details in a full model.

The modelling documented here uses recently developed techniques to characterise the landscape dose object in a way that was not standard practice even in the early 2010s. The development of site characterisation methods, started with license application for the long-term disposal of spent nuclear fuel in Sweden and Finland repositories (SKB 2011;

POSIVA 2012). In this way the site description derived here is much more representative of the site than was the case in earlier assessments in conditional clearance applications. As may be discerned in these conclusions the perspective here is very much on the assessment of potential radiological consequences. It is a subtle point but this is a difference in this view compared to that of modelling the site for other purposes, say in terms of hydrology or more generalised contaminant transport. Earlier models were of their time in that less site specific information could be included without major investment in site characterisation studies. The use of GIS methods and access to online national databases means that more can now be achieved and this turns attention back to the conceptual understanding of the wasteform and potential releases therefrom on longer timescales. Results from this assessment indicate that some site investigation would benefit future dose assessments, particularly in respect of the near surface hydrology of the site and the understanding of the release of radionuclides in the waste disposed in the landfill.

SSM may wish to consider the need to develop more structured guidance for the assessment of radiological consequences in applications of conditional clearance for waste disposal in a conventional landfill.

7. References

References with report numbers

Kemakta AR 2005-01. Svensson, H., Sundqvist, U., Graffner, O. and Gustavsson, S. (2005). Kvarntorpsområdet - Studie av grundvattensystemet.

Kemakta AR 2014-21. Elert, M., Keith-Roach, M., Lindgren, M. and Svensson, H. (2014). Beräkning av doskonsekvens från uranhaltigt avfall från rivning i Ranstad vid deponering på SAKAB – Reviderat inventarium

Kemakta AR 2015-42. Elert, M., Lindgren, M. and Asperö, M. (2016). Doskonsekvens vid deponering av avfall från WSE på avfallsanläggningarna Gryta och Norrtorp.

Kemakta AR 2020-02. Keith-Roach, M. (2020). Memo – Dose assessment for the disposal of conditionally cleared steel slag and melting furnace refractory at Fortum Waste Solutions' hazardous waste landfill in Kumla.

SKB DokumentID 1579757. Keith-Roach, M., Jones, C., Elert, M. and Lindgren, M. (2021). Clearance of decommissioning wastes for disposal in conventional waste facilities or re-use.

SSM Dokumentnr: 21-1773. (2021). Sammanställning av avfall som genom riktad friklassning deponerats vid Fortums deponi i Norrtorp, Kumla.

Other references

Beresford N A, Barnett C L, Howard B J, Scott W A, Brown J E, Coplestone D, (2008). Derivation of transfer parameters for use within the ERICA Tool and the default concentration ratios for terrestrial biota. *Journal of Environmental Radioactivity* 99, 1393–1407.

BIOMOVS II (1996). Development of a Reference Biospheres Methodology for Radioactive Waste Disposal. Final report of the Reference Studies Working Group of the BIOMOVS II Study. Technical Report No 6, published by the Swedish Radiation Protection Institute on behalf of the BIOMOVS II Steering Committee, Stockholm

Brown J E, Alfonso B, Avila R, Beresford N A, Coplestone D, Pröhl G, Ulyanovsk A, (2008). The ERICA Tool. *Journal of Environmental Radioactivity* 99, 1371–1383.

Ecolego (2018). Ecolego website. <http://ecolego.facilia.se>. Retrieved 19.12.2018.

Grolander S, (2013). Biosphere parameters used in radionuclide transport modelling and dose calculations in SR-PSU. SKB R-13-18, Svensk Kärnbränslehantering AB.

Guerfi, R., Dverstorp, B., Kłos, R.A., Nordén, M. and Xu, S. (2019). A simple and transparent modelling approach for biosphere assessment in post-closure safety assessment, International High-Level Radioactive Waste Management Conference (IHLRWM) (2019).

Hultqvist, F. (2020). Environmental radiological studies of Kvarntorpshögen Dose and radiological risk assessments of humans and biota. Master Thesis. University of Gothenburg.

IAEA (2003a#). "Reference Biospheres" for Solid Radioactive Waste Disposal, Report of BIOMASS Theme 1 of the BIOSphere Modelling and ASSESSment Programme, International Atomic Energy Agency report IAEA-BIOMASS-6, Vienna, Austria.

IAEA (2003b#). Derivation of activity limits for the disposal of radioactive waste in near surface disposal facilities (ISAM Programme), IAEA TECDOC-1380, Vienna, 2003.

IAEA (2004a). Safety Assessment Methodologies for Near Surface Disposal Facilities (ISAM) - Results of a co-ordinated research project - Vol.1: Review and Enhancement of Safety Assessment Approaches and Tools, IAEA, Vienna, 2004.

IAEA (2004b). Safety Assessment Methodologies for Near Surface Disposal Facilities (ISAM) - Results of a co-ordinated research project - Vol.2: Test cases, IAEA, Vienna, 2004.

IAEA (2011a#). Disposal of radioactive waste. IAEA Safety Standards Series No. SSR-5. IAEA, Vienna.

IAEA (2012). The safety case and safety assessment for the disposal of radioactive waste. IAEA Safety Standards Series No. SSG-23. IAEA, Vienna.

IAEA (2014). Near surface disposal facilities for radioactive waste. IAEA Safety Standards Series No. SSG-29, IAEA, Vienna (2014).

Karlsson, S., Bergström, U. and Meili, M. (2001). Models for dose assessments Models adapted to the SFR-area, Sweden. SKB TR-01-04. Svensk Kärnbränslehantering AB.

Kirchner, G. (1998). Applicability of compartmental models for simulating the transport of radionuclides in soils. J. Environ. Radioact. 38 (3), 339e352

Kłos, RA and Thorne MC. (2020). Use of interaction matrices to formalise the development of conceptual models of contaminant transport in the biosphere and the translation of those conceptual models into mathematical models. J. Radiol. Prot. 40-67, 40(1), 2020.

Löfgren A (ed), 2010. The terrestrial ecosystems at Forsmark and Laxemar-Simpevarp. SR-Site Biosphere. SKB TR-10-01, Svensk Kärnbränslehantering AB.

Lindgren, M. and Lindström, F. (1999). SR 97 Radionuclide transport calculations. SKB TR-99-23. Svensk Kärnbränslehantering AB.

NEA (2012). Methods for safety assessment of geological disposal facilities for radioactive waste. Outcomes of NEA MeSA Initiative. NEA No. 6923. Nuclear Energy Agency (NEA). ISBN 978-92-64-99190-3.

POSIVA (2012). Safety case for the disposal of spent nuclear fuel at Olkiluoto – Synthesis 2012. Eurajoki, Finland: Posiva Oy. POSIVA 2012-12. ISBN 978-951-652-193-3.

POSIVA (2013). Terrain and Ecosystems Development Modelling in the Biosphere Assessment BSA-2012. Safety Case for the Disposal of Spent Nuclear Fuel at Olkiluoto, POSIVA Report 2012-29, www.posiva.fi.

Saetre, P., Nordén, S., and Keesmann, S. (2013). The Biosphere model for radionuclide transport and dose assessment in SR-PSU. SKB R-13-46. Svensk Kärnbränslehantering AB.

SKB (2006). Long-term safety for KBS-3 repositories at Forsmark and Laxemar – a first evaluation Main Report of the SR-Can project, SKB TR-06-09. Svensk Kärnbränslehantering AB.

SKB (2011). Long-term safety for the final repository for spent nuclear fuel at Forsmark Main report of the SR-Site project. SKB TR-11-01. Svensk Kärnbränslehantering AB.

SKB (2014). Data report for the safety assessment SR-PSU. SKB TR-14-10. Svensk Kärnbränslehantering AB.

Stark, K. (2022). Personal communication (email dated 2022-03-28).

Tröjbom M, Grolander S, Rensfeldt V, Nordén S, (2013). Kd and CR used for transport calculation in the biosphere in SR-PSU. SKB R-13-01, Svensk Kärnbränslehantering AB.

Thorne MC, Lindborg, T, Brown, J, Ikonen, ATK, Smith, GM, Smith, K and Walke, R. (2022). A research and development roadmap to support applications of the enhanced BIOMASS methodology. J. Radiol. Prot. **42** (2022) 020508

Xu, S., Wörman, A., Dverstorp, B. (2007). Criteria for resolution-scales and parametrisation of compartmental models of hydrological and ecological mass flow in watersheds, Journal of Hydrology. 335, 364-373.

Xu, S. and Kłos, R. (2022). A study of methodologies for assessing the safety of different options for disposal of very low-level radioactive waste. SSM report 2022:XX. (in press).

Xu, S., Kłos, R., Dverstorp, B., Sandberg, V., Stark, K. and Gisca, I. (2022). Experiences in radiological risk assessment of a surface waste disposal facility in Chişinău, Moldova. J. Environ. Radioact. **42** (2022) 011515.

Appendix A – Hydrology of the biosphere model

Fig A-1 shows the stylised structure of the model.

Inflows and outflows:

$$F_{UL} = (P - E)A_{upslope}$$

Upslope catchment to local aquifer

$$F_{OL} = (P - E)A_{LDO}$$

Whole landscape dose object to lake

$$F_{WE} = PA_L + (P - E)A_{LDO}$$

outflow from lake downstream in aquifer

Internal fluxes:

$$F_{LT} = d_{irri}A_{garden}$$

Irrigation from local aquifer (well)

$$F_{TD} = (d_{irri} + P - E)A_{garden}$$

Drainage topsoil to deep soil

$$F_{DT} = EA_{garden}$$

Capillary rise deep soil to topsoil

$$F_{DL} = (d_{irri} + P - E)A_{garden}$$

Percolation through deep soil to local aquifer

$$F_{LW} = F_{UL} + F_{TD}$$

Groundwater throughflow in aquifer to lake

The corresponding 10 transfer coefficients are then as shown below.

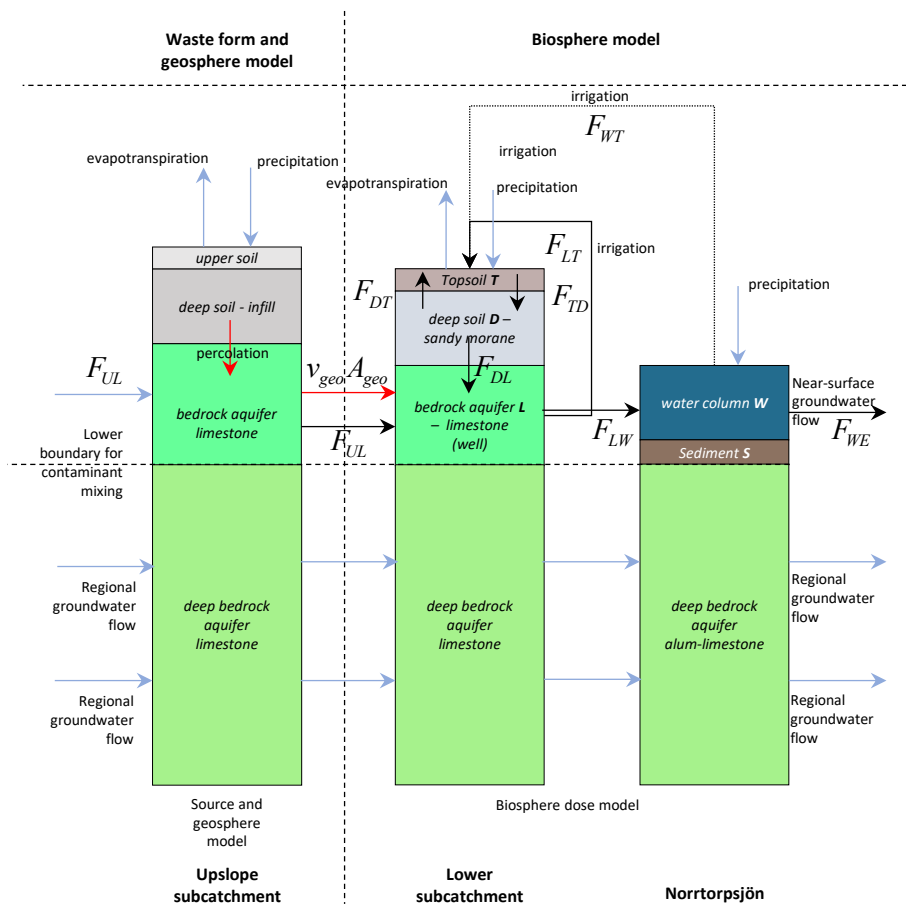


Fig A-1 Schematic hydrology of the biosphere dose assessment model.

Input from disposal area and overall loss from lake:

| | |
|--|--|
| $\lambda_{geoL} = \frac{v_{geo}}{\varepsilon_{geo}R_{geo}l_{geo}}$ | Implicit cross-sectional area of geosphere path is 1 m ² |
| $\lambda_{WE} = \frac{PA_{lake}+(P-E)A_{LDO}}{V_{lake}}$ | Total water flux out of the biosphere system via the lake to Elsewhere |

Internal transfers

| | |
|--|---|
| $\lambda_{LT} = \frac{F_{LT}}{\varepsilon_{geo}R_{geo}V_L} = \frac{d_{irri}}{\varepsilon_{geo}R_{geo}z_L}$ | Irrigation |
| $\lambda_{LW} = \frac{v_{geo}+F_{UL}}{\varepsilon_{geo}R_{geo}V_L}$ | Flow from local aquifer to lake water, volume of local aquifer is $V_L = z_L A_{garden}$, $F_{UL} = (P - E)A_{upslope}$ |
| $\lambda_{DL} = \frac{F_{DL}}{s_D \varepsilon_D R_D V_D} = \frac{d_{irri}+P-E}{s_D \varepsilon_D R_D z_D}$ | Percolation to local aquifer |
| $\lambda_{DT} = \frac{F_{DT}}{s_D \varepsilon_D R_D V_D} = \frac{E}{s_D \varepsilon_D R_D z_D}$ | Capillary rise |
| $\lambda_{TD} = \frac{F_{TD}}{s_T \varepsilon_T R_T V_T} = \frac{d_{irri}+P-E}{s_T \varepsilon_T R_T z_T}$ | Drainage |
| $\lambda_{SW} = \frac{2D_{eff}}{z_{lake}(z_{lake}+z_S)\varepsilon_S R_S}$ | Diffusion from bed sediment to lake water |
| $\lambda_{WS} = \frac{2D_{eff}}{z_{lake}(z_{lake}+z_S)}$ | Sedimentation and diffusion from lake water to bed sediment |

No irrigation is assumed from the lake in this model although it is used as a source of fish for human consumption. The well is taken to be the source of irrigation abstraction since it has a dilution determined by the size of the upslope subcatchment based in a restrictive boundary condition for the contaminant plume from the disposal mound (see Fig 3-8). The total water flux entering the lake is based on the full upslope subcatchment and the lower subcatchment, of which the cultivated area is a smaller part. Dilution in the lake is therefore clearly considerably higher, prompting the focus on the well water as the irrigation source.

Appendix B – Numerical data

Data used in the main scenario

Table B-1 Element specific distribution coefficient (Kd) for saturated and unsaturated mediums, the distribution function is assumed in this study. Value is used as GM.

| Element | Kd_geo [m ³ /kg] | PDF | GSD |
|---------|--------------------------------|-----------|-----|
| Ac | 1.0 | lognormal | 2.0 |
| Am | 1.0 | lognormal | 2.0 |
| Bi | 0.5 | lognormal | 2.0 |
| C | 0.0 | | |
| Co | 0.05 | lognormal | 2.0 |
| Cs | 0.1 | lognormal | 2.0 |
| H | 0.0 | | |
| K | 0.0 | | 2.0 |
| Pa | 0.5 | lognormal | 2.0 |
| Pb | 0.5 | lognormal | 2.0 |
| Po | 0.5 | lognormal | 2.0 |
| Pu | 1.0 | lognormal | 2.0 |
| Ra | 0.05 | lognormal | 2.0 |
| Rn | 0.0 | | |
| Th | 1.0 | lognormal | 2.0 |
| U | 0.05 | lognormal | 2.0 |

Table B-2 Element specific distribution coefficient (Kd) for soil and backfill material, the distribution function is assumed in this study. Value is used as GM.

| Element | Kd_infill [m ³ /kg] | PDF | GSD |
|---------|-----------------------------------|-----------|-----|
| Ac | 1.7 | lognormal | 2.0 |
| Am | 2.0 | lognormal | 2.0 |
| Bi | 0.0 | lognormal | 2.0 |
| C | 0.48 | lognormal | |
| Co | 1.2 | lognormal | 2.0 |
| Cs | 0.0 | | 2.0 |
| H | 0.013 | lognormal | |
| K | 2.0 | lognormal | 2.0 |
| Pa | 2.0 | lognormal | 2.0 |
| Pb | 2.0 | lognormal | 2.0 |
| Po | 0.48 | lognormal | 2.0 |
| Pu | 0.74 | lognormal | 2.0 |
| Ra | 2.5 | lognormal | 2.0 |
| Rn | 0.0 | | |
| Th | 1.9 | lognormal | 2.0 |
| U | 0.2 | lognormal | 2.0 |

Table B-3 Element specific distribution coefficient (Kd) for cement material, the distribution function is assumed in this study. Value is used as GM.

| Element | Kd_cement [m ³ /kg] | PDF | GSD |
|---------|-----------------------------------|-----------|-----|
| Ac | 10.0 | lognormal | 2.0 |
| Am | 10.0 | lognormal | 2.0 |
| Bi | 3.0 | lognormal | 2.0 |
| C | 0.0001 | lognormal | 2.0 |
| Co | 0.2 | lognormal | 2.0 |
| Cs | 0.002 | lognormal | 2.0 |
| H | 0.0 | | |
| K | 0.002 | lognormal | 2.0 |
| Pa | 10.0 | lognormal | 2.0 |
| Pb | 3.0 | lognormal | 2.0 |
| Po | 3.0 | lognormal | 2.0 |
| Pu | 30.0 | lognormal | 2.0 |
| Ra | 0.1 | lognormal | 2.0 |
| Rn | 0.0 | | |
| Th | 30.0 | lognormal | 2.0 |
| U | 30.0 | lognormal | 2.0 |

Table B-4 Transfer coefficient to cows meat, milk and soil to plant concentration factors

| Elements | TF_meat [days kg ⁻¹ fw] | TF_grain [Bq kg ⁻¹ fw/Bq kg ⁻¹ dry soil] | TF_milk [days l ⁻¹] | TF_pasture [Bq kg ⁻¹ fw/Bq kg ⁻¹ dry soil] | TF_root [Bq kg ⁻¹ fw/Bq kg ⁻¹ dry soil] | TF_veg [Bq kg ⁻¹ fw/Bq kg ⁻¹ dry soil] |
|----------|---------------------------------------|---|------------------------------------|---|--|---|
| Ac | 1.6E-04 | 1.0E-03 | 4.0E-07 | 1.0E-03 | 1.0E-03 | 1.0E-03 |
| Am | 4.0E-05 | 1.0E-05 | 1.5E-06 | 5.0E-03 | 1.0E-03 | 1.0E-03 |
| Bi | 4.0E-04 | 1.0E-02 | 3.0E-04 | 1.0E-02 | 1.0E-02 | 1.0E-02 |
| C | 1.2E-01 | 1.0E-01 | 1.0E-02 | 1.0E-01 | 1.0E-01 | 1.0E-01 |
| Co | 1.0E-02 | 3.0E-02 | 3.0E-04 | 6.0E-03 | 3.0E-02 | 3.0E-02 |
| Cs | 5.0E-02 | 2.0E-02 | 7.9E-03 | 3.0E-02 | 3.0E-02 | 3.0E-02 |
| H | 2.9E-02 | 5.0E+00 | 1.5E-02 | 5.0E+00 | 5.0E+00 | 5.0E+00 |
| K | 2.0E-02 | 1.3E+00 | 7.2E-03 | 1.3E+00 | 1.0E+00 | 1.3E+00 |
| Pa | 5.0E-05 | 4.0E-02 | 5.0E-06 | 4.0E-02 | 4.0E-02 | 4.0E-02 |
| Pb | 4.0E-04 | 1.0E-02 | 3.0E-04 | 1.0E-02 | 1.0E-02 | 1.0E-02 |
| Po | 5.0E-03 | 2.0E-04 | 3.4E-04 | 2.0E-04 | 2.0E-04 | 2.0E-04 |
| Pu | 1.0E-05 | 3.0E-05 | 1.1E-06 | 1.0E-03 | 1.0E-03 | 1.0E-04 |
| Ra | 5.0E-05 | 4.0E-02 | 1.3E-03 | 4.0E-02 | 4.0E-02 | 4.0E-02 |
| Rn | 2.9E-02 | 0.0E+00 | 1.5E-02 | 5.0E+00 | 5.0E+00 | 5.0E+00 |
| Th | 2.7E-03 | 5.0E-04 | 5.0E-06 | 5.0E-04 | 5.0E-04 | 5.0E-04 |
| U | 3.0E-04 | 1.0E-04 | 4.0E-04 | 1.0E-03 | 1.0E-03 | 1.0E-03 |

Table B-5 Dose coefficients for ingestion, inhalation and external irradiation

| Radionuclide | DF_ext [Sv h ⁻¹ Bq ⁻¹ kg] | DF_inh [Sv Bq ⁻¹] | DF_intag [Sv Bq ⁻¹] | Radionuclide | DF_ext [Sv h ⁻¹ Bq ⁻¹ kg] | DF_inh [Sv Bq ⁻¹] | DF_intag [Sv Bq ⁻¹] |
|--------------|---|----------------------------------|------------------------------------|--------------|---|----------------------------------|------------------------------------|
| Ac-227 | 6.0E-11 | 5.7E-04 | 1.21E-06 | Pu-238 | 1.2E-15 | 1.1E-04 | 2.3E-07 |
| Ac-228 | 6.0E-11 | 5.7E-04 | 1.21E-06 | Pu-239 | 4.6E-15 | 1.2E-04 | 2.5E-07 |
| Am-241 | 6.4E-13 | 9.6E-05 | 2E-07 | Pu-240 | 1.4E-15 | 1.2E-04 | 2.5E-07 |
| Bi-211 | 2.5E-13 | 5.7E-06 | 6.9E-07 | Pu-241 | 3.0E-16 | 2.3E-06 | 4.8E-09 |
| Bi-212 | 2.5E-13 | 5.7E-06 | 6.9E-07 | Ra-223 | 5.7E-10 | 1.6E-05 | 2.8E-07 |
| Bi-214 | 2.5E-13 | 5.7E-06 | 6.9E-07 | Ra-224 | 5.7E-10 | 1.6E-05 | 2.8E-07 |
| C-14 | 0.0E+00 | 5.8E-09 | 5.8E-10 | Ra-226 | 5.7E-10 | 9.5E-06 | 2.8E-07 |
| Co-60 | 5.5E-10 | 3.1E-08 | 3.5E-09 | Ra-228 | 1.6E-10 | 1.6E-05 | 6.8E-07 |
| Cs-137 | 1.2E-10 | 2.0E-08 | 1.3E-08 | Rn-219 | 0.0 | 2.6E-10 | 1.8E-11 |
| H-3 | 0.0E+00 | 2.6E-10 | 1.8E-11 | Rn-220 | 0.0 | 2.6E-10 | 1.8E-11 |
| K-40 | 6.0E-12 | 2.1E-09 | 6.2E-09 | Th-227 | 3.2E-10 | 4.4E-05 | 4.4E-05 |
| Pa-231 | 5.7E-10 | 1.4E-04 | 7.1E-07 | Th-228 | 3.2E-10 | 4.4E-05 | 1.4E-07 |
| Pa-234m | 6.1E-12 | 1.4E-04 | 7.1E-07 | Th-230 | 2.4E-14 | 1.0E-04 | 2.1E-07 |
| Pb-210 | 2.5E-13 | 5.7E-06 | 6.9E-07 | Th-232 | 9.4E-15 | 1.1E-04 | 2.3E-07 |
| Pb-211 | 2.5E-13 | 5.7E-06 | 6.9E-07 | Th-234 | 9.4E-15 | 1.1E-04 | 2.1E-07 |
| Pb-212 | 2.5E-13 | 5.7E-06 | 6.9E-07 | U-232 | 3.4E-14 | 9.6E-06 | 5.1E-08 |
| Pb-214 | 2.5E-13 | 5.7E-06 | 6.9E-07 | U-234 | 6.7E-15 | 9.4E-06 | 4.73E-08 |
| Po-210 | 1.9E-15 | 4.3E-06 | 1.2E-06 | U-235 | 1.9E-11 | 8.5E-06 | 4.73E-08 |
| Po-212 | 1.9E-15 | 4.3E-06 | 1.2E-06 | U-236 | 2.8E-15 | 8.7E-06 | 4.7E-08 |
| Po-216 | 1.9E-15 | 4.3E-06 | 1.2E-06 | U-238 | 6.3E-12 | 8.0E-06 | 4.73E-08 |

Data used in evaluation of alternative scenario

Bathubbing scenario:

Except for the source terms, radionuclide and element dependent data all the parameter values used in the calculation of the flooding scenario are given below:

- water overflow to the garden in one year (OF) = 0.1 m
- the volume of the disposal unit = 3200 [m³]
- the moisture content of the disposal unit = 0.7 [-]
- for external exposure, a shielding factor (*sf*) of 0.1 for indoor activities is assumed.
- breathing rate indoor = 0.75 [m³/h]
- breathing rate outdoor = 1 [m³/h]
- time spent indoor = 6575 [h/y]
- time spent outdoor = 2191 [h/y]
- consumption rate of root vegetables = 118 [kg/y]
- consumption rate of green vegetables = 31 [kg/y]
- inadvertent soil ingestion rate = 3×10⁻² [kg/y]
- soil thickness = 0.25 [m]
- soil dry bulk density = 1800 [kg/m³]
- indoor dust level = 1×10⁻⁸ [kg/m³]
- outdoor dust level = 2×10⁻⁸ [kg/m³]

Data used in evaluation of human intrusion scenarios

On-site residence scenario:

Except for the source terms, radionuclide and element dependent data all the parameter values used in the calculation of the on-site residence scenario are given below:

- dilution factor is 0.1
- the amount of the waste = 5000 [ton]
- for external exposure, a shielding factor of 0.1 for indoor activities is assumed.
- breathing rate indoor = 0.75 [m³/h]
- breathing rate outdoor = 1 [m³/h]
- time spent indoor = 6575 [h/y]
- time spent outdoor = 2192 [h/y]
- root vegetables consumption rate = 118 [kg/y]
- green vegetables consumption rate = 31 [kg/y]
- inadvertent soil ingestion rate = 3×10^{-2} [kg/y]
- indoor dust level = 1×10^{-8} [kg/m³]
- outdoor dust level = 2×10^{-8} [kg/m³]

Road construction scenario:

Except for the source terms, radionuclide and element dependent data all the parameter values used in the calculation of road construction scenario are given below:

- dilution factor = 0.1
- the amount of the waste = 5000 [ton]
- inadvertent soil ingestion rate = 3×10^{-2} [kg/y]
- exposure duration = 88 [h]
- Breathing rate of the intruder = 1.2 [m³/h]
- Inadvertent soil ingestion rate of the intruder = 3.4×10^{-5} [kg/h]
- Dust level experienced by the intruder = 1×10^{-6} [kg/m³]

Data used in Non-human biota calculations

Table B-6 DCC_int_alpha, DCC_int_beta_gamma and DCC_int_low_beta for limnic organisms benthic fish and pelagic fish [($\mu\text{Gy h}^{-1}$)/(Bq kgfw $^{-1}$)]

| Radionuclides | DCC_int_alpha | DCC_int_beta_gamma | DCC_int_low_beta |
|---------------|---------------|--------------------|------------------|
| Ac-227 | 3.93E-05 | 4.74E-06 | 4.45E-06 |
| Ac-228 | 3.93E-05 | 4.74E-06 | 4.45E-06 |
| Am-241 | 3.17E-03 | 3.20E-05 | 0.0 |
| Bi-211 | 4.15E-03 | 2.45E-04 | 4.80E-06 |
| Bi-212 | 5.08E-03 | 2.45E-04 | 4.80E-06 |
| Bi-214 | 0.0 | 2.45E-04 | 4.80E-06 |
| C-14 | 0.0 | 2.87E-05 | 2.90E-07 |
| Co-60 | 0.0 | 2.30E-04 | 0.0 |
| Cs-137 | 0.0 | 1.90E-04 | 0.0 |
| H-3 | 0.0 | 8.25E-07 | 2.48E-06 |
| K-40 | 0.0 | 3.00E-04 | 0.0 |
| Pa-231 | 2.87E-03 | 3.90E-05 | 7.58E-06 |
| Pa-234m | 2.87E-03 | 3.90E-05 | 7.58E-06 |
| Pb-210 | 0.0 | 2.45E-04 | 4.80E-06 |
| Pb-211 | 0.0 | 2.45E-04 | 5.00E-06 |
| Pb-212 | 0.0 | 2.45E-04 | 5.00E-06 |
| Pb-214 | 0.0 | 2.45E-04 | 5.00E-06 |
| Po-210 | 3.10E-03 | 0.0 | 0.0 |
| Po-212 | 3.10E-03 | 0.0 | 0.0 |
| Po-216 | 3.10E-03 | 0.0 | 0.0 |
| Pu-238 | 3.20E-03 | 0.0 | 0.0 |
| Pu-239 | 3.00E-03 | 0.0 | 0.0 |
| Pu-240 | 3.00E-03 | 0.0 | 0.0 |
| Pu-241 | 6.20E-08 | 8.37E-07 | 2.20E-06 |
| Ra-223 | 1.43E-02 | 7.50E-04 | 1.05E-05 |
| Ra-224 | 1.43E-02 | 7.50E-04 | 1.05E-05 |
| Ra-226 | 1.43E-02 | 7.50E-04 | 0.0 |
| Ra-228 | 0.0 | 3.40E-04 | 9.90E-06 |
| Rn-219 | 0.0 | 8.25E-07 | 2.48E-06 |
| Rn-220 | 0.0 | 8.25E-07 | 2.48E-06 |
| Th-227 | 1.82E-02 | 7.60E-04 | 9.75E-06 |
| Th-228 | 1.82E-02 | 7.60E-04 | 0.0 |
| Th-230 | 2.70E-03 | 0.0 | 0.0 |
| Th-232 | 2.30E-03 | 0.0 | 0.0 |
| Th-234 | 2.70E-03 | 0.0 | 9.00E-06 |
| U-232 | 3.06E-03 | 1.01E-05 | 9.65E-07 |
| U-234 | 2.80E-03 | 0.0 | 0.0 |
| U-235 | 2.57E-03 | 1.35E-04 | 0.0 |
| U-236 | 2.60E-03 | 6.61E-06 | 7.59E-07 |
| U-238 | 2.40E-03 | 0.0 | 0.0 |

Table B-7 DCC_ext_beta_gamma and DCC_ext_low_beta for limnic organisms
benthic fish and pelagic fish $[(\mu\text{Gy h}^{-1})/(\text{Bq l}^{-1})]$

| Radionuclides | DCC_ext_beta_gamma | DCC_ext_low_beta | DCC_ext_beta_gamma | DCC_ext_low_beta |
|---------------|--------------------|------------------|--------------------|------------------|
| | Benthic fish | | Pelagic fish | |
| Ac-227 | 6.67E-08 | 6.03E-16 | 6.81E-08 | 4.22E-16 |
| Ac-228 | 6.67E-08 | 6.03E-16 | 6.81E-08 | 4.22E-16 |
| Am-241 | 1.10E-05 | 0.0 | 8.07E-06 | 0.0 |
| Bi-211 | 2.97E-05 | 0.0 | 2.97E-05 | 0.0 |
| Bi-212 | 6.85E-04 | 0.0 | 6.85E-04 | 0.0 |
| Bi-214 | 7.60E-04 | 0.0 | 7.60E-04 | 0.0 |
| C-14 | 1.70E-08 | 0.0 | 1.80E-08 | 0.0 |
| Co-60 | 1.30E-03 | 0.0 | 1.30E-03 | 0.0 |
| Cs-137 | 2.80E-04 | 0.0 | 2.90E-04 | 0.0 |
| H-3 | 3.70E-13 | 0.0 | 3.60E-13 | 0.0 |
| K-40 | 8.58E-05 | 0.0 | 2.90E-04 | 0.0 |
| Pa-231 | 1.86E-05 | 5.98E-16 | 1.89E-05 | 4.09E-16 |
| Pa-234m | 1.86E-05 | 5.98E-16 | 1.89E-05 | 4.09E-16 |
| Pb-210 | 3.80E-06 | 0.0 | 4.00E-06 | 0.0 |
| Pb-211 | 3.80E-06 | 0.0 | 4.00E-06 | 0.0 |
| Pb-212 | 3.80E-06 | 0.0 | 4.00E-06 | 0.0 |
| Pb-214 | 3.80E-06 | 0.0 | 4.00E-06 | 0.0 |
| Po-210 | 4.30E-09 | 0.0 | 4.30E-09 | 0.0 |
| Po-212 | 4.30E-09 | 0.0 | 4.30E-09 | 0.0 |
| Po-216 | 4.30E-09 | 0.0 | 4.30E-09 | 0.0 |
| Pu-238 | 1.40E-07 | 0.0 | 1.50E-07 | 0.0 |
| Pu-239 | 7.80E-08 | 0.0 | 8.20E-08 | 0.0 |
| Pu-240 | 1.30E-07 | 0.0 | 1.40E-07 | 0.0 |
| Pu-241 | 8.20E-10 | 0.0 | 8.40E-10 | 0.0 |
| Ra-223 | 9.10E-04 | 0.0 | 9.20E-04 | 0.0 |
| Ra-224 | 9.10E-04 | 0.0 | 9.20E-04 | 0.0 |
| Ra-226 | 9.10E-04 | 0.0 | 9.20E-04 | 0.0 |
| Ra-228 | 4.90E-04 | 0.0 | 5.00E-04 | 0.0 |
| Rn-219 | 3.70E-13 | 0.0 | 3.60E-13 | 0.0 |
| Rn-220 | 3.70E-13 | 0.0 | 3.60E-13 | 0.0 |
| Th-227 | 8.20E-04 | 0.0 | 8.30E-04 | 0.0 |
| Th-228 | 8.20E-04 | 0.0 | 8.30E-04 | 0.0 |
| Th-230 | 2.40E-07 | 0.0 | 2.50E-07 | 0.0 |
| Th-232 | 1.40E-07 | 0.0 | 1.50E-07 | 0.0 |
| Th-234 | 1.40E-07 | 0.0 | 1.50E-07 | 0.0 |
| U-232 | 2.41E-07 | 7.08E-17 | 2.52E-07 | 4.84E-17 |
| U-234 | 1.50E-07 | 0.0 | 1.60E-07 | 0.0 |
| U-235 | 8.20E-05 | 0.0 | 8.30E-05 | 0.0 |
| U-236 | 1.20E-07 | 5.58E-17 | 8.30E-05 | 3.82E-17 |
| U-238 | 9.50E-08 | 0.0 | 1.00E-07 | 0.0 |

Table B- 8 Parameters values for cR_lake_fish_NHB for benthic fish and pelagic fish [m³/kg fw]

| Radionuclides | cR_lake_fish_NHB | Radionuclides | cR_lake_fish_NHB |
|---------------|------------------|---------------|------------------|
| Ac-227 | 2.6E-03 | Pu-238 | 2.0E-02 |
| Ac-228 | 2.6E-03 | Pu-239 | 2.0E-02 |
| Am-241 | 2.6E-03 | Pu-240 | 2.0E-02 |
| Bi-211 | 3.7E-01 | Pu-241 | 2.0E-02 |
| Bi-212 | 3.7E-01 | Ra-223 | 2.0E-02 |
| Bi-214 | 3.7E-01 | Ra-224 | 2.0E-02 |
| C-14 | 0.0E+00 | Ra-226 | 2.0E-02 |
| Co-60 | 3.6E-02 | Ra-228 | 2.0E-02 |
| Cs-137 | 1.3E+00 | Rn-219 | 0.0 |
| H-3 | 0.0 | Rn-220 | 0.0 |
| K-40 | 0.0 | Th-227 | 7.8E-02 |
| Pa-231 | 2.6E-03 | Th-228 | 7.8E-02 |
| Pa-234m | 2.6E-03 | Th-230 | 7.8E-02 |
| Pb-210 | 3.7E-01 | Th-232 | 7.8E-02 |
| Pb-211 | 3.7E-01 | Th-234 | 7.8E-02 |
| Pb-212 | 3.7E-01 | U-232 | 1.7E-04 |
| Pb-214 | 3.7E-01 | U-234 | 1.7E-04 |
| Po-210 | 1.6E-01 | U-235 | 1.7E-04 |
| Po-212 | 1.6E-01 | U-236 | 1.7E-04 |
| Po-216 | 1.6E-01 | U-238 | 1.7E-04 |

Appendix C – Dose Conversion Factors

Table C-1 Dose conversion factors (DCFs) calculated based on site-specific biosphere in this study [Sv/Bq]. EXD denotes extreme low dilution, MID denotes minimum dilution, MAD denotes maximum dilution (as defined in Table 3-3).

| Radionuclides | EXD | MID | MAD | Radionuclides | EXD | MID | MAD |
|---------------|----------|----------|----------|---------------|----------|----------|----------|
| U-238 | 3.04E-11 | 7.27E-12 | 3.53E-12 | U-232 | 1.66E-13 | 1.61E-13 | 1.54E-13 |
| U-234 | 1.91E-11 | 4.56E-12 | 2.22E-12 | U-236 | 1.89E-11 | 4.52E-12 | 2.19E-12 |
| U-235 | 5.36E-11 | 1.28E-11 | 6.22E-12 | Ac-228 | 2.71E-09 | 6.53E-10 | 3.17E-10 |
| Th-234 | 2.79E-11 | 6.67E-12 | 3.24E-12 | Bi-211 | 1.33E-20 | 1.33E-20 | 1.33E-20 |
| Th-230 | 1.03E-10 | 4.58E-11 | 2.62E-11 | Bi-212 | 4.74E-09 | 1.14E-09 | 5.55E-10 |
| Th-232 | 3.17E-10 | 7.65E-11 | 3.72E-11 | Bi-214 | 1.24E-19 | 1.24E-19 | 1.24E-19 |
| Th-228 | 5.74E-09 | 1.38E-09 | 6.73E-10 | C-14 | 4.28E-13 | 1.02E-13 | 4.98E-14 |
| Ra-226 | 2.21E-08 | 7.54E-09 | 3.47E-09 | Cs-137 | 4.05E-14 | 4.03E-14 | 3.99E-14 |
| Ra-228 | 2.50E-08 | 6.02E-09 | 2.92E-09 | H-3 | 9.65E-15 | 4.08E-15 | 2.27E-15 |
| K-40 | 5.94E-11 | 1.42E-11 | 6.90E-12 | Pa-234m | 7.40E-21 | 7.40E-21 | 7.40E-21 |
| Ac-227 | 8.30E-10 | 3.56E-10 | 2.06E-10 | Pb-211 | 2.24E-19 | 2.24E-19 | 2.24E-19 |
| Pa-231 | 8.87E-09 | 3.79E-09 | 2.19E-09 | Pb-212 | 4.74E-09 | 1.14E-09 | 5.55E-10 |
| Pb-210 | 5.49E-09 | 1.87E-09 | 8.64E-10 | Pb-214 | 1.66E-19 | 1.66E-19 | 1.66E-19 |
| Po-210 | 1.46E-09 | 4.93E-10 | 2.25E-10 | Po-212 | 1.62E-09 | 3.90E-10 | 1.89E-10 |
| Am-241 | 2.31E-13 | 2.28E-13 | 2.25E-13 | Po-216 | 2.53E-09 | 6.09E-10 | 2.96E-10 |
| Co-60 | 6.69E-15 | 6.67E-15 | 6.65E-15 | Ra-224 | 1.91E-08 | 4.60E-09 | 2.23E-09 |
| Pu-238 | 4.84E-14 | 4.83E-14 | 4.82E-14 | Ra-223 | 4.24E-16 | 4.24E-16 | 4.24E-16 |
| Pu-239 | 2.05E-11 | 1.40E-11 | 9.76E-12 | Rn-219 | 7.77E-23 | 7.77E-23 | 7.77E-23 |
| Pu-240 | 5.68E-12 | 4.98E-12 | 4.24E-12 | Rn-220 | 1.87E-10 | 4.51E-11 | 2.19E-11 |
| Pu-241 | 1.62E-16 | 1.62E-16 | 1.62E-16 | Th-227 | 5.39E-15 | 5.39E-15 | 5.39E-15 |

The Swedish Radiation Safety Authority has a comprehensive responsibility to ensure that society is safe from the effects of radiation. The Authority works from the effects of radiation. The Authority works to achieve radiation safety in a number of areas: nuclear power, medical care as well as commercial products and services. The Authority also works to achieve protection from natural radiation and to increase the level of radiation safety internationally.

The Swedish Radiation Safety Authority works proactively and preventively to protect people and the environment from the harmful effects of radiation, now and in the future. The Authority issues regulations and supervises compliance, while also supporting research, providing training and information, and issuing advice. Often, activities involving radiation require licences issued by the Authority. The Swedish Radiation Safety Authority maintains emergency preparedness around the clock with the aim of limiting the aftermath of radiation accidents and the unintentional spreading of radioactive substances. The Authority participates in international co-operation in order to promote radiation safety and finances projects aiming to raise the level of radiation safety in certain Eastern European countries.

The Authority reports to the Ministry of the Environment and has around 300 employees with competencies in the fields of engineering, natural and behavioral sciences, law, economics and communications. We have received quality, environmental and working environment certification.

Publikationer utgivna av Strålsäkerhetsmyndigheten kan laddas ned via stralsakerhetsmyndigheten.se eller beställas genom att skicka e-post till registrator@ssm.se om du vill ha broschyren i alternativt format, som punktskrift eller daisy.

Strålsäkerhetsmyndigheten
171 16 Stockholm
08-799 40 00
www.stralsakerhetsmyndigheten.se
registrator@ssm.se

©Strålsäkerhetsmyndigheten